U.PORTO
FEUP FACULDADE DE ENGENHARIA
UNIVERSIDADE DO PORTO

U.PORTO
INSTITUTO DE CIÊNCIAS BIOMÉDICAS ABEL SALAZAR
UNIVERSIDADE DO PORTO

ASTROCYTE-OLIGODENDROCYTE CROSSTALK IN THE CONTEXT OF ASTROGLIOSIS

Eva Daniela de Sousa Maia Carvalho

Master Dissertation

Integrated Master in Bioengineering

Specialization in Molecular Biotechnology

Supervisor: Doutora Ana Paula Gomes Moreira Pêgo

Co-supervisor: Doutora Daniela Nogueira da Rocha Mar

October, 2016

Astrocyte-oligodendrocyte crosstalk in the context of astrogliosis

Eva Daniela de Sousa Maia Carvalho

Dissertation submited to Faculdade de Engenharia da Universidade do Porto and to Instituto de Ciências Biomédicas Abel Salazar to obtain the degree of

Masters in Bioengineering

October, 2016

The research described in this dissertation was financed by:

- Santa Casa da Misericórdia de Lisboa – Prémio Melo e Castro (grant MC-1068-2015).

- Project NORTE-01-0145-FEDER-000008, supported by Norte Portugal Regional Operational Programme (NORTE 2020), under the PORTUGAL 2020 Partnership Agreement, through the European Regional Development Fund (ERDF).

- Fundo Europeu de Desenvolvimento Regional funds through the COMPETE 2020.

- Operacional Programme for Competitiveness and Internationalisation (POCI), Portugal 2020, and by Portuguese funds through FCT - Fundação para a Ciência e a Tecnologia/ Ministério da Ciência, Tecnologia e Ensino Superior in the framework of the project "Institute for Research and Innovation in Health Sciences" (POCI-01-0145-FEDER-007274).

“...Põe quanto és
No mínimo que fazes”

Ricardo Reis

Agradecimentos

É com enorme satisfação pessoal que hoje revejo os cinco anos de curso que findam, e em especial este semestre, que teve um brilho diferente! A realização que hoje sinto deve-se muito aos que se foram cruzando comigo e me foram ajudando. A todos eles tenho que deixar um enorme obrigada.

Em primeiro lugar, à professora Ana Paula, orientadora desta tese. Por ser a minha grande guia este semestre, por me ter incutido a vontade de querer, ambicionar mais e sonhar. Obrigada por todos os conselhos, por todas as discussões e por todas as lições sobre ciência. Foi tão bom aprender ter tido a oportunidade de aprender consigo (quer na secretária, ou na bancada do laboratório! ☺). Obrigada também por acreditar em mim e mais importante, por me fazer acreditar, confiar e olhar sempre para o lado bom da ciência. À Daniela, minha co-orientadora, muito obrigada por, apesar de ausente estares presente e tentares ajudar à distância. Os teus conselhos realistas foram fulcrais para o desenrolar do trabalho.

Ao grupo Glial Cell Biology, do i3S. A Maria, a Sofia, a Joana e a Ana foram peças essenciais nesta tese. Obrigada por me terem introduzido ao misterioso mundo dos oligodendrócitos e me terem ensinado que quem dita as regras são sempre eles e nunca nós! Obrigada por terem sempre tempo para atender às minhas mil e uma dúvidas cada vez que corria para o 209; obrigada por todos os reagentes que me foram emprestando e obrigada por tudo o que me deram a nível pessoal: reavivaram-me o valor do dar e do dar-se sem esperar nada em troca!

Ao grupo nBTT, em especial, à Sofia pela disponibiidade em me ensinar a trabalhar *in vivo* e por ser a minha tutora no curso animal e à Vicky pela ajuda na síntese do polímero e na análise dos NMR. Obrigada também a todos os outros que me foram dando apoio nas mais variadas áreas e muito obrigada por me irem ensinando ao longo do semestre a ser resiliente e a saber lidar com as frustrações. Aos outros membros do i3S, deixo um especial obrigada à Paula Sampaio pela ajuda incansável no estudo live imaging dos oligodendrócitos nos pilares.

Ademais, fora do i3S, tenho que expressar o meu profundo agradecimento ao Dr. Eduardo Mendes (TU Delft) e ao Dr. Piotr Glazer (TU Delft) pela produção dos moldes de silica para a fabricação dos micropilares de PDMS e pela ajuda inicial e introdução a esta área. Agradeço também ao grupo de investigação do professor Jorge Coelho do Departamento de Química da Universidade de Coimbra pela realização das análises GPC dos polímeros (Joana Mendes) e pelo tratamento de plasma dos micropilares (Dr. Ana Fonseca).

Para além de todas estas pessoas que fui referindo, estes cinco anos e este semestre só foram superados porque tive o apoio incansável de quem esteve sempre do meu lado. E todos eles também merecem estar aqui.

Às minhas meninas bioengenheiras, companheiras de curso e companheiras de vida, obrigada mil vezes por aturarem todos os meus dramas, todos os meus “não vou conseguir” ou “vai correr mal”. Obrigada por terem feito destes cinco anos, anos memoráveis e recheados de momentos que vou levar para a vida! Às meninas biotecs do 214, obrigada por partilharem comigo esta experiência laboratorial, por não me deixarem ir abaixo quando tudo parecia correr mal e por partilharem das minhas pequenas alegrias quando algo corria bem. Aos outros biotecs que este semestre invadiram o i3S, um obrigada também por todas as pausas, quebras de rotina e companhia nas horas de trabalho que pareciam não ter fim!

Ao Eurico, obrigada por aceitares os meus ideais e por continuares ao meu lado, apesar de todas as minhas ausências. Tudo o que fui conseguindo nestes anos é também graças a ti!

Por fim, mas acima de tudo, à minha mãe, ao meu pai, ao Dani e à Filipa. Obrigada. Por tudo. Mas em especial por me ensinarem continuamente a dar sempre tudo o que sou no mínimo que faço.

Eva

List of Contents

- This page was intentionally left blank. -

Abbreviation List

BBB Blood-brain barrier

CL ε-caprolactone

CM Conditioned Medium

CNS Central Nervous System

CSPG Chondroitin sulphate proteoglycans

CTCF Corrected total cell fluorescence

DCM Dichloromethane

DMEM Dulbecco's Modified Eagle Medium

DMF Dimethylformamide

DRG Dorsal root ganglia

EAE Encephalomyelitis

ECM Extracellular matrix

FBS Foetal Bovine Serum

FGF Fibroblast Growth Factor

GFAP Glial fibrillary acidic protein

GFP Green fluorescent protein

GPC Gel permeation chromatography

HBSS Hank's Balanced Salt Solution (HBSS)

HTS High throughput screening

LPS lipopolysaccharide

MAG Myelin associated glicoprotein

MBP Myelin basic protein

MOG Myelin oligodendrocyte glicoprotein

Mn number average molecular weight

MS Multiple Sclerosis

Mw weight average molecular weight

NGS Normal Goat Serum

NMR Nuclear Magnetic Resonance

OPC Oligodendrocyte precursor cell

P(TMC-CL) Poly(trimethylene carbonate-co-ε-caprolactone)

PBS Phosphate Buffer Saline

PDGFR-α Platelet derived growth factor receptor-α

PDI Polydispersity index

PDMS Poly(dimethylsiloxane)

PFA Paraformaldehyde

PLL Poly-L-lysine

PLP Proteolipid protein

PNS Peripheral Nervous System

qRT-PCR Quantitative real time Polymerase Chain Reaction

RT Room temperature

ROCK Rho-associated protein kinase

SD Standard deviation

SEM Scanning Electron Microscopy

TCPS Tissue culture polystyrene

TE Tissue engineering

TMC Trimethylene carbonate

UV Ultraviolet

List of Figures

List of Tables

- This page was intentionally left blank. -

Abstract

Myelin is an insulating layer or sheath that forms around nerves, that is constituted by protein and fatty substances. In the central nervous system (CNS), this structure is produced by oligodendrocytes that extend their plasma membrane and enwrap neurons in a tightly organized way, forming an electrically insulating layer. Consequently, myelin is a fundamental player in the process of electric impulse conduction along the axons and is also involved in the crosstalk between axons and oligodendrocytes. One of the major mechanisms responsible for the loss of function observed in several neurological diseases is the loss of the myelin sheath. In the adult CNS, myelin loss can only be partially rescued by remyelination of spared axons. The newly formed myelin is not made by oligodendrocytes surviving an episode of demyelination, but from oligodendrocyte progenitor cells (OPCs), which become activated, proliferate and give rise to remyelinating oligodendrocytes. However, after disease progression, remyelination fails, leading to irreversible functional failure.

Under the context of demyelinating conditions, other glial cells are also severely affected, namely astrocytes. These cells switch their phenotype and become activated, hence playing a pivotal role in the modulation of the CNS extracellular environment. In this context, a glial scar, mainly composed by reactive astrocytes that secrete altered signalling molecules (as growth factors, cytokines, and ECM constituents) may have profound impacts in demyelinating diseases.

However, so far, little is known about the effects of reactive astrocytes on the process of remyelination, in particular in terms of astrocyte activation impact on OPC recruitment to the lesion site and differentiation to a mature state. The lack of knowledge on demyelinating diseases provides from the lack of screening platforms that allow the study of the specific influence of neural and glial cells in the progression of these diseases.

Here, a 3D *in vitro* myelination platform composed of electrospinning polymeric (poly(trimethylene carbonate-co-ε-caprolactone) copolymer, P(TMC-CL)) nanofibers combined with a tissue engineered glial scar model of astrocytes embedded in alginate matrices is explored. This platform was previously established by our group therefore, this project aimed to deepen the study of the influence of activated astrocytes on OPC differentiation and myelination capacity.
Besides, a novel *in vitro* platform based on poly(dimethylsiloxane) (PDMS) pillars to allow the study of myelination and wrapping of oligodendrocytes around pillars is also here described.

OPCs were found to extensively adhere, proliferate and differentiate in oligodendrocytes without the need of any coating base on a cell adhesion molecule, highlighting the possibility of uncoupling the axons effects' on the study of astrocyte-oligodendrocyte crosstalk. Moreover, astrocytes were shown to remain viable within the alginate matrices and become activated after three days of culturing with meningeal fibroblasts conditioned medium. When activated astrocytes were co-cultured with OPCs in fibers, the differentiation ability of OPCs in oligodendrocytes (assessed in terms of myelin basic protein gene expression) was significantly impaired after 5 days of culture, showing a potential negative role of the astrogliosis in the course of a demyelinating disease.

Moreover, OPCs were also found to adhere, proliferate and differentiate in oligodendrocytes in a reproducible manner when cultured on PDMS micropillars. Importantly, oligodendrocytes have shown a vast propensity to wrap micropillars at early stages of differentiation (day 3). Nonetheless, detailed conclusions could not be taken regarding the process of oligodendrocyte wrapping, as these studies are still in their infancy.

Overall, the work presented in this thesis highlights the importance exploring *in vitro* platforms that can serve as a tool to dissect myelination processes or the crosstalk between neural cell types. In the future, this may be of added value in the search for new therapeutical molecules and targets to demyelinating diseases.

Key words: oligodendrocytes, myelin, astrogliosis, tissue engineering, high throughput screening platforms, electrospinning, poly(trimethylene carbonate-co-ε-caprolactone), alginate, poly(dimethylsiloxane) micropillars

CHAPTER 1

GENERAL INTRODUCTION

- This page was intentionally left blank. -

OVERVIEW OF DEMYELINATING DISEASES

Myelin is an insulating layer, or sheath that forms around nerves, including those in the central and peripheral nervous system, being constituted by protein and fatty substances. Myelin is essential for the correct function of the nervous system, so that myelin loss is one of the major mechanisms responsible for several neurodegenerative diseases. The concept of demyelination refers to pathologies in which myelin loss occurs before axonal degeneration and atrophy [1].

There are several central nervous system (CNS) demyelinating diseases and their origin is very diversified: genetic defects, inflammatory processes and acquired metabolic derangements are examples of demyelinating diseases' causes [1].

Multiple sclerosis (MS), which is an inflammatory mediated demyelinating disease, is considered nowadays one of the most common causes of incapacity in young adults, especially in Europe and North America. It is estimated that this disease affects around 2.5 million people worldwide (89.3 per 100,000 people – MS Society client data [2]). Moreover, statistics point out that women are more affected than men (three in four patients are women) and that the peak of appearance of the disease is at 30 years old. MS has a profound impact on patients' social life. As the disease progresses, physical disabilities such as fatigue, depression and cognitive impairments are observed among MS patients. Recent data predicts an increase of the prevalence of the disease in the next years. In addition to its huge social significance, MS's associated economic impact is also high. Yearly costs are estimated to be 49,000 US dollars per patient (2010), which arise essentially from indirect costs rather from direct costs (prescription medications) once people with MS are not able to perform professional activities [2].

To achieve a possible treatment to demyelinating diseases some strategies have been tried. For instance, for MS, plasma exchange to act on severe relapses has been proposed as a short term therapy [3]. Interestingly, having a specific nutritional plan composed of anti-inflammatory nutrients (omega-6 and omega-3), dietary polyphenols [4] and vitamins like vitamin D [5] can minimize the progress and comorbidities of this disease. Besides, over the last decades, the scientific and pharmacological community have been trying to induce immunosuppression either through cytotoxic drugs to induce immune cells' apoptosis or bone marrow transplantation to substitute immune cells and extinguish the autoimmune ones [6] but the results obtained with these therapies are far from being optimal. Like for MS, other approaches have been searched for other CNS demyelinating diseases, such as acute disseminated encephalomyelitis, Krabbe's disease, Alexander disease or Contusion type-spinal injury. However, currently, there is not an established and valuable treatment to these diseases.

In fact, one of the reasons behind the inexistence of efficient therapies against demyelinating diseases arises from the lack of knowledge of the biological and biochemical mechanisms underlying these diseases. In order to understand these diseases it is very important to understand first the basic biology of the nervous system, the mechanism behind the pathological condition and how the degeneration and possible regeneration occurs.

DEGENERATION AND REGENERATION IN THE CENTRAL NERVOUS SYSTEM

Components of the nervous system

The nervous system comprises the CNS, which is constituted by the brain and the spinal cord, and the peripheral nervous system (PNS), including the peripheral nerves (bundles of axons) responsible for connecting the CNS to the rest of the body. Neurons are the cells that define the nervous system. Their major function is to send electrochemical synaptic signals through axons that may inhibit, stimulate or modulate the receiving cells. The neuronal network within the body determines individual's behaviours [7].

Nonetheless, neurons would not be able to perform their main functions if supporting cells did not exist. The maintenance of the nervous system is conducted by a specialized type of cells known as glial cells. The term "glia" arises from the Greek and means "glue", thus glial cells are seen as the glue that holds the nervous system together. In the PNS, these supporting cells are the Schwann cells and satellite cells and in the CNS are the astrocytes, oligodendrocytes, microglia and ependymal cells [8].

Astrocytes constitute approximately 90% of the cells of the brain and are responsible for numerous processes that are known to be pivotal to CNS homeostasis. Generally, astrocytes are responsible to maintain the appropriate chemical environment for the signalling between neurons by the regulating the ion and pH of the microenvironment and also by clearing neuronal debris. Besides, astrocytes allow the survival of neurons and of the other glial cells by releasing neuronal surviving factors [9]. Moreover, astrocytes are determinant in modulating the integrity of the blood brain barrier (BBB), which is a selective physical barrier that separates the CNS parenchyma from the circulating blood. This is especially important during inflammation as astrocytes alter the permeability of the BBB therefore allowing the influx of immune cells and other components to the CNS [9].

On the other hand, microglia are of hematopoietic origin and their activities are very often connected to macrophage functions. These cells are capable of removing cellular debris from sites of normal cell turnover or injury, fact that explains why microglia are seen as the CNS resident macrophages [8].

Ependymal cells line the cerebral spinal fluid-filled ventricles in the brain and the central canal of the spinal cord [10].

Lastly, oligodendrocytes are the myelin producing cells of the CNS. These cells establish a tight crosstalk with axons which is fundamental for correct metabolic function and transport, ion channel organization and cytoskeletal arrangement [11].

Myelin is an electric insulator and protective sheath that surrounds some, but not all axons in a spiral way. In the PNS, the myelin sheath is produced by the Schwann cells [12] that in opposite to oligodendrocytes, can just myelinate one single axon (**Figure 1.1**) [13].

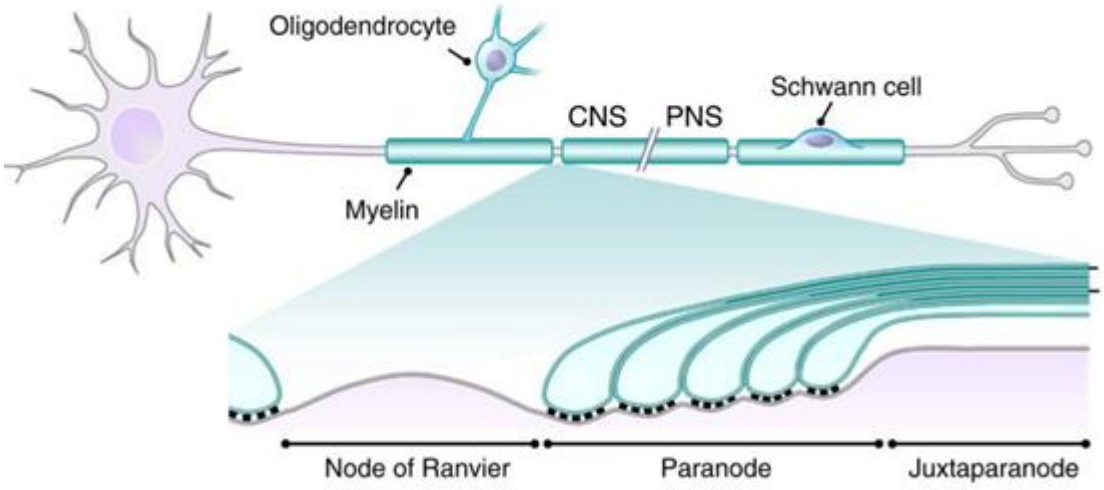

Figure 1.1 *Structure of myelinated axons.* In the CNS, oligodendrocytes produce myelin that tightly enwrap neurons, and one oligodendrocyte can myelinate several neurons. Myelin segments are separated from each other through nodes of Ranvier that optimize the saltatory electric conduction characteristic of these neurons. In the PNS, Schwann cells myelinate neurons. However, one Schwann cell only enwraps one neuron. Adapted from Chang *et al* (2015) [14].

The presence of myelin in axons enables the efficient propagation of the electrical signal through saltatory conduction in gaps, called Ranvier nodes [13]. In the CNS, Ranvier nodes directly contact with perinodal astrocytes and their extremes are flanked by paranodes followed by adjacent juxtaparanodes. Myelin segments are delimitated by internodes and together these structures contribute to the complexity and highly organization seen in a myelinated axon (**Figure 1.1**) [15]. The effective saltatory conduction is also established because of the increased resistance and diminished capacitance of the axons [13].

In the mammalian CNS, the myelin membrane is a lipid bilayer in which proteins are embedded or attached to the surface by weak bounds in an asymmetrically way. The high percentage of lipids (70-85%) relatively to the low percentage of proteins (15-30%) is one of the unique characteristics that differs the myelin membrane from other biological membranes. Although there is no lipid that characterizes the myelin membrane, the most common is galactocerebroside (galactosyl ceramide), which is, in fact, used to estimate the proportion of the existent myelin in the brain. Besides, cholesterol and phospholipids are other major lipids constituting the CNS myelin sheath [16]. In spite of being in lower percentage in the brain, myelin's proteins are crucial to maintain axonal functionality. The most abundant are the myelin basic protein (MBP) and proteolipid protein (PLP), which account for 60-80% of the total protein in most species and play fundamental roles in axonal myelination [17, 18]. Moreover, myelin associated glycoprotein (MAG) is crucial for the induction of myelin production [19] and the enzyme CNPase (2,3-cyclic nucleotide 3-phosphodiesterase) produced in mature

oligodendrocytes is also crucial for the homeostasis of axons once its deletion provokes swollen and further degeneration of myelinated neurons [11, 20].

Apart from cells, the nervous system is also constituted by extracellular matrix (ECM) components. Although in the brain the ECM comprises only 20% of its total volume [21], the ECM is crucial to assure the proper brain tissue architecture. It is mainly composed by proteoglycans of the lectican/hyalectan family and their binding molecules, glicosaminoglycans like heparin sulphate or hyaluronic acid, and other proteins as tenascins [22]. Lecticans are components responsible for the primary organization of the brain and they are included in the chondroitin sulphate proteoglycans (CSPGs) family [23]. Tenascins are glycoproteins capable of connecting proteoglycans and act as binding sites for cells. Hyaluronan is a glycosaminoglycan that plays an important role in brain due to its negatively charged nature enabling the attaching of positive ions (for instance, sodium) and charged proteins. This effect strongly increases brains' hydration [21]. Collagen, namely collagen type I and collagen IV are also present as well as laminin which together with collagen IV are responsible for basal lamina composition [24].

Specific mechanisms involved in degeneration and regeneration in the nervous system

When an insult that causes the death of oligodendrocytes or Schwann cells occurs, myelin normal function is extensively disturbed. Demyelination and further axonal degeneration and dysfunction drastically affect the homeostasis of CNS. Conversely, in the PNS the effects are not so adverse since Schwann cells just myelinate one single axon. Hence, the loss of Schwann cells has a lesser impact on the extent of the axonal degeneration process. Furthermore, in the PNS, the response to an insult is more effective than in the CNS. Resident macrophages are rapidly recruited to the local of the lesion by factors secreted by Schwann cells and injured neurons. Myelin and axonal debris is efficiently cleaned and macrophages in turn also secrete factors that are beneficial for Schwann cell migration and axonal regeneration (see reference [25] for a review).

In contrast, in the CNS the effects of demyelination can have very adverse outcomes. Once demyelination occurs, the lesion site is characterized by the presence of myelin debris [26] whose clearance is achieved by microglia [11] that if efficient, contributes to the permissive environment for remyelination. To achieve regeneration, the mature oligodendrocytes in the proximity of the lesion that have survived are not able to enwrap neurons and overcome the damages due to their post-mitotic status, however they can extend some processes [27]. On the other hand, endogenous non-committed stem cell populations, oligodendrocyte precursor cells (OPCs) and neural progenitor cells (NPCs), respond to products released by activated glia and actively express genes related to their mature state (OPCs express Olig2 and Nkx2.2, for example [28]). In general, in the early stages of demyelinated diseases remyelination is

well succeeded once some oligodendrocytes mature from OPCs and spontaneously remyelinate axons [29]. This event leads to a partial recovery of the disability characteristic that identifies, for example, MS as a relapsing and remitting disease. The interval between relapses vary among patients and can be many years [1]. Nonetheless, at some point and as the disease progresses the extent of this differentiating phenomena is not sufficient, thus remyelination is not efficiently achieved. Several studies have been conducted to understand why the process of remyelination is not well succeeded. Some hypothesis are that the new oligodendrocytes also suffer injury with the same extent of the previous ones [11]; the source of OPC is not producing enough cells to provide an effective remyelination [30]; or the inhibitory environment of the lesion inhibits the differentiation [26]. The last hypothesis, formulated by Robin Franklin has been widely supported among the scientific community [26, 31].

As soon as demyelination happens resident astrocytes are the first cells to be recruited to lesion sites [32]. Astrocytes become reactive, upregulating the expression of intermediate glial fibrillary acidic protein (GFAP) and vimentin, among other genes, in a process referred as astrogliosis [33]. In this process reactive astrocytes induce modifications in the ECM by secreting some ECM molecules like laminin, fibronectin and tenascin-C. It has been reported through animal model-based studies that ECM composition changes during demyelination [24]. For example, in MS collagen type IV, laminin and heparin sulphate proteoglycans are overexpressed and this influences the stiffness of the ECM. Also, fibronectin is abnormally expressed, fact that is related with the degree of inflammation once macrophages respond to this protein migrating to the site of injury [34, 35]. Tenascins are other crucial ECM molecules for myelination. They have a key role in the maintenance of the structural stability as well as in oligodendrocytes' functionality (by influencing their survival, proliferation, differentiation and migration). Together, the abnormal deposition of these molecules creates an inhibitory environment to regeneration, which is synonym of progressive neuronal degeneration. The expression ratio between inhibitory molecules and supportive molecules dictates the progress of demyelination or remyelination [24]. Besides, it is worth noting that the inefficient clearance of myelin debris by microglia also induces some modifications in the ECM composition [36] that also contribute to the progression of demyelinating diseases.

In the majority of the cases, all these factors (ECM modifications, astrogliosis, accumulation of myelin debris and degenerated neurons) contribute to the possible formation of a glial scar [11]. Glial scar is a neuroprotective mechanism that CNS uses to avoid the invasion of inflammatory cells or pathogens into surrounding normal tissue as a consequence of BBB disruption. Consequently, glial scar acts on the closure of BBB, thus avoiding a devastating inflammatory response [37]. Besides, glial scar is of great importance to the revascularization of the site of injury [24]. Nonetheless, in spite of being initially a protective mechanism, as the disease progresses the glial scar is seen as a barrier to the regeneration and this changed environment can prevail for long term or even forever [38]. The scar is mainly composed of hypertrophic reactive astrocytes, meningeal fibroblasts and collagenous ECM. Some myelin

debris' characteristic proteins (for example, MAG and oligodendrocyte-myelin glycoprotein) [39] and increased levels of CSPGs and semaphorins can also be found in the glial scar [24]. All the above-mentioned features happening within the lesion site (myelin debris, the presence of astrocytes, the glial scar and the inhibitory proteins) contribute to the failure of regeneration. Ultimately, the balance between demyelination and remyelination, as well as axonal degeneration/regeneration regulates the outcome of the neurodegenerative diseases.

MODELS TO STUDY THE BIOLOGICAL FUNDAMENTALS OF DEMYELINATING DISEASES

The difficulty in reaching efficient therapies against demyelinating diseases in a significant part arises from the lack of knowledge on the biology and the pathogenesis of these diseases [40]. Despite all of the advances in the field, yet there is no model capable of truly recapitulating demyelination processes.

Animal models of demyelination

Traditionally animals such as mice or rat are considered the gold standard models to mimic diseases. In fact, the majority of the actual therapies for MS have arisen from tests in these animals For this demyelinating disease, three categories of animal models are now well established and include the toxin-induced models (for example, the cuprizone model, in which oligodendrocytes rapidly die after the administration of cuprizone, and after removing it, myelination occurs again), the viral-induced models (for example, the Theiler's murine encephalomyelitis virus (TMEV) infection results in the generation of myelin-specific T cells which leads to a progressive disease course) and the autoimmune models (model of experimental autoimmune encephalomyelitis, EAE, in which mice are immunized with myelin antigens or pre-activated myelin specific T cells, both infiltrating the CNS causing pathologies in mice similar to MS in humans [41]) [42].

However, with these models it is hard to isolate distinct features of diseases and correctly interpret and extrapolate them to human conditions. In fact, there have been a crescent number of clinical trial failures over the years. High associated costs with animal research and all the ethical issues it can raise are other factors that highlight the necessity for changing the way science in the demyelination field has been conducted [43]. For that reason, researchers have been focusing their studies on more human-relevant models, and there has been a specifically growing tendency to establish *in vitro* models.

In vitro models of demyelination

In vitro models of disease are simplified systems in which distinct features of a certain disease are mimicked. Despite not being possible to fully translate disease complexity within such platforms, these models are simple and a suitable source of knowledge on specific biochemical and morphological mechanisms observed *in vivo*, hence, allowing the study of individual variables, which may not be achievable in an animal model.

In *in vitro* cellular models the biologic pathological environment is mimicked as far as possible with the aim of studying a signalling pathway [44], specific biomarkers [45], among others.

Cellular platforms of demyelinating diseases are either 2D or 3D. These cell culture systems are very diverse, including monocultures, co-cultures, neuronal organoids, organotypic cultures or tissue explants. Monocultures are the simplest and easiest way to culture cells and are of extreme importance to study cell specific behaviours' and mechanisms'. Numerous studies using only oligodendrocytes revealed important mechanisms these cells are responsible for [46]. However, this type of culture is not able to reproduce interactions between different cell types. Cellular crosstalk is known to play an important role in tissue homeostasis and to influence several processes including (de)myelination. Consequently, more complex models, that include additional cells types, provide more physiologically relevant models to study cellular mechanisms [47]. Besides, neuronal cellular platforms can be originated from different sources namely, primary cultures, cell lines or neuronal derived pluripotent stem cells (human or non-human). Nonetheless, independently of their source, the used neural cells in culture should accomplish a series of parameters, such as, show the appropriate cell morphology and behaviour, express the genes that are expressed *in vivo* and translate functional proteins [21].

Two-dimensional (2D) cell-based platforms

Over the years, *in vitro* cell models were usually achieved using flat glass coverslips or tissue culture polystyrene (TCPS) flasks. CNS neural cells can be easily and reliably cultured on these 2D surfaces, normally requiring the use of coating with molecules capable of promoting cell adhesion (namely, poly-L-lysine – PLL – or laminin) [21, 48]. 2D models are easy to manipulate and very reproducible, making them adequate to maintain cells in culture and achieve results on neurobiological processes. Nevertheless, it is now well known that TCPS or glass substrates offer cells a very different mechanical environment in comparison to the one experienced in physiological conditions *in vivo*. Besides, the surface topographies of these substrate do not resemble the *in vivo* as well and mammalian cells were shown to respond differently to different nanotopography substrates, either in terms of morphology features or even differentiation abilities [49]. For that reason, it has been developed some more physiological relevant *in vitro* assays using 2D materials that can better achieve *in vivo* mechanical properties.

In terms of 2D cultures, in the last two decades, the use of microfluidic platforms allowed the introduction of new features that allowed the achievement of more physiological systems to study neurobiology. Microfluidics is a technology in which fluids are controlled and manipulated at the sub-millimetre scale in engineered devices [50]. This technique has been proving the ability to precise control cells' microenvironment and to mimic molecular gradients that are found in the majority of tissues. Firstly, microfluidics chambers were used to force the physical isolation of axons from each other and from their cell bodies, however now some devices for neurons co-cultures have been produced in 2D microenvironments [51-53]. Microfluidics introduced an easy and feasible way of studying neurobiology once cell microenvironment is

well controlled and molecular and cellular interactions can be both achieved with this methodology. Examples of microfluidics platforms are represented in **Figure 1.2**.

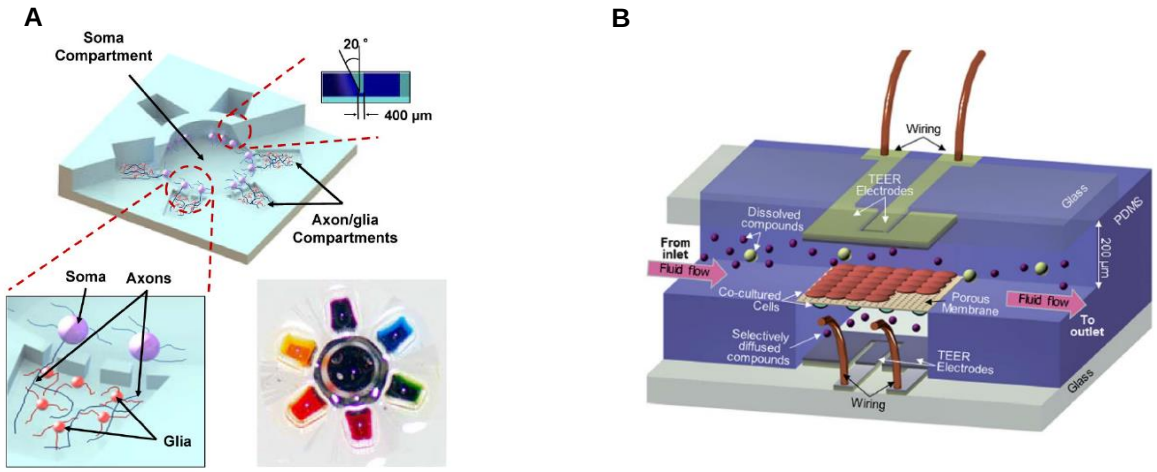

Figure 1.2 *Example of microfluidic devices used in studies of neurobiology.* **A)** Device where both OPCs and axons were grown. It is shown the six compartments that are capable of conducting multiple treatments at the same time. Adapted from Park, J., *et al* (2012) [53] **B)** Microfluidic system to mimic BBB. Cells are co-cultured in the middle of the device in a porous membrane and the fluid flows in parallel. Adapted from Booth, R., *et al* (2012) [54].

Three-dimensional (3D) cell-based platforms

Although 2D models present evident benefits for neurodegenerative disease studies due to the precise control of individual components of a system, the complexity of neural tissue arising from the three-dimensionality is not correctly reproduced when using this type of platforms. To approach this complexity, an ideal culture requires a 3D matrix to better mimic the natural cell-cell and cell-ECM interactions, as well as biochemical gradients [55]. By comparing 2D and 3D cell culture architectures several authors observed significant differences in cell behaviour, suggesting that cells behave more closely to those *in vivo* in the latter conditions. For that reason, many consider data obtained from 3D cultures more biologically relevant [56].

In these substrata, neuronal cells may grow in more adequate densities than the ones reached in the 2D models. In most of the cases, this is crucial to replicate neuronal architectures [21]. 3D microenvironments can be designed to protect cells from external perturbations like media changes, thus cells present higher stability and survival rates. Besides, these substrata can also be thought in terms of optimal permeability for nutrients and waste, therefore resembling closer the neuronal tissue permeability [57].

Nowadays, there are several ways of obtaining 3D reliable architectures. Explants, neural organoids or tissue engineering (TE) based platforms are some examples. Neural tissue

derived explants are brain/spinal cord derived tissue slices in which cells and the architecture of the tissue is fully preserved [58]. They have the advantage of being cultured for a long periods of time. However, in this type of model it is impossible to modify cellular composition, thus, it is crucial to choose a region with distinctive characteristics of myelination and remyelination. In neuronal organoids cells are grown as spherical cell clusters at a microscale level. There are many ways of producing these clusters, namely using the hanging drop technique or microwells [59]. TE approaches to mimic diseases are becoming widely popular among the scientific community. The conventional TE paradigm relies on using scaffolds combined with cells to create an engineered tissue graft that may be used to repair or regenerate a lesion site. More recently, these TE grafts are being explored as *in vitro* disease models. In this case, the engineered construct is used to study biological issues of diseases, find new therapeutic targets, test new drug candidates, as well as study cell-drugs interaction, neuronal networks formation and combined effects [60]. One can develop these platforms using bottom-up or top-down approaches. In a bottom-up process the matrix is the first component being designed. After, cells and growth factors or other biochemical components are added in a space-time controlled manner. On the other hand, in top-down approaches cells are embedded in a substratum and form their adequate ECM by spontaneously degradation and reconstruction of the substratum [21]. With a 3D TE platform, taking conclusions about cells' behaviour is easier as this complexity simulates more the *in vivo* situation [60]. Besides, TE platforms allow the study of several cues that can be presented in different ways, namely synergistically or competitively which enables the study of their importance [60]. TE platforms can be created in many ways. For instance, polymeric substrates are commonly used as neuronal platforms. An ideal polymer for neuronal cell culture must meet features as a low elastic modulus to resemble brain's elastic modulus, porous structure to enable the diffusion of gases and nutrients and an appropriate electrical conductance to facilitate electric signalling between neurons. Besides, they should allow cell growth and facilitate characterization of cell behaviour [21]. Hydrogels are a class of polymer networks that met many of the above-mentioned characteristics. They can be tuned to replicate the CNS ECM in terms of physicochemical properties [61]. Besides, they present adequate mechanical properties (low elastic modulus and similar and adjustable stiffness to neuronal tissue) and can be designed to promote the extension of axons [62]. In addition to hydrogels made of natural polymers or photopolymerized hydrogels, synthetic polymer scaffolds, self-assembling peptide scaffolds, micro- or nano- patterned substrates and also microgravity bioreactors are other possibilities for a neuronal reliable matrix [63].

In the past years, 3D bioprinting revealed to be a revolutionary technique providing valuable tools in constructing platforms to better understand tissue complex architectures. Bioprinting can be defined as a process of patterning cells, molecules and "non-living" materials aided by a computer program with the aim of creating structures to be used in the field of TE and

regenerative medicine [64]. Some, but not many studies have been published about bioprinting in neuronal TE [65].
To sum up, TE platforms are valuable tools to address *in vitro* features of *in vivo* mechanisms. Therefore they are beneficial concerning other types of possible models for the study of demyelinating diseases.

Figure 1.3 shows an example of a 3D *in vitro* model of myelination composed by a tubular scaffold with pores allowing the oligodendrocytes to grow.

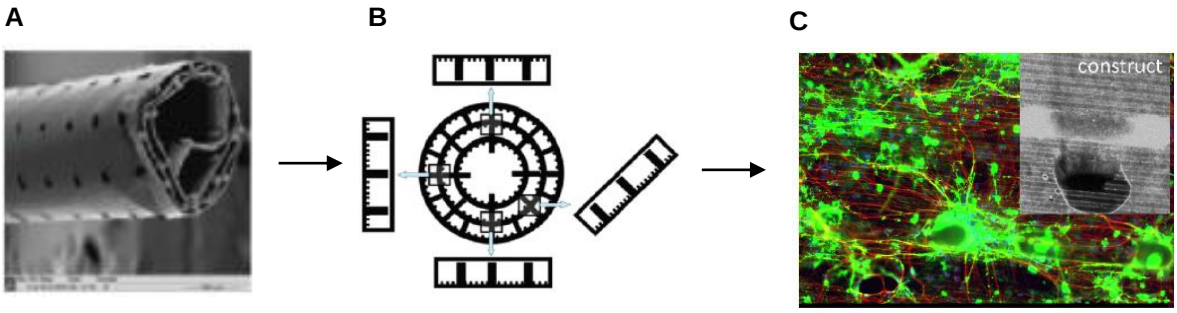

Figure 1.3 *Scheme of tubular scaffold used to simulate CNS myelination.* **A)** Image of Scan Electron Microscopy of the tubular construct. **B)** Representation of the interior of the scaffold and the various positions in which the scaffold was manipulated to conclude about cell distribution and survival. **C)** Myelination within the pores of the tubular scaffold. Adapted from Donoghue, P.S. (2014) [66].

High throughput models

High throughput screening (HTS) techniques rely on automated testing a large quantity of compounds against supposed targets of diseases with easy to access readouts. HTS has been widely used among researchers and also in pharmaceutical industry. Currently, HTS platforms enable the screenning of thousands of compounds. These methodologies have several advantages including the simplicity, speed, the high efficiency, the significant low costs and the vast number of results that it is possible to achieve. Fluorescence, chromatography, gene or protein microarrays, nuclear-magnetic resonance or surface plasmon resonance are examples of readout techniques [67].
HTS can be categorized in cellular and biochemical assays. While in a biochemical assay, interactions between proteins, proteases and enzymes are studied, in a cellular assay more complex systems and entire pathways are analysed. For that reason, cell based HST are advantageous for the screening of specific compounds for intercellular activities [68]. When thinking about nervous system it is important to highlight that HTS are hard to establish in these systems due to neurons intrinsic characteristics. These cells are post-mitotic, limited in supply and their extraction is difficult and costly. Despite this, there is a growing need to develop strategies that enable the screening of great amount of neurons in a costly safe way [69]. Not many reports using HTS for neuronal functions studies have been published and

concerning demyelinating diseases there are still few reliable reports. For further reading on high throughput platforms for studies of neurodegeneration and discovering of targets for demyelination see **Appendix A** that includes the review recently published by us on Drug Discovery Today (10th May 2016).

Taking all this into account, there is a growing need to develop platforms where the processes of demyelination and/or remyelination are replicated. These *in vitro* models where glial cells are put together to recreate a simple, yet valuable model, are becoming popular among researchers and may be one important way of concluding about the mysterious complexity of the nervous system in the context of a disease.

REFERENCES

1. Love, S., *Demyelinating diseases.* Journal of Clinical Pathology, 2006. **59**(11): p. 1151-1159.
2. Palmer, A.J., et al., *The economic impact of multiple sclerosis in Australia in 2010.* Mult Scler, 2013. **19**(12): p. 1640-6.
3. Keegan, M., et al., *Plasma exchange for severe attacks of CNS demyelination: predictors of response.* Neurology, 2002. **58**(1): p. 143-6.
4. Adamo, A.M., *Nutritional factors and aging in demyelinating diseases.* Genes & Nutrition, 2014. **9**(1): p. 360.
5. Smolders, J., et al., *Vitamin D as an immune modulator in multiple sclerosis, a review.* J Neuroimmunol, 2008. **194**(1-2): p. 7-17.
6. Rieckmann, P., et al., *Escalating Immunotherapy of Multiple Sclerosis.* Therapeutic Advances in Neurological Disorders, 2008. **1**(3): p. 181-192.
7. Tanaka, E.M. and P. Ferretti, *Considering the evolution of regeneration in the central nervous system.* Nat Rev Neurosci, 2009. **10**(10): p. 713-723.
8. Purves, D., et al., *Neuroscience 2nd Edition. Sunderland (MA) Sinauer Associates*. 2001, Inc.
9. Nair, A., T.J. Frederick, and S.D. Miller, *Astrocytes in Multiple Sclerosis: A Product of their Environment.* Cellular and molecular life sciences : CMLS, 2008. **65**(17): p. 2702-2720.
10. Jiménez, A.J., et al., *Structure and function of the ependymal barrier and diseases associated with ependyma disruption.* Tissue Barriers, 2014. **2**: p. e28426.
11. Alizadeh, A., S.M. Dyck, and S. Karimi-Abdolrezaee, *Myelin Damage and Repair in Pathologic CNS: Challenges and Prospects.* Frontiers in Molecular Neuroscience, 2015. **8**.
12. Nave, K.A. and B.D. Trapp, *Axon-glial signaling and the glial support of axon function.* Annu Rev Neurosci, 2008. **31**: p. 535-61.
13. Poliak, S. and E. Peles, *The local differentiation of myelinated axons at nodes of Ranvier.* Nat Rev Neurosci, 2003. **4**(12): p. 968-980.
14. Chang, K.-J., S.A. Redmond, and J.R. Chan, *Remodeling myelination: implications for mechanisms of neural plasticity.* Nat Neurosci, 2016. **19**(2): p. 190-197.
15. Abad-Rodriguez, J. and N. Diez-Revuelta, *Axon glycoprotein routing in nerve polarity, function, and repair.* Trends Biochem Sci, 2015. **40**(7): p. 385-96.
16. Morell P and Q. RH, *Characteristic Composition of Myelin*, in *Basic neurochemistry: Molecular, Cellular and Medical Aspects*, G.J. Siegel, et al., Editors. 1999: Philadelphia: Lippincott-Raven.
17. Griffiths, I., et al., *Axonal swellings and degeneration in mice lacking the major proteolipid of myelin.* Science, 1998. **280**(5369): p. 1610-3.
18. Boggs, J.M., *Myelin basic protein: a multifunctional protein.* Cell Mol Life Sci, 2006. **63**(17): p. 1945-61.
19. Biffiger, K., et al., *Severe hypomyelination of the murine CNS in the absence of myelin-associated glycoprotein and fyn tyrosine kinase.* J Neurosci, 2000. **20**(19): p. 7430-7.
20. Rittchen, S., et al., *Myelin repair in vivo is increased by targeting oligodendrocyte precursor cells with nanoparticles encapsulating leukaemia inhibitory factor (LIF).* Biomaterials, 2015. **56**: p. 78-85.
21. Hopkins, A.M., et al., *3D in vitro modeling of the central nervous system.* Progress in Neurobiology, 2015. **125**: p. 1-25.
22. Bonneh-Barkay, D. and C.A. Wiley, *Brain Extracellular Matrix in Neurodegeneration.* Brain pathology (Zurich, Switzerland), 2009. **19**(4): p. 573-585.
23. Zimmermann, D.R. and M.T. Dours-Zimmermann, *Extracellular matrix of the central nervous system: from neglect to challenge.* Histochem Cell Biol, 2008. **130**(4): p. 635-53.

24. Harlow, D.E. and W.B. Macklin, *Inhibitors of myelination: ECM changes, CSPGs and PTPs.* Exp Neurol, 2014. **251**: p. 39-46.
25. Gaudet, A.D., P.G. Popovich, and M.S. Ramer, *Wallerian degeneration: gaining perspective on inflammatory events after peripheral nerve injury.* Journal of Neuroinflammation, 2011. **8**: p. 110-110.
26. Kotter, M.R., et al., *Myelin impairs CNS remyelination by inhibiting oligodendrocyte precursor cell differentiation.* J Neurosci, 2006. **26**(1): p. 328-32.
27. Keirstead, H.S. and W.F. Blakemore, *Identification of post-mitotic oligodendrocytes incapable of remyelination within the demyelinated adult spinal cord.* J Neuropathol Exp Neurol, 1997. **56**(11): p. 1191-201.
28. Wegener, A., et al., *Gain of Olig2 function in oligodendrocyte progenitors promotes remyelination.* Brain, 2015. **138**(Pt 1): p. 120-35.
29. Hanafy, K.A. and J.A. Sloane, *Regulation of remyelination in multiple sclerosis.* FEBS Letters, 2011. **585**(23): p. 3821-3828.
30. Miron, V.E., T. Kuhlmann, and J.P. Antel, *Cells of the oligodendroglial lineage, myelination, and remyelination.* Biochimica et Biophysica Acta (BBA) - Molecular Basis of Disease, 2011. **1812**(2): p. 184-193.
31. Franklin, R., *Why does remyelination fail in multiple sclerosis?* Nature Reviews Neuroscience, 2002. **3**(9): p. 705-714.
32. Silver, J. and J.H. Miller, *Regeneration beyond the glial scar.* Nat Rev Neurosci, 2004. **5**(2): p. 146-56.
33. Eng, L.F. and R.S. Ghirnikar, *GFAP and astrogliosis.* Brain Pathol, 1994. **4**(3): p. 229-37.
34. Stoffels, J.M., et al., *Fibronectin aggregation in multiple sclerosis lesions impairs remyelination.* Brain, 2013. **136**(Pt 1): p. 116-31.
35. Zhao, C., et al., *Up-regulation of oligodendrocyte precursor cell alphaV integrin and its extracellular ligands during central nervous system remyelination.* J Neurosci Res, 2009. **87**(15): p. 3447-55.
36. Karimi-Abdolrezaee, S., et al., *Chondroitinase and growth factors enhance activation and oligodendrocyte differentiation of endogenous neural precursor cells after spinal cord injury.* PLoS One, 2012. **7**(5): p. e37589.
37. Kawano, H., et al., *Role of the lesion scar in the response to damage and repair of the central nervous system.* Cell and Tissue Research, 2012. **349**(1): p. 169-180.
38. Sofroniew, M.V. and H.V. Vinters, *Astrocytes: biology and pathology.* Acta Neuropathologica, 2010. **119**(1): p. 7-35.
39. Talbott, J.F., et al., *Endogenous Nkx2.2+/Olig2+ oligodendrocyte precursor cells fail to remyelinate the demyelinated adult rat spinal cord in the absence of astrocytes.* Exp Neurol, 2005. **192**(1): p. 11-24.
40. Hemmer, B. and H.P. Hartung, *Toward the development of rational therapies in multiple sclerosis: what is on the horizon?* Ann Neurol, 2007. **62**(4): p. 314-26.
41. McCarthy, D.P., M.H. Richards, and S.D. Miller, *Mouse Models of Multiple Sclerosis: Experimental Autoimmune Encephalomyelitis and Theiler's Virus-Induced Demyelinating Disease.* Methods in molecular biology (Clifton, N.J.), 2012. **900**: p. 381-401.
42. Mayo, L., F.J. Quintana, and H.L. Weiner, *The Innate Immune System in Demyelinating Disease.* Immunological Reviews, 2012. **248**(1): p. 170-187.
43. Jakel, R.J., B.L. Schneider, and C.N. Svendsen, *Using human neural stem cells to model neurological disease.* Nat Rev Genet, 2004. **5**(2): p. 136-44.
44. Seyb, K.I., et al., *Identification of Small Molecule Inhibitors of beta-Amyloid Cytotoxicity Through a Cell-based High-Thourhput Screening Platform.* J Biomol Screening, 2009. **13**(9): p. 870-878.
45. Guodong Li, W.Z., Huazong Zeng, Lei Chen, Wenjing Wang, Jilong Liu, Zhiyu Zhang Nad Zhengdong Cai, *An integrative multi-platform analysis for discovering biomarkers of osteosarcoma.* BMC Cancer, 2009. **9**.
46. Sharma, K., et al., *Involvement of MeCP2 in Regulation of Myelin-Related Gene Expression in Cultured Rat Oligodendrocytes.* J Mol Neurosci, 2015. **57**(2): p. 176-84.

47. Kipp, M., et al., *Experimental in vivo and in vitro models of multiple sclerosis: EAE and beyond.* Multiple Sclerosis and Related Disorders, 2012. **1**(1): p. 15-28.
48. Eide, L. and C.T. McMurray, *Culture of adult mouse neurons.* Biotechniques, 2005. **38**(1): p. 99-104.
49. Yim, E.K.F., et al., *Nanotopography-induced changes in focal adhesions, cytoskeletal organization, and mechanical properties of human mesenchymal stem cells.* Biomaterials, 2010. **31**(6): p. 1299-1306.
50. Sackmann, E.K., A.L. Fulton, and D.J. Beebe, *The present and future role of microfluidics in biomedical research.* Nature, 2014. **507**(7491): p. 181-189.
51. Majumdar, D., et al., *Co-culture of neurons and glia in a novel microfluidic platform.* J Neurosci Methods, 2011. **196**(1): p. 38-44.
52. Park, J., et al., *A multi-compartment CNS neuron-glia Co-culture microfluidic platform.* J Vis Exp, 2009(31).
53. Park, J., et al., *Multi-compartment neuron-glia co-culture platform for localized CNS axon-glia interaction study.* Lab Chip, 2012. **12**(18): p. 3296-304.
54. Booth, R. and H. Kim, *Characterization of a microfluidic in vitro model of the blood-brain barrier (muBBB).* Lab Chip, 2012. **12**(10): p. 1784-92.
55. Paivalainen, S., et al., *Myelination in mouse dorsal root ganglion/Schwann cell cocultures.* Mol Cell Neurosci, 2008. **37**(3): p. 568-78.
56. Edmondson, R., et al., *Three-Dimensional Cell Culture Systems and Their Applications in Drug Discovery and Cell-Based Biosensors.* Assay and Drug Development Technologies, 2014. **12**(4): p. 207-218.
57. LaPlaca, M.C., et al., *Three-dimensional neuronal cultures.* Methods in bioengineering: 3D tissue engineering Norwood, MA: Artech House 2010: p. 187-204.
58. Lancaster, M.A., et al., *Cerebral organoids model human brain development and microcephaly.* Nature, 2013. **501**(7467): p. 373-9.
59. Mori, H., et al., *Effect of neurosphere size on the growth rate of human neural stem/progenitor cells.* J Neurosci Res, 2006. **84**(8): p. 1682-91.
60. Li, G.N. and D. Hoffman-Kim, *Tissue-engineered platforms of axon guidance.* Tissue Eng Part B Rev, 2008. **14**(1): p. 33-51.
61. Tam, R.Y., et al., *Regenerative Therapies for Central Nervous System Diseases: a Biomaterials Approach.* Neuropsychopharmacology, 2014. **39**(1): p. 169-188.
62. McMurtrey, R.J., *Patterned and functionalized nanofiber scaffolds in three-dimensional hydrogel constructs enhance neurite outgrowth and directional control.* J Neural Eng, 2014. **11**(6): p. 066009.
63. Lai, Y., K. Cheng, and W. Kisaalita, *Three Dimensional Neuronal Cell Cultures More Accurately Model Voltage Gated Calcium Channel Functionality in Freshly Dissected Nerve Tissue.* PLoS ONE, 2012. **7**(9): p. e45074.
64. Dababneh, A.B. and I.T. Ozbolat, *Bioprinting Technology: A Current State-of-the-Art Review.* Journal of Manufacturing Science and Engineering, 2014. **136**(6): p. 061016.
65. Lee, W., et al., *Three-dimensional bioprinting of rat embryonic neural cells.* Neuroreport, 2009. **20**(8): p. 798-803.
66. Donoghue, P.S., et al., *Development of a novel 3D culture system for screening features of a complex implantable device for CNS repair.* Mol Pharm, 2014. **11**(7): p. 2143-50.
67. Liu, B., S. Li, and J. Hu, *Technological advances in high-throughput screening.* Am J Pharmacogenomics, 2004. **4**(4): p. 263-76.
68. Macarron, R., et al., *Impact of high-throughput screening in biomedical research.* Nat Rev Drug Discov, 2011. **10**(3): p. 188-195.
69. Gordon, K.R., et al., *Magnetic Alignment of Microelements Containing Cultured Neuronal Networks for High-Throughput Screening.* J Biomol Screen, 2015. **20**(9): p. 1091-100.

CHAPTER 2

AIM OF THE THESIS

- This page was intentionally left blank. -

During development astrocytes and oligodendrocytes communicate so that myelination can occur in an accurate and timely manner [1, 2]. Under the context of demyelinating conditions, astrocytes are also severely affected, playing a pivotal role in the modulation of the CNS extracellular environment. Nonetheless, so far, little is known about the effects of reactive astrocytes on the process of remyelination. In particular in terms of astrocyte activation impact on OPC recruitment to the lesion site and differentiation to a mature state.

Our group has previously studied the effects of astrogliosis on OPC differentiation ability and concluded that the activation of astrocytes impairs the differentiation of the OPCs and the recovery of astrocyte phenotype to non-reactive was seen to recover OPC differentiation ability in astrocyte-OPC co-cultures [3]. These conclusions were taken by using an *in vitro* rapid myelinating artificial axon system composed of electrospinning polymeric (poly(trimethylene carbonate-co-ε-caprolactone) copolymer, P(TMC-CL)) nanofibers [4] combined with a tissue engineered glial scar model of astrocytes embedded in alginate matrices [5]. However, detailed quantification of OPC protein/gene expression after exposition to reactive astrocytes was not performed. Beyond, although this platform provides valuable tools to study dynamics occurring during demyelination, it does not allow the monitorization of myelin wrapping around the fibers. Consequently, the major two aims of the proposed thesis were:

1. the exploration of the established *in vitro* rapid myelinating artificial axon system to deepen the study of the crosstalk between OPCs and astrocytes, particularly exploring the influence of the latter on OPCs differentiation and myelination ability;
2. the development of a new 3D platform based on poly(dimethylsiloxane) (PDMS) pillars to allow the study of myelination and wrapping of oligodendrocytes around pillars.

The work developed and the data obtained during the thesis is described in **Chapter 3** and **Chapter 4**, respectively.

REFERENCES

1. Sorensen, A., et al., *Astrocytes, but not olfactory ensheathing cells or Schwann cells, promote myelination of CNS axons in vitro.* Glia, 2008. **56**(7): p. 750-63.
2. Ishibashi, T., et al., *Astrocytes promote myelination in response to electrical impulses.* Neuron, 2006. **49**(6): p. 823-32.
3. Rocha, D.N., *Impact of Mechanotrasduction in the Context of Central Nervous System Diseases (Unplublished doctoral thesis)*. 2015, University of Porto: Portugal.
4. Pires, L.R., et al., *Ibuprofen-loaded poly(trimethylene carbonate-co-epsilon-caprolactone) electrospun fibres for nerve regeneration.* J Tissue Eng Regen Med, 2013.
5. Rocha, D.N., et al., *Extracellular Environment Contribution to Astrogliosis – Lessons learned from a Tissue Engineered 3D Model of the Glial Scar.* Front. Cell. Neurosci., 2015. **9:377**.

- This page was intentionally left blank. -

CHAPTER 3

IN VITRO RAPID MYELINATION PLATFORM TO STUDY OLIGODENDROCYTE-ASTROCYTE CROSSTALK

- This page was intentionally left blank. -

INTRODUCTION

The process of CNS myelination is complex and the mechanisms responsible for chronic remyelination failure have not yet been fully explained. Nevertheless, over the past years, it has been observed the presence of both OPCs and post-mitotic oligodendrocytes in lesion sites in sufficient number [1]. The apparent contradiction between the existence of OPCs and oligodendrocytes in the lesion sites and the failure of remyelination has been widely discussed among scientific community [2]. It is believed that on the one hand the resident surviving oligodendrocytes cannot rearrange their compact myelin sheath and form new myelin due to the lack of expression of the early progenitor markers. On the other hand, recruited OPCs do not remyelinate normally; although myelin composition is similar to developmental myelin, its size is thinner and shorter in comparison to the axonal diameter [2]. These facts clearly suggest the existence of a regulatory mechanism inhibiting OPC differentiation under pathological scenarios.

The existence of some inhibitors within the demyelinated lesion has been proposed and so far, several signalling pathways have been identified as mediators of OPC differentiation. Within those signalling pathways, the ones that actively induce modifications in the cytoskeleton are of special interest. Namely, the Rho/ROCK signalling pathway has been widely emphasized as a major mediator of OPC differentiation and maturation [3-5].

The Rho family of GTPases is a subfamily of the small GTPases Ras superfamily constituted by eight members, being RhoA the best studied and characterized. It is generally associated with cytoskeleton organization and regulation, integrin mediated signalling and migration controlling. Generally, the signalling through RhoA is initiated by a series of plasma membrane receptors like integrins that progressively activate the downstream receptors. After RhoA activation, it interacts with the downstream target protein ROCK (Rho-associated protein kinase), which in turns produces the cellular effects [6]. The possible involvement of Rho/ROCK signalling pathway in the OPC differentiation phenotype definition points out the important role of ECM molecules in the process of OPC remyelination after an insult.

As described in **Chapter 1**, the lesion microenvironment is characterized by the presence, among others, of astrocytes that switch their quiescent phenotype to an activated state thus creating a modified environment in which signalling molecules (as growth factors, cytokines, and ECM constituents) are altered [7-9]. The consequent formation of the glial scar is a barrier to neuronal regeneration and all these factors may also alter the course of OPC differentiation and remyelination of damaged areas [10-12].

Astrocytes and oligodendrocytes are known to intrinsically communicate during development and in the homeostasis CNS. However, if in pathological scenarios this crosstalk is affected is a theme still under debate and some contradictory studies have been published [13, 14]. In this project, it is hypothesized that the astrocyte activation is involved in the impairment of the normal course of OPC differentiation. Nevertheless, very little is known about the mechanisms that underlie astrocyte activation in the aftermath of a lesion. It has been previously shown by our group that the acquisition of the reactive state by astrocytes is influenced by matrix mechanical properties, being probably mediated via a mechanosensing pathway. The Rho/ROCK signalling was demonstrated as a possible mediator of this process, having RhoA a pivotal role in this process. Besides, the pharmacological inhibition of this pathway with ibuprofen showed to reduce the RhoA levels and therefore allowed the recovering of astrocytes to a quiescent phenotype [9].

In this work, a co-culture platform composed by a tissue engineered glial scar model and a rapid myelination axon system was used to dissect the interaction between astrocytes and oligodendrocytes in the context of an insult.

Tissue engineered glial scar model

In our group, Rocha *et al* [9] developed a 3D glial scar platform composed of astrocytes seeded within alginate gels and induced a lesion environment using meningeal fibroblasts conditioned medium to mimic the possible stimuli resultant from fibroblast infiltration that occurs in the follow up of an injury.

Alginate is a natural anionic polymer obtained from marine brown algae. Due to its favourable characteristics such as biodegradability, biocompatibility, low toxicity, low costs and mild gelation, it has been widely explored for biomedical applications [15]. Structurally, alginate is a block linear co-polymer of D-mannuronic acid (M units) and L-guluronic acid (G units) (**Figure 3.1A**) with ratios of the residues varying depending on the source of alginate. The regions within the alginate molecule vary between sequential M units, G units or alternated M and G units. Alginate hydrogels may be produced recurring to several cross-linking methods. The most common is the ionic crosslinking, in which crosslinking agents, as divalent cations (e.g. Ca^{2+}) are combined with the alginate solution to form the hydrogel (**Figure 3.1B**). The structure of the gel is achieved when the alginate chains form junctions with adjacent chains (egg-box model of crosslinking). Some examples of the most used crosslinking agents are calcium chloride ($CaCl_2$), calcium sulphate ($CaSO_4$) and calcium carbonate ($CaCO_3$). Whereas $CaCl_2$ has disadvantages regarding the insufficient control of the gelation rate that occurs rapidly, $CaSO_4$ and $CaCO_3$ have a low solubility, which slows the gelation process. However, for Ca^{2+} to be generated, a dissociation agent needs to be added to the solution. For $CaCO_3$, glucono-δ-lactone (GDL) is the commonly used agent. This molecule is responsible for lowering the pH

of the reaction medium thus allowing the dissociation of the Ca^{2+} from the $CaCO_3$, which at neutral pH is not soluble in water [15].

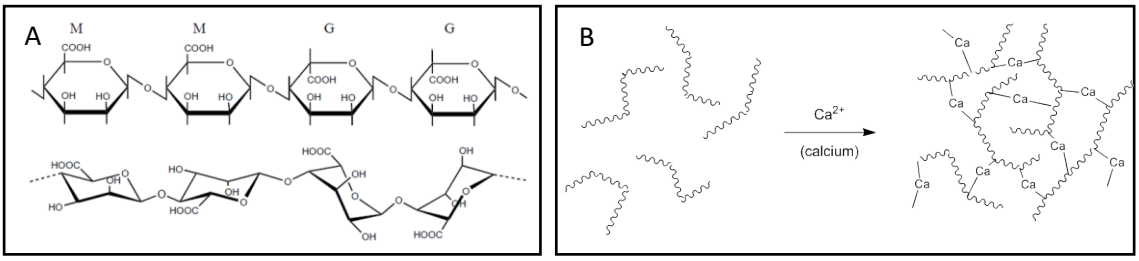

Figure 3.1 *Alginate chemical structure (**A**) and scheme of ionic crosslinking using Ca^{2+} as the crosslinking agent (**B**).* Alginate is a linear co-polymer composed by blocks of D-mannuronate (M) and L-guluronate (G) residues, either consecutive or alternated in the chain. The content of M and G varies depending on alginate source. The crosslinking with divalent cations enables the formation of a hydrogel being that linking only made by the G-blocks of the alginate.

Besides ionic crosslinking, other methods of crosslinking have been explored, namely covalent crosslinking and thermal gelation. Covalent crosslinking emerged as a reliable technique to overcome some of the ionic crosslinking problems such as the easy plastic deformation of the hydrogels after the application of stress forces. However some of the reagents of the covalent crosslinking are toxic and should be removed from the gels if one has a biological application in mind. On the other hand, hydrogels formed by thermal gelation respond to temperature changes, which is beneficial in the field of drug delivery systems. It is also possible to modify alginate with cell adhesion ligands that promote the crosslinking via receptor-ligand interactions without the need of adding other crosslinking agents. Among the vast range of applications of alginate hydrogels, a very important one relies on their use as synthetic ECMs. In this project, alginate based matrices were used as the 3D microenvironment surrounding astrocytes. Alginate's unique features made it the ideal choice for mimicking brain's extracellular space. Alginate matrices are highly reproducible and easy to obtain. In addition, alginate functions as a relative inert background once protein adsorption is not promoted, therefore cell interaction with the hydrogel is minimal [16]. This facilitates the control of the system complexity. Alginate structure also allows the recovery of the cells after culture through the use of quelators, thus further biochemical or cellular analysis can be performed. Besides, alginate's mechanical properties are tunable to be identical to brain's mechanical properties [17] and its 3D structure allows the formation of a more physiologically relevant model. In fact, astrocytes in the brain form a 3D network thus a 3D model is expected to better recapitulate cellular interactions occurring *in vivo*.

Mimicking axons using electrospun fibers

Electrospinning is a simple fiber producing method that relies on the use of electrical forces to produce polymer fibers with variable diameters in the nano to micron scale, and different

organization/orientation. This ninetieth century-technique is nowadays being widely used among the scientific community for diverse applications due to the standardized and consistent fiber production in the submicron range with small and tunable porosity and high surface-to-volume ratio [18].

Electrospinning can be performed using a horizontal or a vertical setup (**Figure 3.2**). However, both have the same associated principals: the system consists of a high voltage power supply, a spinneret and a collecting plate that can either be static or rotating. The polymer solutions previously dissolved in appropriate solvents or melts are introduced in the spinneret to which an electric field is applied. An electric charge on the liquid surface is produced and the charged solution is then accelerated in the direction of the collector. A jet of the solution is ejected from the Taylor cone in a way that allows the solvent to evaporate and the deposition of the polymer on the collector to occur.

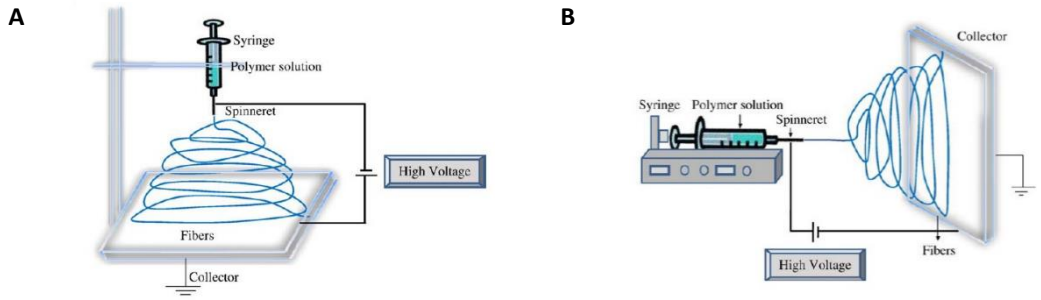

Figure 3.2 *Electrospinning setup.* **A)** Vertical setup. **B)** Horizontal setup. Adapted from Bhardwaj, N. *et al* (2010) [18].

Electrospun nanofibers have been used for several applications. The possibility of adjusting the parameters allows the production of a broad spectrum of fibers. In the context of nerve repair, aligned fibers have been widely explored and can in fact serve as a reliable nerve conduit. Electrospinning fibers can also be seen as a drug delivery systems allowing the release of promising agents for neuronal regeneration [19].

Another promising approach is the use of electrospinning fibers to mimic axons, which may be achievable due to the possibility of producing fibers with diameters similar to axons' diameters (ranging from 0,1μm to 10μm [20]).

The first publication on the use of fibers to act as surrogate axons was developed by Howe [21]. Later, Lee and co-workers, have used electrospinning polystyrene nanofibers to conclude about the influence of diameter in myelination processes [22]. Up until now, these are the only studies on this field.

In the context of this project the use of engineered polymeric nanofibers enabled the study of the crosstalk between astrocytes and oligodendrocytes uncoupling the influence of axonal cellular and/or biochemical signals. The chosen strategy is undoubtedly interesting when one

intends to study a particular effect of one neuronal cell and at the same time approaching the *in vivo* conditions. In the study of myelination and remyelination, fibres enable the examination of OPC gene expression as well as biochemical signalling pathways involved in the formation and wrapping of the myelin without the influence of neurons. Also, biophysical and molecular cues that enable OPC differentiation and migration can be easily seen.

Several polymers are reported to be suitable for electrospinning. Electrospinning fibers from natural (e.g., collagen, gelatin, etc), synthetic (poly(lactic acid), polyurethane, etc) or even a mixture of both type of polymers with proteins, nucleic acids, polysaccharides or drugs are being described over the past years. While natural polymers have advantages regarding biocompatibility and immunogenicity, synthetic polymers degrade slower and their fabrication processes are simpler. Besides, it is easier to adjust synthetic polymers' mechanical properties such as viscoelasticity and strength [18].
One synthetic polymer that is successfully ascribed for electrospinning fiber production is poly(trimethylene carbonate-co-ε-caprolactone) (P(TMC-CL)) [19].
P(TMC-CL) is a biodegradable elastomer and a co-polymer composed of poly(trimethylene carbonate) (P(TMC)) and poly-ε-caprolactone (PCL) (**Figure 3.3**).

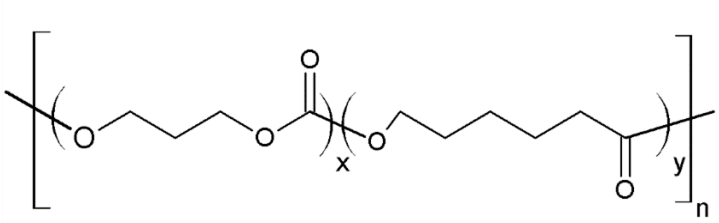

Figure 3.3 *TMC-CL co-polymer.* **x** identifies trimethylene carbonate (TMC) and **y** is ε-caprolactone (CL).

P(TMC) is hydrophobic, amorphous and rubbery, having glass temperature transitions around 15-20ºC. Beyond, what makes P(TMC) interesting for tissue engineering applications is its enhanced lifetime due to slow degradation rates and generation of non-acidic products after *in vitr*o hydrolysis. However, *in vivo* enzymatic degradation happens at high rates when high molecular weight polymer chains are used, disadvantage that pushed researchers to find solutions to meet many biomedical needs. One of them was the incorporation of other monomers in the P(TMC) chain. Besides having the aim of slowing the rate of biodegradation, this strategy also allows the tuning of TMC mechanical properties. The incorporation of PCL, which is a semi-crystalline, thought and characterized by a low glass transition temperature, aided the control of degradation rates of TMC [23, 24]. P(TMC-CL) has been previously proposed for the preparation of nerve conduits to promote nerve regeneration [24, 25]. Specifically, it was reported that Schwann cells, the myelinating forming cells of the PNS, can easily attach and proliferate on P(TMC-CL) surfaces [26].

In this study, a previously established 3D *in vitro* myelination platform composed of electrospinning polymeric (poly(trimethylene carbonate-co-ε-caprolactone) copolymer, P(TMC-CL)) nanofibers combined with a tissue engineered glial scar model of astrocytes embedded in alginate matrices [27] will be explored and the study on the effects of activated astrocytes in oligodendrocytes differentiation will be deepened.

MATERIALS AND METHODS

Poly(trimethylene carbonate-co-ε-caprolactone) (P(TMC-CL)) synthesis and purification

Poly(trimethylene carbonate-co-ε-caprolactone) with a molar ratio of 10:90 mol% was synthetized as previously reported [24]. ε-caprolactone (CL) and trimethylene carbonate (TMC) were polymerized through ring-opening polymerization in the melt, using stannous octoate ($SnOct_2$) as the catalyst (**Figure 3.4**).

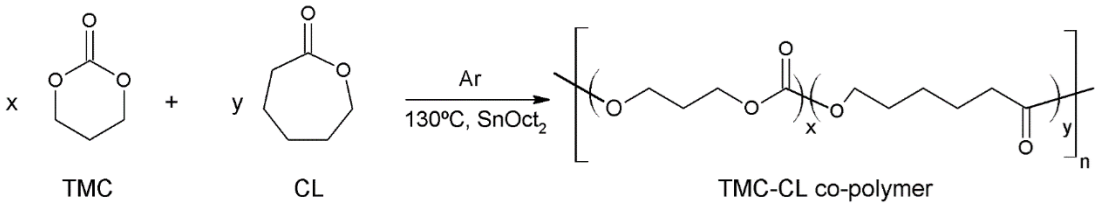

Figure 3.4 *Chemical reaction between TMC and CL*.

TMC (from Boehringer Ingelheim, Germany) was dried overnight under vacuum at room temperature (RT) prior use. CL (Merk) was purified by drying overnight under calcium hydride (CaH_2) and, subsequently, distilled under a reduced argon atmosphere (**Figure 3.5**).

Figure 3.5 *Photograph of CL distillation set-up.* Legend: **1**. condensation column, 2. balloon filled with argon, **3**. Argon supply, **4**. cold trap, **5**. distilled ε-caprolactone.

At the end of the distillation, the CL was kept under argon until further use.

The polymerization reaction was carried on in a previously washed, silanized (Serva) and dried overnight (105ºC) glass ampoule. Firstly, the ampoule and an adaptor were mounted and three argon purges were done to keep the system under a reduced argon atmosphere. The ampoule and the adaptor were then weighted and TMC was added to the ampoule. After 3 argon purges, the system (ampoule, adaptor and TMC) was weighted and TMC weight was calculated. Hereafter, the needed volume of CL to be added to TMC in order to achieve a 10:90 mol% ratio of TMC:CL was estimated. CL was added to the system previously purged with argon, the final weight of the system was measured and the weight of CL estimated.

Afterwards, the catalyst, $SnOct_2$ was added to the reaction in a proportion of $2x10^{-4}$ mol per mol of monomer. $SnOct_2$ is the most common initiator system for polymerizations of lactones and TMC and was chosen due to its high efficiency and capability of completely convert monomers even at high ratios between the monomers and the catalyst [25]. The synthesis was carried out for a period of three days in the ampoule vacuum-sealed at a temperature settled to 130ºC in an oil bath. Afterwards, the reaction was stopped, by immersing the ampoule in cold water. Next, the glass ampoule was broken with a hammer and transferred to liquid nitrogen that makes easier the removal of the broken pieces of glass.

Subsequently, the polymer was purified, firstly by dissolving overnight (room temperature, RT) at 3% (w/v) in chloroform (Merk) and then by precipitating it in a ten-fold volume of technical grade ethanol (99%). The precipitated polymer was dried at RT in a vacuum hoven under a stream of air during three days. The purified polymer (yield of recovery 85%) was stored at RT until further use.

P(TMC-CL) polymer characterization

Chemical composition

The purified P(TMC-CL) was analysed in terms of chemical composition by ^{1}H nuclear magnetic resonance (NMR). For that purpose, the polymer was dissolved in chloroform at a final concentration of 1mg/mL and sent to *Centro de Materiais da Universidade do Porto* (CEMUP) for the NMR experiments. NMR spectra were recorded with a Bruker Avance III 400 MHz spectrometer in $CDCl_3$. Chemical shifts are reported in ppm (δ units). Mathematical spectrum analysis was conducted by Dr. Victoria Leiro (INEB/i3S).

Molecular weight

The number average molecular weight (Mn) and polydispersity index were calculated by gel permeation chromatography (GPC) using tetrahydrofuran as the mobile phase and conventional calibration to determine samples Mn. Procedures were performed at

Departamento de Química da Universidade de Coimbra by Joana Mendes (Professor Jorge Coelho's group).

P(TMC-CL) electrospinning fibers preparation and characterization

In order to obtain nanofibers with a desired diameter and morphology, a wide range of electrospinning variables was tested: polymer concentration; polymer solvent ratio (dichloromethane (Merk) and dimethylformamide (Sigma) – DCM:DMF); needle diameter; distance between the collector and the syringe; flow rate and the applied electrical field. Variables tested are presented in **Appendix B**. To sum up, concentrations were varied between 9% and 12.5% (w/v), flow rate 0.8 mL/h and 1.2 mL/h, applied electrical field between 10 kV and 17 kV and distance between collector and needle from 10 cm to 20 cm. Based on the morphology of the fibers (**Appendix B**) the best conditions were chosen for subsequent experiments: 10% of P(TMC-CL) dissolved in DCM and DMF at a ratio of 6:1 was dispensed at 0.9 mL/h using a 0.8 mm outer diameter spinneret and syringe (Soft-Jet, 4.26mm diameter) connected to a pump (Ugo Basile), distanced 16 cm from the collector (flat copper plate 15x15cm), and applying an electrical field of 16kV. Fibers were collected to 13 mm pre-washed and dried coverslips (neuVitro) distributed along an aluminium foil during approximately 1h-1.5h. Coverslips were then vacuum dried (Raypa or Binder vacuum ovens) overnight and stored at RT until further use.

Fiber morphology was assessed by scanning electron microscopy (SEM). SEM was performed using a high resolution SEM with X-Ray Microanalysis: JEOL JSM 6301F/Oxford INCA Energy 350. Prior analysis samples were coated with an Au/Pd thin film for 70s and with a 15mA current, by sputtering, using the SPI Module Sputter Coater equipment. Fiber diameter measurements (fiber mean diameter and fiber distribution) were estimated from SEM images and were calculated based on 100 different measurements from three different regions of the glass coverslip using image analysis software (ImageJ, version 1.50b; Rasband, W.S., ImageJ, U. S. National Institutes of Health, Bethesda, Maryland, USA, http://imagej.nih.gov/ij/, 1997-2016).

Primary cell cultures

All experiments involving animals and their care were performed in agreement with institutional ethical guidelines (IBMC/INEB/i3S), the EU directive (2010/63/EU) and Portuguese law (DL 113/2013). Consequently, in order to be able to work in the animal facility, a Laboratory Animal course following FELASA B recommendations was performed and successfully concluded (see Final Report of the Tutorial Training in **Appendix C**).

All described procedures had the approval of the Portuguese official authority on animal welfare and experimentation (*Direção Geral de Alimentação e Veterinária*). Animals had free access to food and water and were kept under a 12h light/12h dark cycle.

Cortex and meningeal tissue isolation

To obtain oligodendrocytes, astrocytes and meningeal fibroblasts, Wistar Han rat pups in post-natal day 2 (P2) were sacrificed by decapitation and brain was removed to further dissociate the cortex and the meningeal tissue. Approximately 8-16 pups were sacrificed every two weeks. Removal of brain was performed using straight micro-scissors and fine forceps previously cleaned and sterilized. The procedure was conducted under a magnifying glass in a Petri dish containing Hank's Balanced Salt Solution (HBSS, Gibbco) without calcium and magnesium supplemented with 2% (v/v) penicillin/streptomycin (P/S) (Gibco). Firstly, the skin of the head was cut until the nose with a sharper scissor with the other hand holding the head (from the ear) with a big forceps. The skin was opened to the corners in order to let the skull bones be visible. Then, with a straight microscissor, the skull bone was cut until the nose and to the sides. The bones were removed with a thinner forceps and a special care was taken to not damage the cortex. With the same forceps, the cortex was carefully removed (from the olfactive bulbs) and cut by the cerebellum. Subsequently, using thinner forceps, the two hemispheres were separated and the meningeal tissue was detached from the cortex. Cortex and meningeal tissue were maintained in ice-cold HBSS without calcium or magnesium with P/S to prevent cell dissociation and death.

Mixed glial cell (MGC) cultures

After cortex and meningeal tissue removal, the cortices were firstly mechanically digested with a 10 mL serological pipette and passed through a 25G needle to dissociate clusters. Cortices were then enzymatically digested with HBSS without calcium or magnesium supplemented with 0,0025% (w/v) trypsin (Sigma) and 0.001mg/mL DNase I (Applichem LifeSciences) for 15 min at 37ºC. The action of the trypsin was inhibited by the addition of Dulbecco's modified Eagle medium (DMEM) Glutamax High glucose (Gibco) supplemented with 10% (v/v) heat inactived Foetal Bovine Serum (FBS, Sigma F7524) and 1% (v/v) P/S and the homogeneized was then centrifuged at 500g during 10 min. The supernatant was poured off, the pellet re-suspended in serum containing DMEM and filtered through a 40 μm nylon cell strainer (BD Falcon) to remove large cell clusters. Finally cells were distributed for T75 cell culture flasks, previously coated with 100 mg/mL poly-L-lysine (PLL, mol wt 30 000-70 000, Sigma) (30 min, 37ºC) at a density of cell suspension obtained from two brains per flask. Cells were cultured with serum containing DMEM at 37ºC, 5% CO_2 during 4 days to allow cell adhesion to the flask and then medium was changed every 2-3 days (changing ¼ of the medium at day 4; ½ at day 6 and all medium from day 8 on). Cells were maintained during 15 days until confluent (see **Figure 3.6**), when the components of the MGC cultures where mechanically separated (see following section).

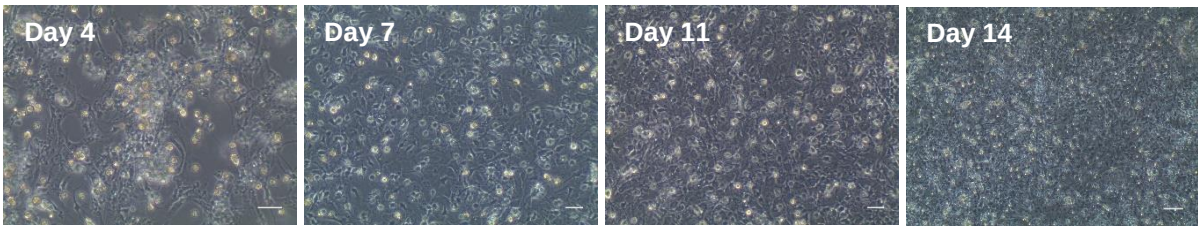

Figure 3.6 *Mixed Glial Cell culture progression over days*. Cell culture confluence increased visibly as a function of time in culture. At day 14 a confluent bed layer of astrocytes (grey phase) with OPCs on the top (dark phase) is easily distinguished. Scale bar represents 30μm.

Oligodendrocyte progenitor cell (OPC) cultures

OPCs were mechanically isolated from MGC as previously described [28, 29]. At day 14 after plating, MGC were confluent with phase-dark OPCs appearing on top of phase-grey bed layers of astrocytes (**Figure 3.6**). On that day, a pre-shake was performed: the T75 lids were tightly sealed and transferred to an horizontal orbital shaker (Infors) during 2h at 210 RPM (37ºC) to remove the majority of loosely adherent microglia cells. After that, medium was replaced and cells were left at 37ºC for 2h to allow the normal metabolism stabilization. An overnight shake (18h-20h) at 230 RPM (37ºC) was then performed to further detach loosely attached microglia and OPCs. After shaking overnight, OPCs were further purified by differential selective adhesion. The cell suspension was transferred to non-treated polystyrene Petri dishes (10 cm of diameter) to allow microglia to adhere during 2h at 37ºC and unattached OPCs were collected, passed through a 40μm cell strainer to remove cell clusters and centrifuged at 450g during 10 min (RT). The cell pellet was then re-suspended, cells counted and seeded on the top of 13 mm glass coverslips previously coated with PLL (as above described) or P(TMC-CL) fibers, previously sterilized (10 min in 70% Ethanol, technical grade, twice). Cells were maintained during 24h-48h in proliferation medium (OPC SATO Medium) (**Table 3.1**). After that period, cells were cultured in differentiation medium (OL SATO Medium) (**Table 3.1**).
The purity of OPC culture was estimated by immunocytochemistry.

Table 3.1 *Medium composition for proliferation (OPC SATO) and differentiation (OL SATO) of OPCs.* A stock of SATO 10x was prepared, aliquoted and frozen at -20ºC until further use. OPC SATO and OL SATO were freshly prepared by supplementing the starting SATO medium.

	Final Concentration
Components	***SATO Medium (10x)***
DMEM Glutamax High Glucose *(Gibco, 31966-047)*	-
Transferrin *(Sigma, T2036)*	1 mg/mL
Putrescine *(Sigma, P5780)*	160μg/mL
Bovine Serum Albumine (BSA) *(BioWest, P6154)*	1 mg/mL
Progesterone *(Sigma, P8783), dissolved in 99% Ethanol*	600 ng/mL
Sodium selenite *(Sigma, S5261), dissolved in 0.1N NaOH*	400 ng/mL
Thyroxine *(Sigma, T1775), dissolved in 0.1N NaOH*	400 ng/mL
Triiodo-L-Thyronine *(Sigma, T6397), dissolved in 0.1N NaOH*	300 ng/mL
OPC SATO (Proliferation medium)	
SATO 10X	1x
Insulin *(Sigma, 19278)*	5μg/mL
Fibroblast Growth Factor (FGF) *(Peprotech (100-18B))*	0.01μg/mL
Platelet-derived growth factor-AA (PDGF-AA) *(Peprotech (100-13A))*	0.01μg/mL
P/S *(Gibco)*	1% (v/v)
OL SATO (Differentiation medium)	
SATO 10X	1x
Insulin *(Sigma, 19278)*	5μg/mL
Foetal Bovine Serum (FBS) *(Sigma Aldrich, F7524), heat inactivated*	0.5% (v/v)
P/S *(Gibco)*	1% (v/v)

Astrocyte culture

The shaken T75 were then cultured at 37ºC 5% CO_2 for additional two weeks and every week flasks were shaken to obtain OPCs. After the third shake, the remaining cells are mainly astrocytes. In order to obtain pure astrocytes, cells were trypsinized and seeded on new T75 flasks at least three times. Astrocytes were maintained in DMEM Glutamax High glucose supplemented with 10% (v/v) heat inactivated FBS (Sigma) and 1% (v/v) P/S (Gibco). Cell culture purity was then analysed and estimated by immunocytochemistry.

Figure 3.7 summarizes the process of cortex isolation, MGC culture and OPCs and astrocytes' obtainment.

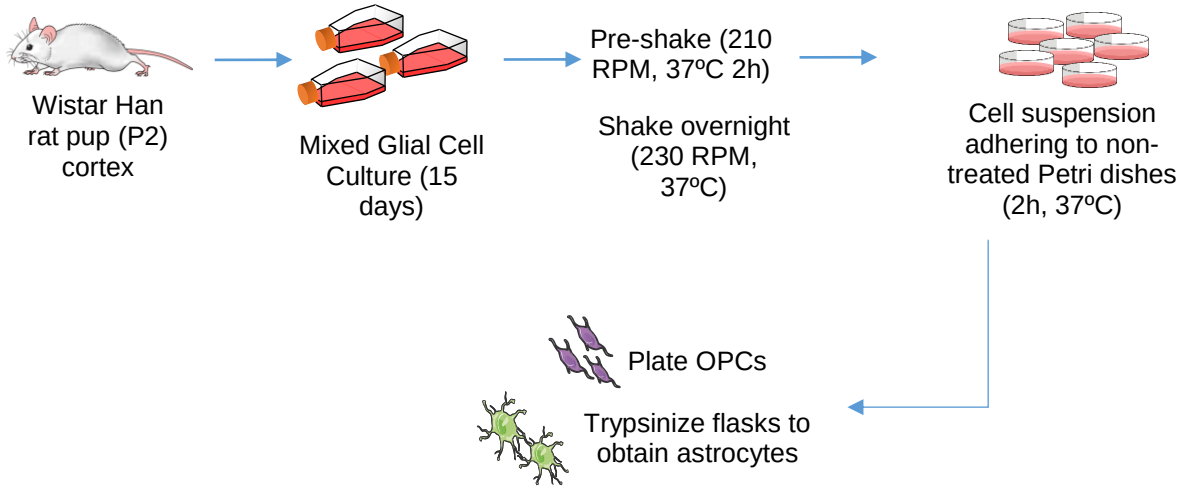

Figure 3.7 *Scheme of the process of OPC and astrocyte isolation.* Firstly, cortex were extracted from P2 rats and plated in T75 flasks (mixed glial cell cultures). After reaching confluency, the components of the MGC cultures were mechanically separated and astrocytes and OPCs obtained.

Meningeal Fibroblasts culture

After removal of pups' brain meninges, the tissue was mechanically and enzymatically digested with HBSS without calcium or magnesium supplemented with 10% (v/v) trypsin for 30 min at 37ºC. Dissociated meninges were seeded in T75 flasks previously coated with PLL (above described) and were maintained at 37ºC, 5% CO_2 in DMEM Glutamax High Glucose supplemented with 10% (v/v) heat inactivated FBS (Sigma) and 1% (v/v) P/S (Gibco). After reaching confluence, cells were trypsinized and frozen down (10% Dimethyl sulfoxide – DMSO in FBS) until passage three.

Fibroblast conditioned medium (CM) was obtained by culturing 1-1.5 x 10^6 meningeal fibroblasts from frozen vials in PLL coated (as described previously) T75 cultured during three days. Medium was collected, centrifuged at 500g during 10 min and stored at 4ºC until use (CM is stable at 4ºC for up to 15 days).

Preparation of 3D alginate discs with astrocytes

Alginate hydrogel discs were produced as described before [30]. Firstly, ultrapure sodium alginates VLVG and LVG (low and high molecular weight) (FMC) with a high glucuronic acid content (68%) were mixed at a proportion of 1:1 and dissolved at a final concentration of 2% (w/v) in a 0.9% NaCl solution. This mixture was then slowly shaken overnight at 4ºC. The alginate solutions were sterilized by filtering with a 0.22μm filter (Millex) and stored until further use.

In situ hydrogel alginate discs were prepared by mixing $CaCO_3$ (FLUKA) (Ca^{2+}/COO^- molar ratio = 0.288), δ-gluconolactone (GDL, Sigma) (Ca^{2+}/GDL molar ratio = 0.125), 2% (w/v) alginate and primary rat astrocytes in order to obtain final concentration of 1% alginate

matrices. Primarily, $4x10^6$ viable cells/mL (determined by the Trypan Blue exclusion assay) were added and homogeneized to 2% (w/v) alginate. For the preparation of the $CaCO_3$ solution it was firstly autoclaved, then weighted and dissolved in NaCl 0.9% at a final concentration of 61.2mg/mL. GDL was prepared at a final concentration of 96.8mg/mL in NaCl 0.9% and subsequently sterilized by filtration (0.22 μm filter). $CaCO_3$ and GDL were rapidly added to the solution of alginate and cells, the suspension homogenised and pipetted to pHEMA-treated culture plates (BD Falcon) (20μL) with a gel pipette. Crosslinking occurred at 37ºC, 5% CO_2 during 1h. After that time, DMEM Glutamax High glucose supplemented with FBS and P/S (hereafter designed as DMEM) or CM was added to alginate discs and maintained in culture at 37ºC, 5% CO_2.

OPCs and astrocytes co-culture system

Co-cultures experiments were performed as schematized in **Figure 3.8**. Firstly, astrocytes were cultured in alginate discs as previously described and cultured either in the presence of DMEM or CM media (day 0). After three days, OPCs were seeded on the top of P(TMC-CL) fibers and allowed to proliferate during 24h (in OPC SATO medium). Afterwards, OPC SATO medium was changed for OL SATO medium and alginate discs were added to a transwell with a 0.4 μm pore (BD Falcon) coupled to the well where OPCs were seeded. Cells were kept at 37ºC, 5% CO_2 for additional five days and OL SATO medium was changed regularly (every 2-3 days). On the day 9 of experiment, RNA from OPCs (300 000 cells) was extracted to further gene expression analysis by quantitative real-time polymerase chain reaction (qRT-PCR) (see section 9).

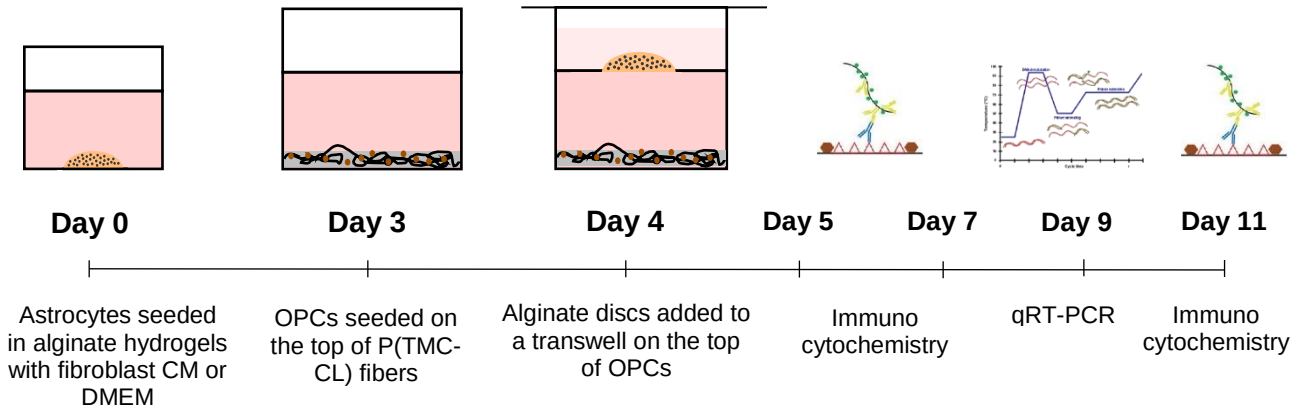

Figure 3.8 *Scheme of the experiment procedure to evaluate gene profile expression of OPCs after co-culturing with activated/non-activated astrocytes.*

In alternative, after the addition of the alginate discs to the OPCs with fibers, cells were fixed after one, three or seven days and analysed by means of immunocytochemistry for the expression of MBP and NG2 (methodology previously described in section 5).

To analyse the effects of the reversion of the activated phenotype of the astrocytes, pharmaceutical grade ibuprofen (purity >99%) (Bluepharma) was added to cultures (0.04M) on the day 9 of the experiment and after 48h, RNA from OPCs was collected for further genetic expression profile analysis.

Live-dead assay

Cells were washed with phosphate buffered saline (PBS) and incubated with a calcein-AM solution (Promega) at a final concentration of 1:250 (in PBS) during 20 min at 37ºC, 5% CO_2, protected from light. After that period, cells were washed three times with PBS to remove the excess of calcein-AM followed by incubation with propidium iodide (PI) (Sigma) during 5 min. The excess of PI was removed by rinsing cells twice with culture medium and immediately observed under a confocal microscope (SP5, Leica, Germany). Cells positive for PI or for calcein-AM were counted from ten different images from two independent samples using image analysis software (ImageJ, version 1.50b; Rasband, W.S., ImageJ, U. S. National Institutes of Health, Bethesda, Maryland, USA, http://imagej.nih.gov/ij/, 1997-2016).

Quantitative real-time Polymerase Chain Reaction (qRT-PCR)

In order to perform quantitative real-time Polymerase Chain Reaction (qRT-PCR), RNA from 300 000 oligodendrocytes cultured on polymeric fibers (50 000 cells per 13mm glass coverslip covered with fibers) was extracted using the Quick-RNA MiniPrep kit (Zymo Research) according to the manufacturer's recommendations. Briefly, cells were lysed using RNA lysis buffer for 7/10 min (time of lysis was optimized before – see in the **Appendix D** for the optimization process), and the lysate was then centrifuged. Afterwards, RNA was precipitated using ethanol (96%, analytical grade) (Merck) and a DNase I treatment was conducted for 15min. RNA recovering was achieved using RNA Prep Buffer. Finally, RNA was eluted in DNase/RNase-Free water (Zymo Research) and concentrations measured in NanoDrop spectrophotometer (Thermo Scientific) at an absorbance of 280nm. Ratios of 260/280 and 260/230 between 1.8 and 2.2 were accepted as non-contaminated samples and proceed to cDNA synthesis. In cases of doubts, a RNA degradation assay by Experion (Biorad) was performed (see **Appendix D**). Samples were stored at -80ºC in low-binding Eppendorf tubes® until further use. After RNA extraction, cDNA was synthetized using NZY First Strand cDNA Synthesis Kit (NZYTech) and following producer's directives. Briefly, on ice, NZYRT 2x Master Mix was mixed with NZYRT Enzyme Mix and with RNA (between 70 and 200ng). The mixture was incubated at 25ºC for 10 min followed by an increase in the temperature to 50ºC, which was maintained during 30 min. Subsequently, the reaction was inactivated by heating at 85ºC for 5 min and then chilled on ice for approximately 5 min. NZY RNase H (*E. coli*) was pipetted to the mixture and the reaction continued for 20 min at 37ºC. At the end, samples were kept at

-20ºC until further usage. It is worth noting that, the temperature cycles were performed in a Thermocycler (Biometra).
After synthetizing cDNA, qPCR was performed using *Ywhaz* as endogenous control to serve as a normalizer to the expression levels of *Mbp. Ywhaz* and *Mbp* primer sequences were gently provided by Dr. Pedro Moreno (INEB/i3S) and Dr. Joana Paes (IBMC/i3S), respectively, and purchased from ThermoScientific. Primer sequences used for qRT-PCR and were the follow:

Mbp sense 5' TGT CAC AAT GTT CTT GAA GAA 3'
Mbp anti-sense 5' GCT CCC TGC CCC AGA AGT 3'
Ywhaz sense 5' ACG ACG TAC TGT CTC TTT TGG 3'
Ywhaz anti-sense 5' GTA TGC TTG CTG TGA CTG GT 3'

Analyses were performed on IQ5 (Biorad) using SYBR Green (SYBR Green Master Mix, Applied Biosystems) according to manufacturer's instructions. Briefly, a master mix containing 10μL iTaq, 0.1μM of each primer (0.25μL each) and 8.5μL nuclease free-water was prepared, in which 1μL of cDNA was added. Reactions were performed in triplicates and qPCR cycle was the follow:

Table 3.2 *qRT-PCR for Mbp and Ywhaz*. Annealing temperature used was 55ºC.

Step	Temperature (ºC)	Time	Number of cycles
Activation	95	3min	1x
Amplification cycle	95	10s	40x
	55	30s	
Storage	4	-	-

To address the specificity of the reactions, melting curves were analysed and found that there was no unspecific reaction product of the qPCR. It is worth noting that, before qPCR analysis for all the samples, both primer sets were tested and their efficiencies calculated. For that purpose, a series of dilutions were done (1/10 and 1/100) and amplification cycles analysed (**Appendix E**). Other housekeeping genes (*Hprt* and *Tbp*) were also tested regarding their amplification cycles and efficiency (**Appendix E**). After a deep analysis, *Ywhaz* was chosen as the reference gene as it was the one that presented the most adequate C_T values and a good efficiency and amplification curve.
qPCR data was analysed using the delta C_T method (ΔC_T) by calculating the difference between reference and target C_T values for each sample. This methodology assumes that the target and reference genes are amplified with efficiency near 100%, which was verified (**Appendix E**).

Immunocytochemistry

For experiments involving immunocytochemistry analysis, before fixation, cells were washed twice with pre-warmed phosphate buffer saline (PBS) (Gibco) solution for 10 min. Afterwards, cells were fixed with 4% (wv/v) paraformaldehyde (PFA) (Merck Milipore) during 10/15min at RT, washed twice with PBS and permeabilized and blocked in PBS containing 5% (v/v) normal goat serum (NGS) (Biosource) and 0.3% Triton X-100 (Sigma) for 1h at 4ºC. Primary antibodies were then diluted in PBS with 1% (v/v) NGS and 0.15% (v/v) Triton X-100 and incubated at 4ºC overnight. Following the primary antibody incubation, cells were washed three times with PBS to remove the excess of the primary antibodies and the secondary antibodies were diluted in PBS containing 1% (v/v) NGS and 0.15% (v/v) Triton X-100 and added to the cells. Secondary antibodies' incubation was conducted at 4ºC for 45min to 1h. Afterwards, cells were washed three times with PBS and incubated with Hoescht (ThermoFisher) diluted in PBS (1:1000) containing 1% (v/v) NGS and 0.15% (v/v) Triton X-100 for 15min at RT. Subsequently, cells were mounted using FluoroMount (Sigma) and observed under an inverted fluorescence microscope (AxioVert) or confocal microscope (SP5, Leica, Germany). The following primary antibodies were used: rat anti-MBP (1:100, Abd Serotec), rabbit anti-NG2 (1:250, Merck), rabbit anti-IBA1 (1:500, Wako), mouse anti-βIII tubulin (1:500, Promega) and rabbit anti-GFAP (1:500, Dako). Secondary antibodies used were 488 donkey anti-rat (1:1000, Invitrogen), 647 donkey anti-rabbit (1:1000, Invitrogen) and 488 donkey anti-mouse (1:1000, Invitrogen). For the evaluation of culture purities, the combination of the used primary antibodies is summarized in **Table 3.3**.

Table 3.3 *Combination of primary and secondary antibodies to evaluate OPCs' and astrocytes' cultures purities.*

	PRIMARY ANTIBODIES		SECONDARY ANTIBODIES	
OPCS' CULTURES	Rat anti-MBP	Rabbit anti-NG2	488 donkey anti-rat	647 donkey anti-rabbit
	Rat anti-MBP	Rabbit anti-IBA1	488 donkey anti-rat	647 donkey anti-rabbit
	Mouse anti-βIII tubulin	Rabbit anti-IBA1	488 donkey anti-mouse	647 donkey anti-rabbit
	Rat anti-MBP	Rabbit anti-GFAP	488 donkey anti-rat	647 donkey anti-rabbit
ASTROCYTES' CULTURES	Mouse anti-βIII tubulin	Rabbit anti-NG2	488 donkey anti-mouse	647 donkey anti-rabbit
	Mouse anti-βIII tubulin	Rabbit anti-IBA1	488 donkey anti-mouse	647 donkey anti-rabbit
	Rat anti-MBP	Rabbit anti-GFAP	488 donkey anti-rat	647 donkey anti-rabbit

In experiments where cell fluorescence intensity measurements were conducted, ten different images of two independent glass coverslips were taken and analysed using an image analysis software (ImageJ, version 1.50b; Rasband, W.S., ImageJ, U. S. National Institutes of Health, Bethesda, Maryland, USA, http://imagej.nih.gov/ij/, 1997-2016). To estimate fluorescence intensity, the cell of interest was selected by drawing a line around the cell and the values for area, mean and integrated density were shown in “Measure” tool. A non-fluorescent region closed to the cell was also selected and appointed as background. The mean fluorescence of the background was also calculated and the corrected total cell fluorescence (CTFC) was estimated by subtracting the integrated density of the cell for the product between the area of selected cell and the mean fluorescence of background readings (CTFC = Integrated density – (area of selected cell x mean fluorescence of background readings).

Statistical analysis

Statistical analysis was performed using GraphPad Prism version 7.00 for Windows, GraphPad Software, La Jolla California USA (www.graphpad.com). Statistical differences between groups were calculated based on *t*-student test (two group comparison) or two-way ANOVA when two factors affected the measurements, followed by Tukey’s multiple comparisons test for multiple comparisons. Gaussian distributions were tested using D’Agostino and Pearson normality tests. When Gaussian distribution could not be tested due to the lack of measurements or failed in the above-mentioned tests, non-parametric tests were performed. Mann-Whitney tests were used in the case of unpaired *t*-tests. A p-value below 0.05 was considered statistically significant and data are shown as mean ± standard deviation (SD).

RESULTS AND DISCUSSION

P(TMC-CL) polymer was successfully synthetized

The reaction between CL and TMC occurred through ring-opening polymerization in the melt at a monomer molar ratio of 10:90 (TMC:CL). In order to determine the resulting chemical composition of the prepared polymer a ^{1}H NMR analysis was performed. The resulting spectrum is depicted in **Figure 3.9**.

The copolymer composition was determined by ^{1}H-NMR analysis of the purified polymer and peaks for polymeric TMC were found in δ=1.93-2.07ppm (multiplet), δ=4.09-4.25ppm (multiplet) and for polymeric CL δ=1.34-1.41ppm (multiplet), δ=1.60-1.68 (multiplet), δ=2.30 (triplet) and δ=4.05 (triplet). The monomeric spectra for separated TMC and CL was not performed, although, according to the literature [24] the peaks showed the expected drift in the spectrum, therefore it was possible to conclude that all monomers reacted between each other. The areas under the curves were measured and assuming the value of the area for CL as the reference (100.000), the area of TMC was estimated as 11.71. The polymer was found to content 89% of CL and 11% of TMC, values that were in accordance with polymer ratio charged (90% CL and 10%TMC). This result indicates that the synthesis reaction was successfully conducted.

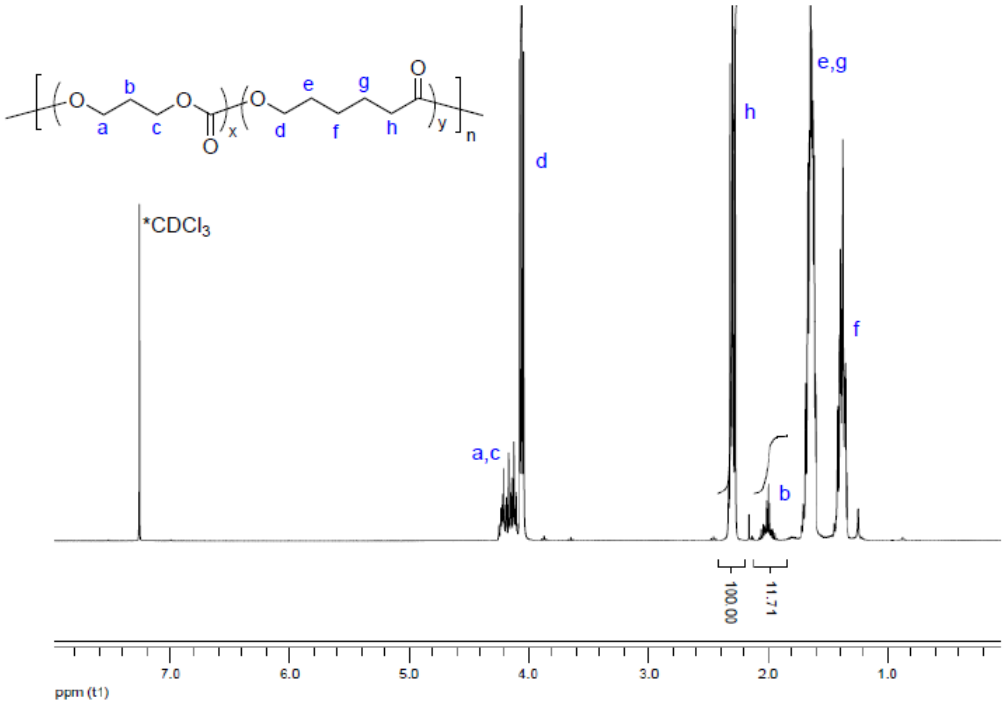

Figure 3.9 *NMR Spectrum of purified P(TMC-CL) (400MHz, $CDCl_3$).* The letters (a-h) correspond to peaks of TMC (a-c) and CL (d-h). The peaks used to estimate the proportion between CL and TMC were the ones corresponding to **h** and **b** letters.

The obtained polymer was subsequently characterized in terms of molecular weight distribution. This characterization is important to infer many physical properties of the polymers, namely, thermal and mechanical properties. In **Table 3.4** the values of the number and weight average molecular weight – Mn and Mw, respectively – and polydispersity index (PDI) are presented. The number average molecular weight (Mn) is the statistical average molecular weight of all the polymer chains in the sample. The weight average molecular weight (Mw) takes into account the molecular weight of individual polymer chains in determining the molecular weight average. By analysing the retention volumes of the samples in specific chromatography columns and comparing with known standards, GPC allows the determination of the average molecular weight of polymers [31]. The polydispersity index (PDI) is used as a measure of the broadness of a molecular weight distribution of a polymer being defined by the Mw/Mn ratio.

P(TMC-CL) was found to have a relatively high molecular weight (Mn=6.8 x 10^4 Da) and a low polydispersity index (PDI) below 2 (**Figure 3.10, Table 3.4**). Guaranteeing that P(TMC-CL) has a high molecular weight is very important to assure the necessary mechanical properties to allow the preparation of fibres with an elastomeric behaviour [24].

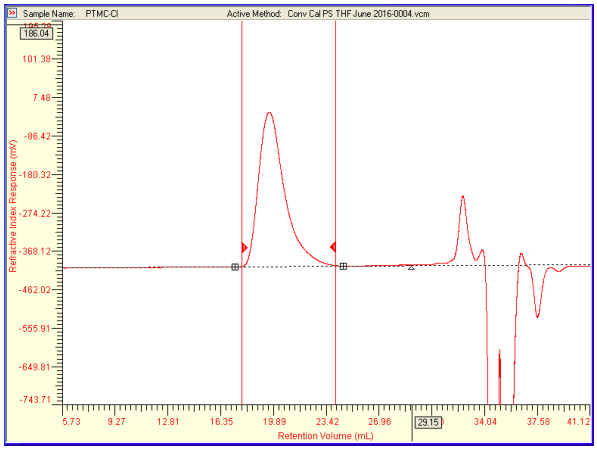

Figure 3.10 *GPC graph for determining P(TMC-CL) molecular weight.*

Table 3.4 *GPC results*.

Polymer molecular weight characteristics	
Mn	6.8 x 10^4
Mw	10.8 x 10^4
PDI (Mw/Mn)	1.58

Legend: ***PDI*** *Polydispersivity index;* ***Mn*** *number average molecular weight;* ***Mw*** *weight average molecular weight.*

P(TMC-CL) nanofibers present similar diameters to CNS axons

In the present study, electrospun fibers were chosen to serve as artificial neurons, hence allowing the specific monitorization of the interaction between oligodendrocytes and astrocytes.

In order to obtain P(TMC-CL) nanofibers with the required characteristics a process of electrospinning optimization was conducted (**Appendix B**). Optimized fibers were obtained using the following conditions: 10% P(TMC-CL) dissolved in DCM:DMF (6:1 ratio) and dispensing it at a flow rate of 0.9mL/h, with an applied voltage of 16kV along a distance of

16cm between the spinneret and the flat collector. P(TMC-CL) nanofibers were observed using high resolution microscopy (SEM) (**Figure 3.11 A,B**) and the distribution of the diameters estimated. The nanofibers were found to have a mean diameter of 0,543 μm ± 0,346 μm with fibers ranging from 0,1μm to 1,9μm (**Figure 3.11 C**).

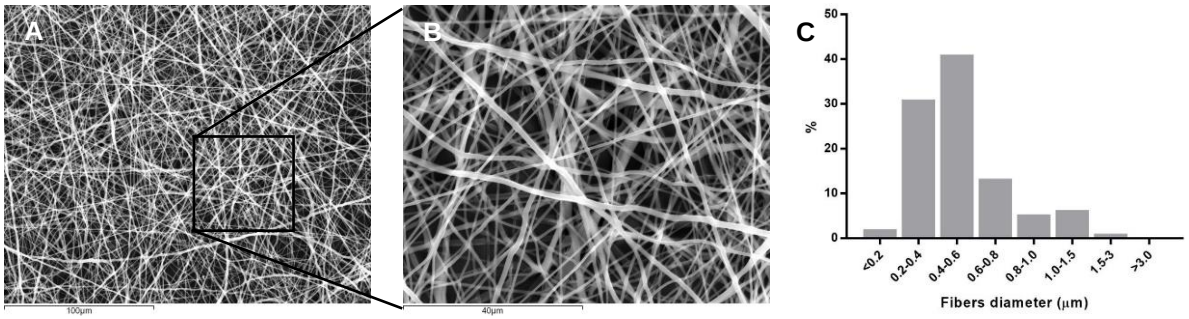

Figure 3.11 *P(TMC-CL) electrospinning nanofibers morphology and diameter distribution measurements.* **A.** and **B.** represent SEM images of optimized electrospinning conditions for P(TMC-CL). Scale bar is depicted in both images. **C.** shows fiber diameter distribution from 100 measurements from three different regions of the glass coverslip.

It has been reported that the majority of CNS myelinated axons have diameters ranging from 0,3μm to 2μm with an average diameter near 1μm [32]. Therefore, P(TMC-CL) fiber diameters close resemble CNS myelinated axons diameters'. Besides, fibers have elongated morphologies and are depicted in a random matrice, facts that make them suitable to mimic axons.

Pure primary rat OPCs and astrocytes cultures were effectively obtained

To investigate if OPCs and astrocytes cultures were free of any other cell type contaminant an immunocytochemistry test against neural cells' characteristic markers was performed. OPC cultures were evaluated for the presence of neurons (through expression of the characteristic marker βIII tubulin [33]), microglia (analysing cell expression of IBA1, a specific calcium binding protein [34]), and astrocytes (for the expression of GFAP, a hallmark of the astrocytes) (**Figure 3.13**). On the other hand, astrocyte cultures were evaluated for the expression of NG2 and MBP (OPC and OL markers, respectively), IBA1 (microglia) and βIII tubulin (neurons) (**Figure 3.12**). Both OPCs and astrocytes were seeded on PLL coated ϕ13 mm glass coverslips (50 000 cells and 30 000 cells per coverslip, respectively) and fixed at day 3 and 5 of culture, respectively. The number of cells that were not astrocytes or oligodendrocytes/OPCs in astrocytes and oligodendrocytes cultures, respectively, was quantified and is shown in **Table 3.5**. Cell culture purity was found to be 92% in both cases**,** which indicates that both cell types were successfully isolated from rat pups' cortex. These results are in accordance with values usually obtained in this kind of primary cell isolation [9, 27].

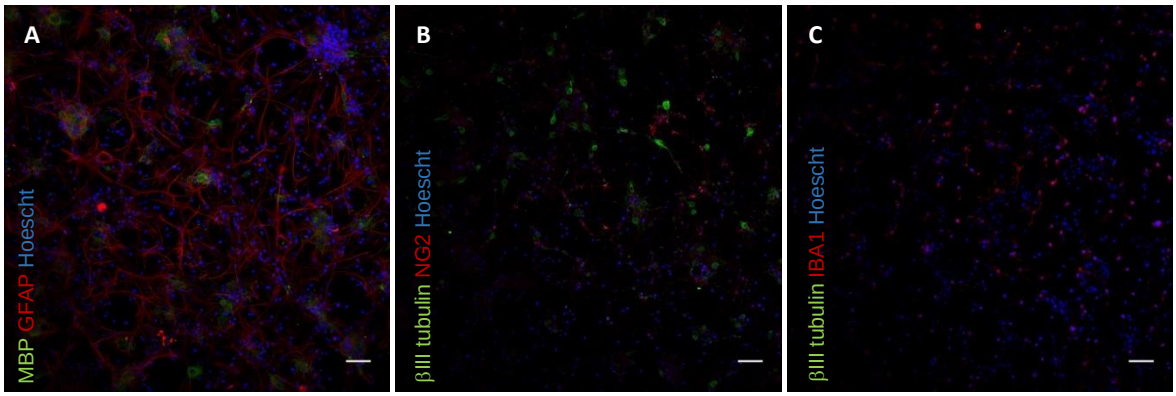

Figure 3.12 *Representative images of astrocytes stained with neuronal and glial characteristic markers.* Staining was made for the presence of oligodendrocytes (MBP) (**A**), neurons (βIII tubulin) (**B** and **C**), OPCs (NG2) (**B**) and microglia (IBA1) (**C**). Scale bar indicates 50μm.

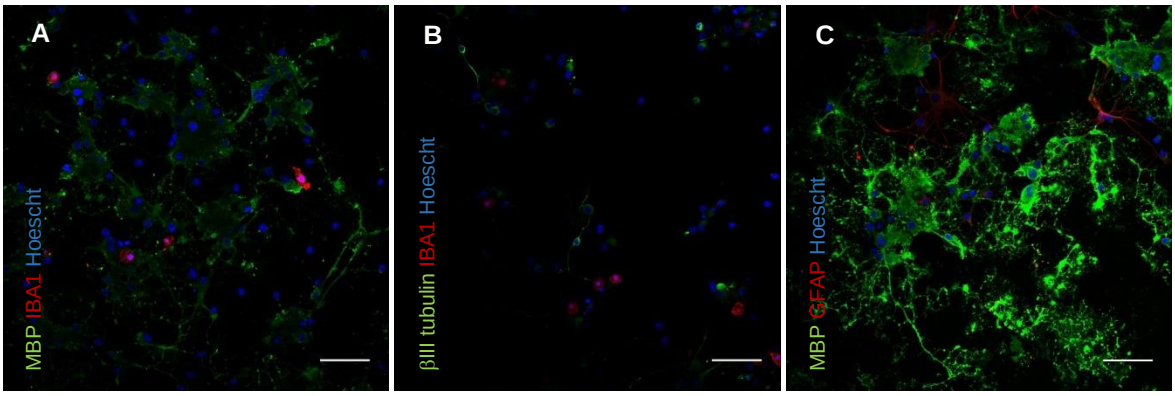

Figure 3.13 *Representative images of oligodendrocytes stained with neuronal and glial characteristic markers.* Staining was made for the presence of microglia (IBA1) (**A** and **B**), neurons (βIII tubulin) (**B**) and astrocytes (GFAP) (**C**). Scale bar indicates 50μm.

Table 3.5 *Quantification of the number of positive cells for non-astrocytic or non oligodendroglial cells in astrocytes and oligodendrocytes cultures, respectively* (n=1).

Positive cells (%)	Astrocyte cultures	OPC cultures
IBA1	6.6	1.8
βIII TUBULLIN	0.3	2.1
MBP	0	-
NG2	0.7	-
GFAP	-	3.4

OPCs are capable to adhere, proliferate and differentiate when cultured on P(TMC-CL) nanofibers

P(TMC-CL) fibers were used to culture OPCs and to serve as surrogate axons. In the presence of appropriate culture medium containing determinant factors for their development, OPCs were found to extensively adhere to fibers. **Figure 3.14** shows a representative bright field confocal image of OPCs cultured with fibers. Engineered nanofibers where therefore proved to be a non-toxic and supportive environment that stimulates oligodendrocytes' adhesion.

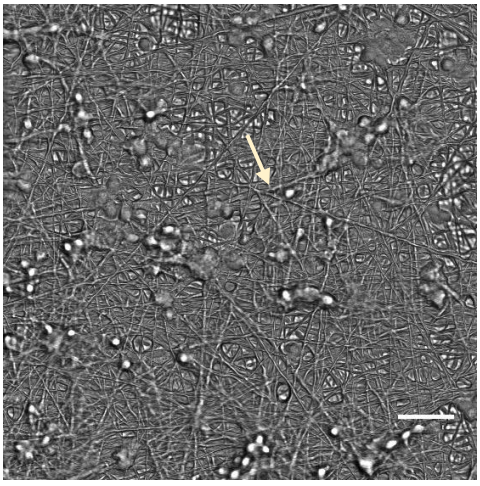

Figure 3.14 *OPC adherence to P(TMC-CL) fibers.* The arrow shows the presence of a cell clearly embedded in the fibers mesh. Scale bar indicates 25μm.

In order to evaluate OPCs' proliferation and differentiation capacities when cultured on the P(TMC-CL) fibers, OPCs were cultured in the presence of OL medium after the culture in proliferation medium for two days. After 1, 3 and 7 days in culture the expression of progenitor or myelin markers (NG2 and MBP, respectively) was evaluated. P(TMC-CL) fibers were found to stimulate proliferation and differentiation of OPCs in a reproducible manner. On the first day, after stimulating cells to differentiate, the majority was extending NG2 processes, indicating a non-differentiated state of the cells (**Figure 3.15, I**). On day 3 it was possible to observe cells with some processes elongated along the fibers (**Figure 3.15, II**). Interestingly, in the last case, at day 7, cells expressing huge and outstanding processes were covering almost all the fiber area (**Figure 3.15, III**). Quantification analysis showed that at day 1, more than 80% of the cells were expressing the progenitor marker NG2 and at day 7, the number of cells expressing NG2 was below 10% of the total cells (**Figure 3.16**).

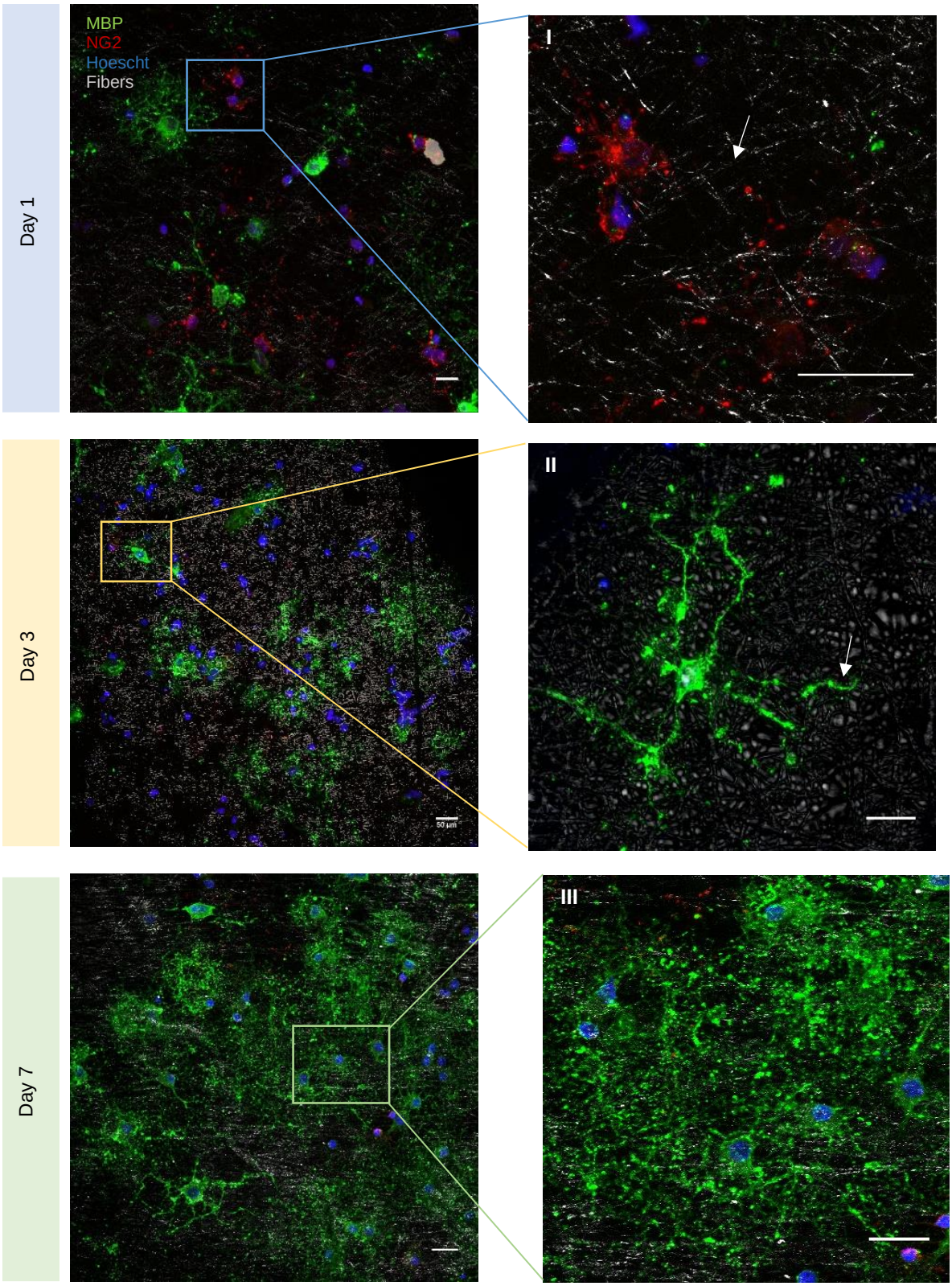

Figure 3.15 *Representative images showing OPC differentiation ability in P(TMC-CL) fibers.* Images I, II and III represent detailed views of the left images. In image I the arrow points out fibers (gray) and in image II a myelin process around a fiber is shown. Scale bar indicates 50μm (images on the left) and 25μm (images on the right).

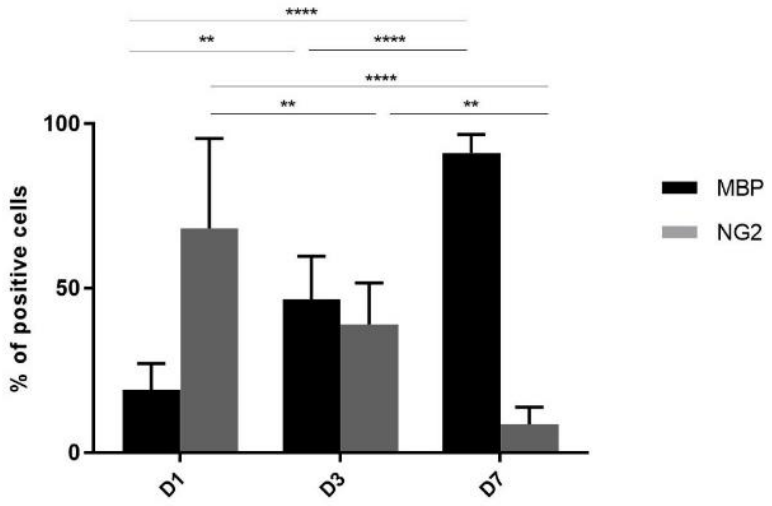

Figure 3.16 *Quantification of the number of cells expressing MBP and NG2 over day 1, 3 and 7 of culture (differentiating conditions).* Results show mean ± standard deviation (n=2 independent experiments), asterisks represents statistical significance (** $p < 0.01$, **** $p < 0.0001$). Statistical analysis was performed using two-way ANOVA and Tukey's multiple comparisons test.

In addition, to quantify the mRNA levels of the myelin marker, qPCR for MBP was performed. Gene expression profile of OPCs cultured on fibers corroborates the previous observation shown by immunocytochemistry: MBP expression increased over the period of culture (**Figure 3.17**). Although just one experiment was performed the visible tendency of OPCs to augment the expression of the *Mbp* gene is in accordance with the expectations. Moreover, it was also noticed that the MBP expression was more prominent in P(TMC-CL) than in glass coverslip controls, highlighting the added value of a 3D microenvironment when trying to mimic *in vivo* conditions. The presented results are in accordance with the ones previously reported by the group (data not published) [27].

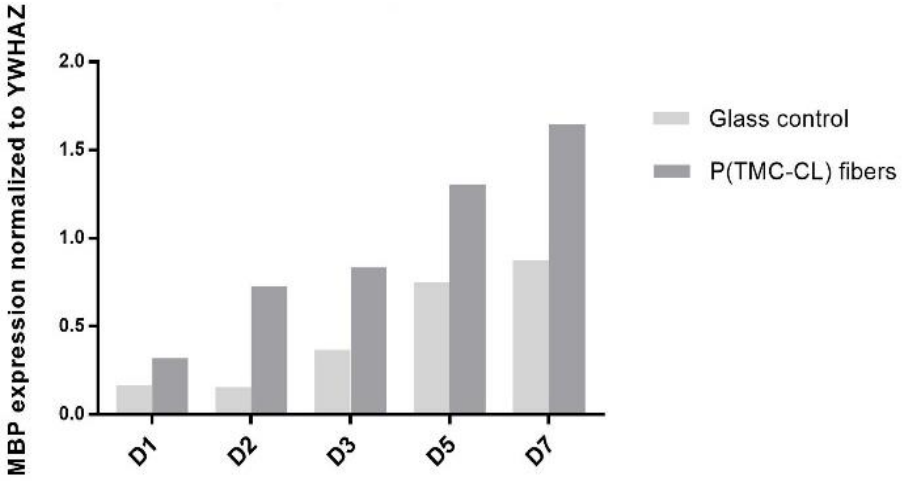

Figure 3.17 *mRNA levels of OPCs cultured either in P(TMC-CL) fibers or in PLL-coated glass coverslips at days 1, 2, 3, 5 and 7. Mbp* expression was normalized to the housekeeping gene *Ywhaz* (n=1).

Using engineered fibers to act as surrogate axons was previously explored by other groups. Howe *et al*, in 2006, showed that Matrigel® coated glass microfibers and vicryl microfibers can act as axons, wrapping myelin in the presence of a cell line of pre-myelinating oligodendrocytes [21]. Besides, Lee and co-workers have used aligned polystyrene electrospinning fibers with a diverse range of diameters to study myelination in closer detail [22]. Therefore, these studies sustain the reliability of this platform as a simple methodology to eliminate axon-OPC crosstalk. However, in the last study, OPC differentiation was achieved after long periods of culture (15 days [22]). Here, cells were shown to be differentiated in a rapid period of time, highlighting the advantages of using P(TMC-CL) fibers regarding polystyrene fibers. These polymers have distinct mechanical properties, which can influence the behaviour of OPCs and their myelination capacities [35]. Therefore, the proposed platform is relevant to obtain significant myelination in a short period of time.

Moreover, it was also observed that OPC differentiation occurs without any additional stimulus besides the seeding on P(TMC-CL) fibers. The fact that these polymeric fibers did not need the commonly used adhesion coating molecules (e.g. poly-lysine) to promote OPC adhesion is an advantage over other similar studies that use fibers to mimic axons and contradicts the postulate that fiber coating is fundamental for OPC differentiation *in vitro* [22]. Therefore, it can be hypothesized that, although interactions between axons and OPCs are crucial to trigger the correct process of myelination, OPC differentiation may not be totally dependent on these signals.

Furthermore, this *in vitro* 3D axonal myelination platform reveals to be advantageous regarding the traditionally used strategies to study myelination. Over time, researchers have gained insight on myelination processes using neurons-OPCs co-cultures. However, these are time consuming and have high associated costs. Besides, so far there is no *in vitro* model of myelination derived uniquely from CNS cells. Conventional models rely on the use of co-cultures of OPCs and dorsal-root ganglia (DRG) neurons [36]. However, these are not purely CNS neurons thus a reliable CNS *in vitro* myelination model remains to be established [37].

Astrocytes remain viable in alginate hydrogels and fibroblast conditioned medium is capable of activating astrocytes cultures

Astrocytes were cultured in 1% (w/v) alginate matrices either in the presence of meningeal fibroblast CM or astrocytic normal culture medium (termed DMEM) and their viability was analysed at day 1, 3 and 7 of culture by a live-dead assay (**Figure 3.18A**). Quantification of the live and the dead cells showed no statistical significant differences between both media and throughout the culture period, although at day 7 a slight decrease in the number of live cells was observed in both conditions (**Figure 3.18B**).

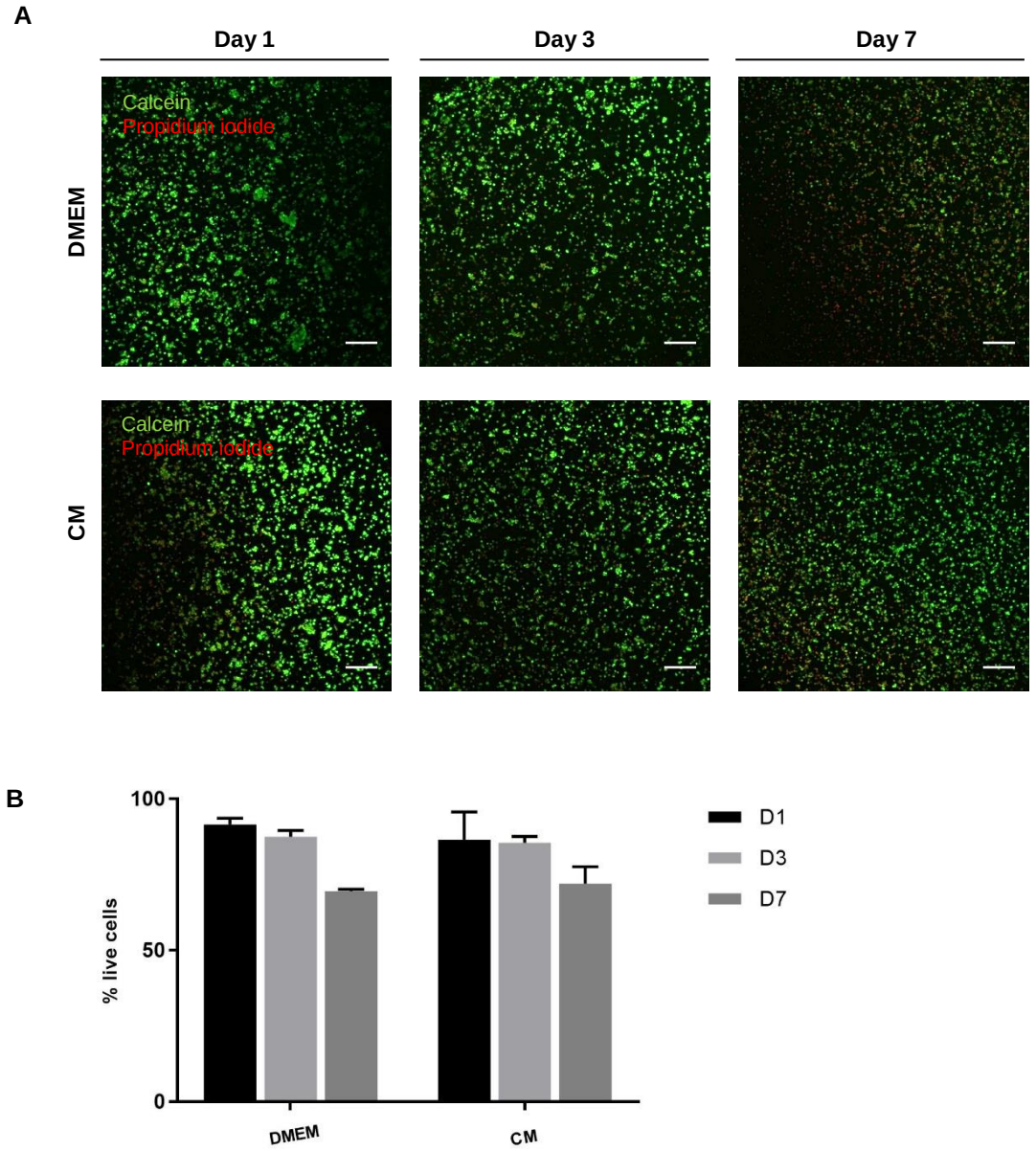

Figure 3.18 *Evaluation of the viability of astrocytes within alginate discs at day 1, 3 and 7.* **A.** Representative images of the live-dead assay. Astrocytes cultured either with DMEM (top) or CM (bottom) were stained with Calcein-AM (green, showing the live cells) and propidium iodide (red, representing the death cells). Scale bar represents 100 μm. **B.** Quantification of the live cells by image analysis (ImageJ). Results show mean ± standard deviation (n=2). No statistical significance among conditions or days was found.

It is worth noting that, contrarily to what has been commonly described in the production of alginate matrices for cell culture, in this study no cell adhesion motif was used. Since cells do not have cell receptors that recognize alginate, some cell adhesion molecules have been used to modify alginate matrices. The most studied case is the sequence arginine–glycine–aspartate (RGD), which was proved to promote cell adaptability to the hydrogels [15]. However, in this case, cells show adequate survival levels and adaptability to the discs which allowed the progression of the present work.

Furthermore, in order to assess the effect of fibroblasts CM on astrocyte phenotype, GFAP fluorescence levels were analysed at day 3 of culture in astrocytes cultured on PLL coated glass coverslips in the presence of DMEM or CM (**Figure 3.19**). This time point was chosen based on our previous observations [9]. It was clearly visible that, in comparison with astrocytes cultured in the presence of DMEM, GFAP fluorescence levels were significantly increased in astrocytes cultured in the presence of CM. Although a quantification of the number of cells expressing GFAP was not performed, based on observations, the number of astrocytes expressing this marker was also superior in CM.

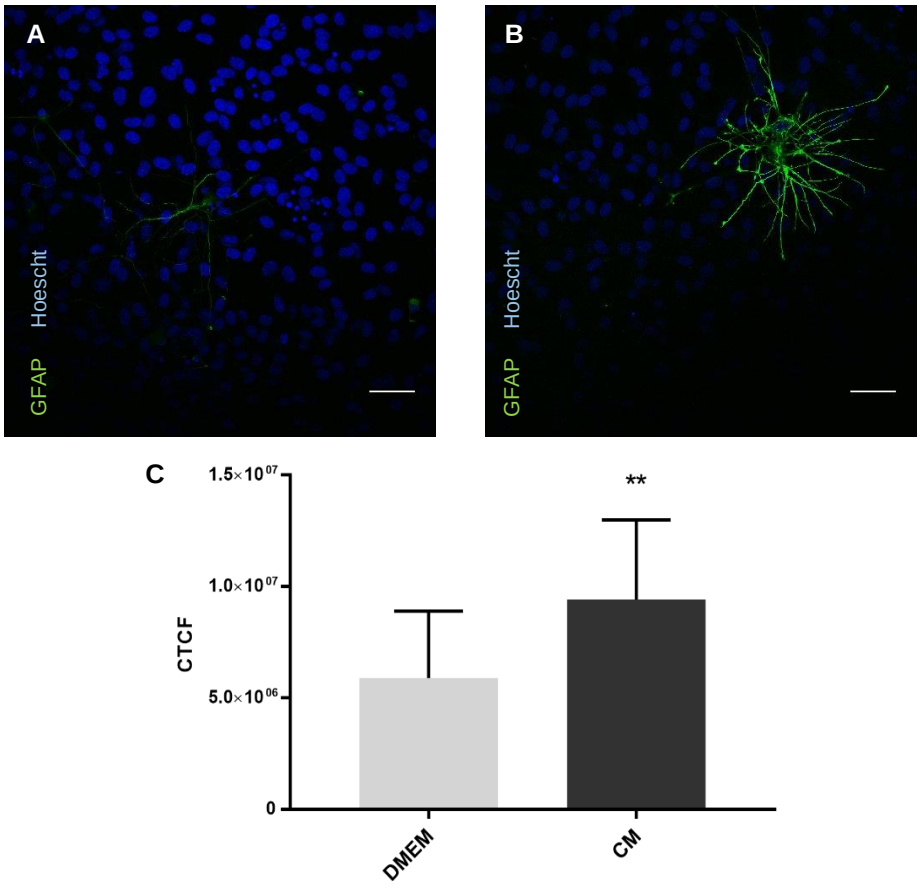

Figure 3.19 *Astrocyte activation by fibroblast conditioned medium at day 3.* **A** and **B**. Representative photos of astrocytes cultured in a glass coverslip in the presence of control medium (A) and fibroblast CM (B). Scale bar 10μm. **C**. Fluorescence intensity quantification by for the expression of GFAP from 10 measurements representing 10 different regions of the coverslip. Results show mean ± standard deviation (n=2) and asterisks represent statistical significances (** $p < 0.01$). Statistical analysis was performed using a *t*-test assuming that there is no Gaussian distribution (non-parametric test) and using Mann-Whitney test (comparing ranks). CTCF represents corrected total cell fluorescence (CTCF = Integrated density – (area of selected cell x mean fluorescence of background readings)).

It is well established that after an insult in the CNS astrocytes change their morphological characteristics to respond to the injury in a process termed astrogliosis. In this process, the expression of proteins, such as GFAP, vimentin and CSPGs is increased. Moreover,

astrocytes start to produce high amounts of ECM characteristic molecules (like collagen IV) and these events culminate in the formation of a glial scar [38]. The glial scar, although mainly composed by astrocytes, also has a fibrotic component derived from meningeal fibroblasts that leave the damaged meninges and infiltrate the local of the lesion. Fibroblasts rapidly proliferate and start secreting ECM components (collagen IV, fibronectin, etc.) therefore contributing to this repair tissue. Together with astrocytes, fibroblasts close the damaged tissue and prevent further invasion of inflammatory cells [39]. The use of meningeal fibroblast CM as a stimulus to trigger astrogliosis was previously reported by the group [9], and the evaluation of the astrocytes' behaviour in the presence of meningeal fibroblast medium was performed with accurate and careful detail, concluding that the gene expression levels of GFAP were significantly increased, as well as the production of CSPG and collagen. Besides, it was also seen that CM activated astrocytes significantly inhibit neuronal outgrowth [9]. For that reason, in the context of this project the 3D engineered astrogliosis model of astrocytes was assumed to be successfully reproduced.

Other approaches to induce the activation of astrocytes have been tried and are described in the literature. For example, Kimura-Kuroda and co-workers established a model in which astrocytes were co-cultured with meningeal fibroblasts and TGF-β1 (a factor involved in the formation of the glial scar) was added to the culture [40]. Jang *et al* [41] have used astrocyte-conditioned media derived from astrocytes cultured in the presence of toll-like receptor ligands (lipopolysaccharide, LPS) or cytokines (IL-4 or IL-10). Moreover, East and colleagues proposed a model of reactive astrogliosis using a 3D collagen gel system in which astrocytes were seeded in addition to TGF-β1 to trigger the reactive phenotype showed by astrocytes in astrogliosis [42].

However the simplicity of the system here described and the fact that the astrocyte survival does not depend on the use of an ECM component makes it advantageous regarding the other established models, and allows the study of a broader range of variables.

OPC differentiation is impaired by activated astrocytes

The 3D glial scar model was then used in combination with the axonal myelination system aiming to study the effects of astrocyte activation in the normal course of OPC differentiation. With that in mind, expression of MBP and NG2 was observed at days 1, 3 and 7 after co-culturing (**Figure 3.20**). When OPCs were cultured with activated astrocytes, a significant decrease in the number of cells producing the myelin sheath was visually perceived. Despite not having performed a quantification for the number of cells expressing MBP and NG2 over days, these effects are more preeminent at day 3 after adding the transwell with the alginate discs to the OPCs cultured on fibers. It is worth to highlight that these observations are in accordance with data previously described by the group (not published) [27].

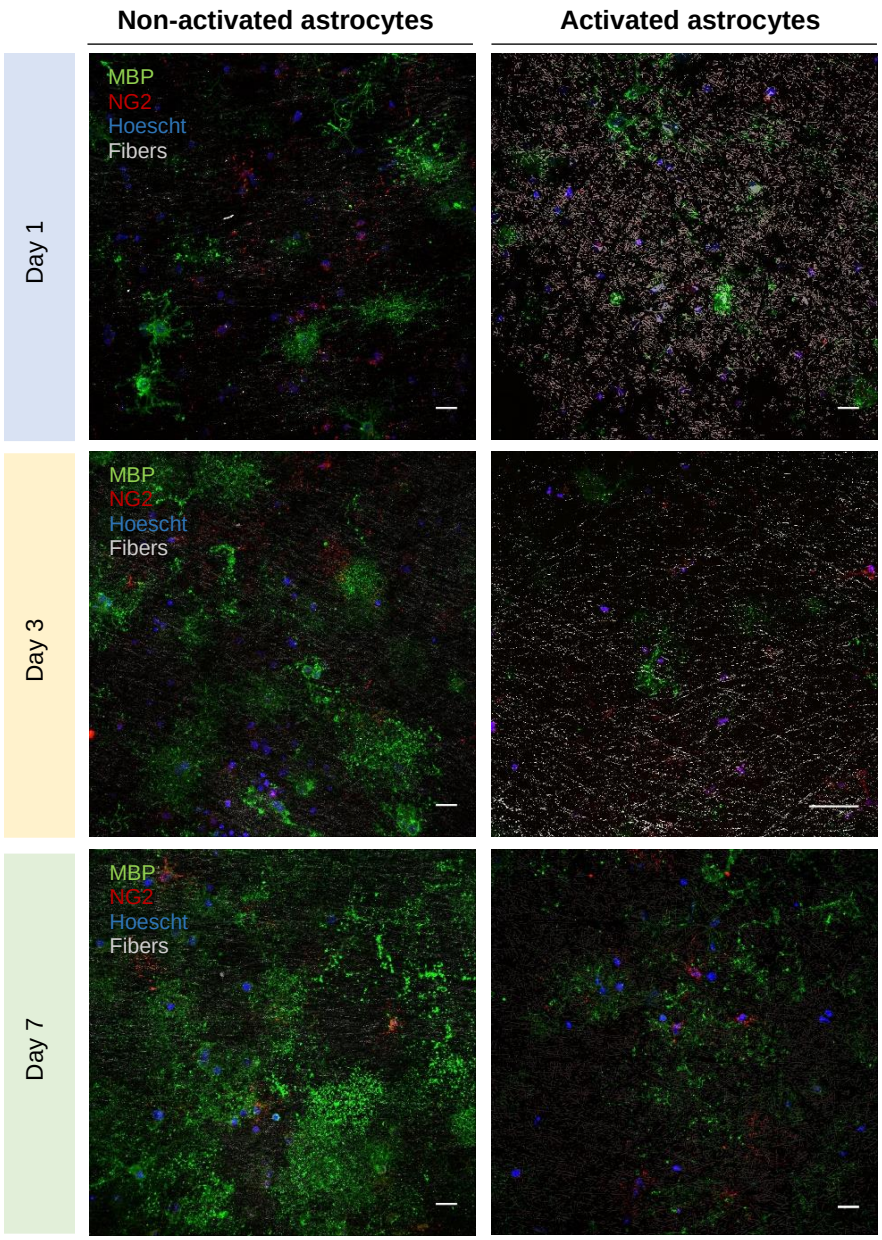

Figure 3.20 *OPC differentiation impairment by reactive astrocytes.* Representative photos of MBP and NG2 immunostaining after co-culturing with non-activated (left) or activated (right) astrocytes. There is a visible reduction in the number of cells expressing MBP when astrocytes were activated with fibroblast CM. Scale bar 50μm.

Furthermore, the expression levels of *Mbp* in both conditions was analysed recurring to qRT-PCR (**Figure 3.21**).

Firstly, the MBP expression of OPCs cultured in fibers in the presence or absence of non-activated astrocytes was evaluated. Surprisingly, no statistical differences were seen between the conditions (**Figure 3.21A**). In the literature, it is well-established that astrocytes support oligodendrocytes' functions by producing, among others, PDGFα and FGF which are potent mitogens that promote OPC survival and self-renewal, inhibiting the premature differentiation

of OPCs [43-45]. Co-culturing astrocytes with OPCs would resemble better the *in vivo* conditions. Although an increase in the expression of MBP was observed for co-cultures, the fact that no statistical significance was seen may be due to protocol limitations in the extraction of the OPCs RNA. Besides, the number of experiments performed was not sufficient to take accurate conclusions (two independent experiments). Moreover, a deep study about the factors that non-activated astrocytes were producing when co-cultured with OPCs was not performed. It is also worth noting that although not determinant, the physical contact between astrocytes and oligodendrocytes (namely through the interaction of laminin in astrocytes and $\alpha 6\beta 1$ integrin in oligodendrocytes) positively influences the maturation of oligodendrocytes [43, 46]. In this co-culture method, the physical contact is not established; therefore this may influence the processes of OPC myelination.

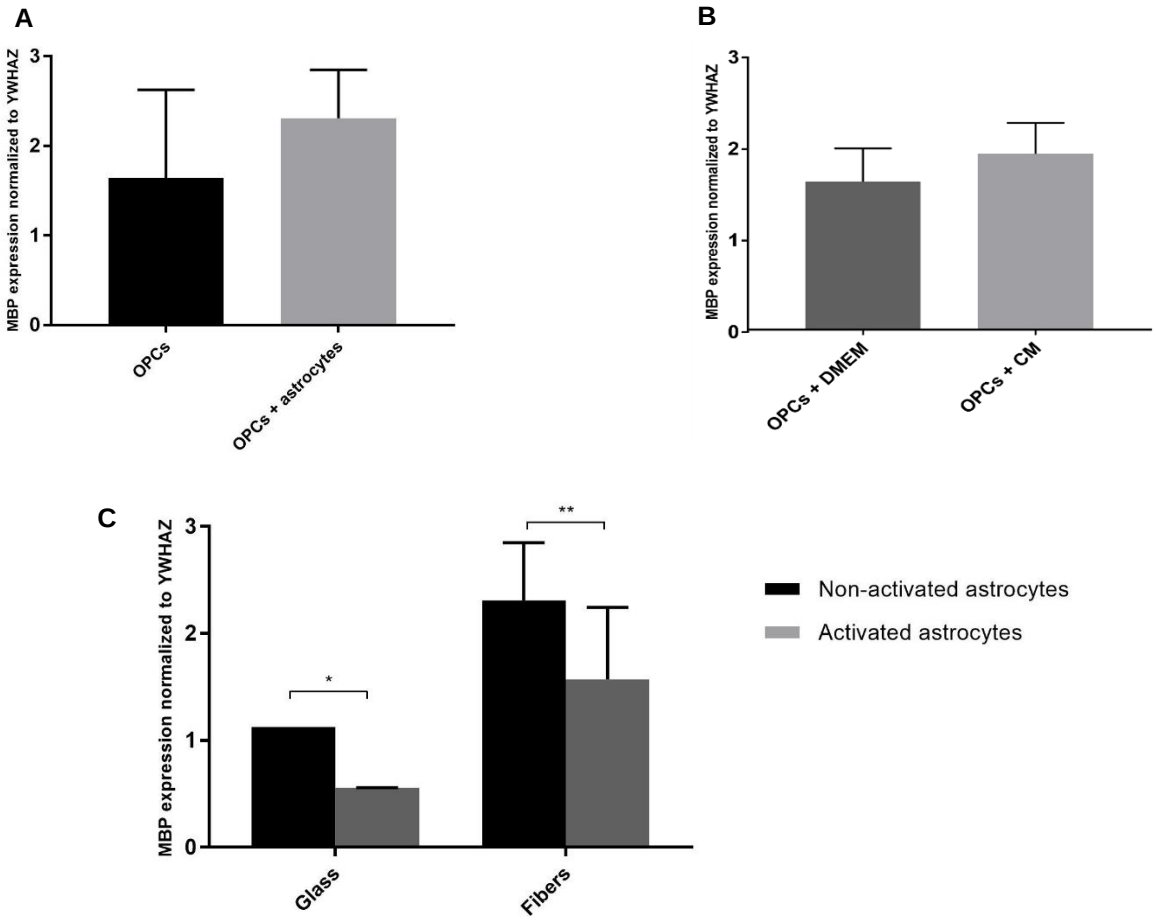

Figure 3.21 *Mbp gene expression levels of OPCs after co-culturing with astrocytes.* **A**. Comparison between the expression levels of OPCs cultured on P(TMC-CL) fibers with OPCs cultured in the presence of non-activated astrocytes. Results show mean ± standard deviation. **B**. Evaluation of the effects of the flux of the medium provided by the transwell on OPC *Mbp* gene expression. Statistical analysis was performed using unpaired t-test (non-parametric) followed by Mann-Whitney test (n=2). No statistical differences between conditions were found. **C.** Comparison between co-cultures in P(TMC-CL) fibers and glass coverslips (n=3). Statistical analysis was performed using two-way ANOVA followed by Tukey's test (n=2). Results show mean ± standard deviation, asterisks represent statistical significance (* $p < 0.05$, ** $p < 0.01$).

Secondly, the influence of the activated state of astrocytes in the course of OPC *Mbp* expression was assessed. A significant decrease in the expression levels of the *Mbp* gene in OPCs when cultured with activated astrocytes was noted. It is worthwhile mentioning that also in OPCs seeded on PLL coated glass coverslips or on P(TMC-CL) fibers the reduction of the levels of MBP was observed (**Figure 3.21C**).
Besides, in order to understand if this effect was due to the CM flow across the transwell, and not due to the activated state of astrocytes, the expression levels of *Mbp* in OPCs cultured with a transwell without astrocytes and filled with DMEM or CM were also measured (**Figure 3.21B**). When comparing *Mbp* gene expression of OPCs cultured with DMEM (without astrocytes) and CM (without astrocytes), no significant differences were observed. However, the differences of the expression of *Mbp* in OPCs cultured with activated astrocytes or cultured without astrocytes but in the presence of CM could not be assessed due to the insufficient number of experiments that were performed. Nevertheless, it is not expectable that the CM exerts an effect *per se* once so far, no study in the literature reports the influence of meningeal fibroblasts or their paracrine signals in OPC differentiation.

The role of astrocytes in processes of myelination and demyelination has been a theme of intense debates and contradictions among biologists [14, 38, 47].
On one hand, reactive astrocytes are viewed as protective tools for injured CNS, preventing inflammatory cells' infiltration through the formation of a glial scar, which is mostly composed by interwoven and tightly connected astrocytes. In the first stages of injuries, astrocytes are believed to be paramount in closing the lesion site, promoting the tissue homeostasis and modulating inflammatory responses [48]. When thinking about remyelination processes, some studies reported that oligodendrocytes show a tendency to remyelinate zones where astrocytes are present, therefore making astrocytes a key component in the process [49].
Nonetheless, other studies report that glial scar rigidity is an obstacle to the entry of OPCs and axons to the lesion sites, thereby inhibiting normal remyelination [47]. Following that point of view, astrocytes could inhibit remyelination either by forming a glial scar or by preventing OPC migration and maturation to the lesion sites. In fact, the astrocytic marker of astrogliosis, GFAP was extensively found in old demyelinated plaques of MS patients [50]. Besides, in the EAE mouse model of demyelination, just a few numbers of OPCs was found to penetrate the glial scar and many were found around the demyelinating lesion local [51, 52]. Corroborating this, other study reported that an extensive number of cells expressing NG2 in the glial scar was found [53]. NG2 is a distinctive marker of oligodendrocyte progenitors and these cells in the glial scar may be cells that are unable to differentiate in oligodendrocytes. In fact, evidences that the processes of differentiation and maturation of OPCs may also be modulated by astrocytes have been shown. Firstly, astrocytes secrete factors that promote OPCs' self-renewal and not the switch to a differentiation phenotype. Moreover, activated astrocytes express high amounts of matrix metalloproteinases (MMPs). Namely, it was observed that

MMP2 is the most activated enzyme in conditions of astrogliosis and that this enzyme degrades MBP [54]. Also, it was seen that the suppression of MMPs in the EAE mouse model attenuates the effects of demyelination [55]. The activity of MMPs is counteracted by specific inhibitors (tissue inhibitors of metalloproteinases, TIMPs), however, in opposite to the augmented expression of MMPs seen in demyelinating plaques, TIMPs expression maintains unaltered [56]. Moreover, after activation, astrocytes secrete various cytokines, including Interleukin 1, 3, 6 (IL-1, IL-6, IL-3) and tumour necrosis factor alpha (TNF-α) [57]. Su and co-workers provided the first evidence that after spinal cord injury, OPC apoptosis and inhibition of differentiation capacity is induced by TNF-α secreted by reactive astrocytes [58]. Another study that reports the possible negative effects of reactive astrocytes in remyelination processes was conducted by Blakemore *et* al [59] that transplanted OPCs to either to areas of demyelination where astrocytes were presented or absence and conclude that the presence of astrocytes was a hallmark in the extent of oligodendrocyte remyelination. Moreover, Wang and co-workers also provided evidences that reactive astrocytes derived from an injured spinal cord inhibit OPC differentiation. In their study, the expression of bone morphogenic proteins was augmented in the damaged spinal cord and the inhibition of the expression of these proteins revealed a reversion of the OPC phenotype [60].

In this study, activated astrocytes were seen to negatively impact the course of OPC differentiation revealed by the decreased expression of MBP when OPCs were cultured with activated astrocytes. Contrarily, Nash *et al* [61] demonstrated that the induction of a quiescent state in astrocytes is not beneficial for OPC remyelination and that the induction of a switch to a reactive astrocytes may lead to an enhanced myelination by OPCs. All together, these studies point out to the fact that despite there are still contradictory evidences, the astrocyte-OPC crosstalk in the modulation of OPC differentiation after an injury is of extreme importance.

Ibuprofen effects on OPC differentiation

Understanding the mechanisms that are behind the possible negative effects of activated astrocytes on OPCs may be key to find possible solutions and new targets to induce remyelination in injured areas.

Previously, the Rho/ROCK signalling pathway was identified as the possible biochemical pathway that triggers the reactivity of astrocytes within alginate based matrices and RhoA was seen to mediate this process. When RhoA activity was inhibited with ibuprofen astrocytes reverted their phenotypes to non-activated decreasing the expression of GFAP and vimentin [9]. Ibuprofen is a non-steroidal anti-inflammatory drug that is also known to block RhoA intracellular signal and, in this manner promote axonal regrowth after an injury [62]. For that reason, ibuprofen was used to determine if the effects of activated astrocytes in OPCs differentiation could be reverted by reverting the astrocyte phenotype to a non-activated status.

The *Mpb* gene expression of OPCs cultured in the presence of activated astrocytes was determined by qPCR 48h after adding ibuprofen to the astrocyte culture media (**Figure 3.22**).

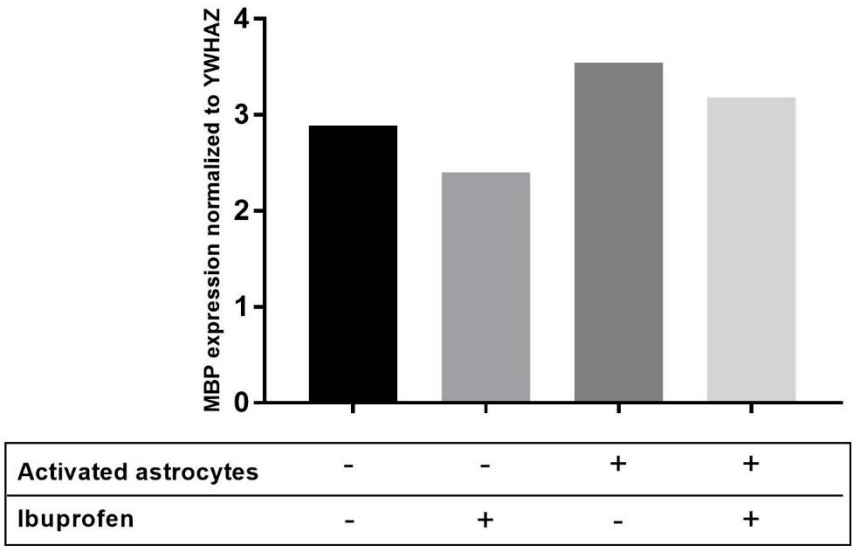

Figure 3.22 *Mbp gene expression levels of OPCs after addition of ibuprofen to the alginate discs* (n=1 independent experiment).

Contrary to expectations, after the treatment with ibuprofen, the *Mbp* expression in activated astrocytes remained similar to non-treated astrocytes. Nevertheless when an immunocytochemistry in the same conditions was performed, an increase in the number of MBP positive cells when OPCs were cultured with activated astrocytes was observed (**Figure 3.23**).

Although this experiment was just performed once, it is in accordance with the previous developed work where MBP protein expression was evaluated [27].

These contradictory results may be explained by timeline in which genetic and proteic expression happen. Once genes are expressed earlier than proteins the time in which the ibuprofen effects was analysed by genetic expression may be not adequate. Besides, the mRNA production is known to happen in a lower rate than proteins and mRNA is less stable than proteins (half-life of 2.6-7h to mRNAs and 46h to proteins) [63]. Therefore the range of gene expression in which ibuprofen effects are analysed should be further studied.

Nevertheless, no definitive conclusion from this study can be taken once both experiments (immunocytochemistry and qRT-PCR) were just performed once.

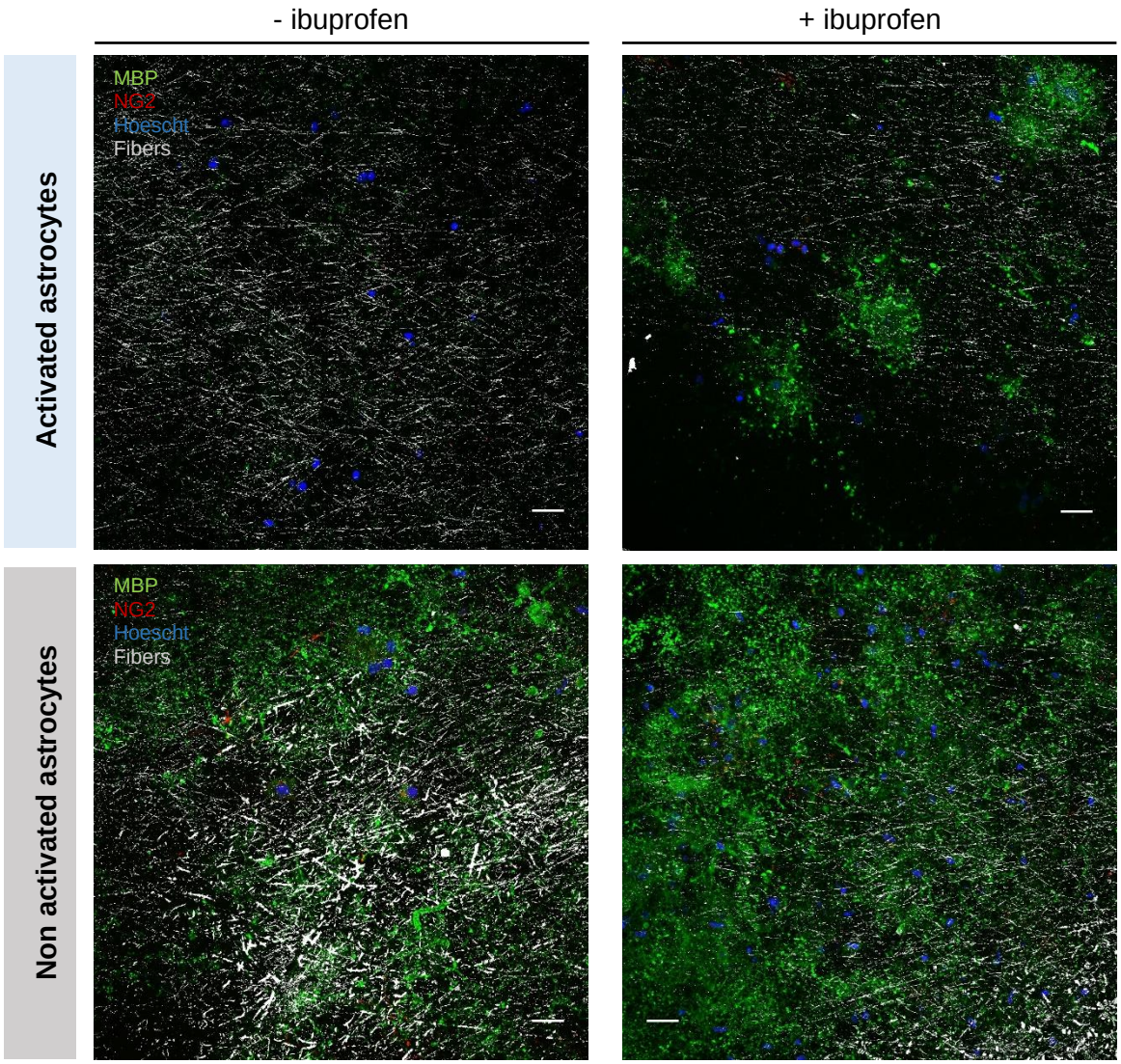

Figure 3.23 *OPCs after addition of ibuprofen to the alginate discs* (n=1 independent experiment). Representative photos of NG2 and MBP positive OPCs/oligodendrocytes cultured with treated (left) or non-treated (right) astrocytes (non-activated, bottom or activated, top). Scale bar 25μm.

CONCLUSIONS

To sum up, these evidences show a key role of astrocytes in the course of remyelination or demyelination processes and also, when considering therapeutical strategies to demyelinating diseases, astrocytes should definitely not be neglected as they may be a potential therapeutic target to these diseases.

Besides, the present study shows that the previously established *in vitro* myelinating platform composed of P(TMC-CL) electrospinning fibers is, in fact, capable of mimicking axons by significantly promoting the normal course of OPC differentiation, highlighting the importance of a 3D microenvironment for the normal cells' behaviour. Moreover, this platform is also interesting to specifically study the interactions between oligodendrocytes and astrocytes dissociated from the effects of axonal signalling. Finally, this platform also shows a huge potential to screen drugs or potential therapeutical molecules for demyelinating diseases.

REFERENCES

1. Prayoonwiwat, N. and M. Rodriguez, *The potential for oligodendrocyte proliferation during demyelinating disease.* J Neuropathol Exp Neurol, 1993. **52**(1): p. 55-63.
2. Franklin, R., *Why does remyelination fail in multiple sclerosis?* Nature Reviews Neuroscience, 2002. **3**(9): p. 705-714.
3. Baer SB, S.Y., Kang SU, Mitteregger D, Vig R, Ffrench-Constant C, Franklin RJM, Altmann F, Lubec G, Kotter MR *Myelin-mediated inhibition of oligodendrocyte precursor differentiation can be overcome by pharmacological modulation of Fyn-RhoA and protein kinase C signalling.* Brain, 2009. **132**: p. 465-481.
4. Pedraza, C.E., et al., *Induction of oligodendrocyte differentiation and in vitro myelination by inhibition of rho-associated kinase.* ASN Neuro, 2014. **6**(4).
5. Zhao, C.F., et al., *Rnh1 promotes differentiation and myelination via RhoA in oligodendrocytes.* Cell Tissue Res, 2013. **353**(3): p. 381-9.
6. Hall, A. and C.D. Nobes, *Rho GTPases: molecular switches that control the organization and dynamics of the actin cytoskeleton.* Philos Trans R Soc Lond B Biol Sci, 2000. **355**(1399): p. 965-70.
7. Hering, T.M., et al., *Proteoglycans of reactive rat cortical astrocyte cultures: Abundance of N-unsubstituted glucosamine-enriched heparan sulfate.* Matrix Biol, 2015. **41**: p. 8-18.
8. Liesi, P. and T. Kauppila, *Induction of Type IV collagen and other basement-membrane associated proteins after spinal cord injury and the adult rat may participate in formation of the glial scar.* Exp. Neurol., 2002. **173**: p. 31-45.
9. Rocha, D.N., et al., *Extracellular Environment Contribution to Astrogliosis – Lessons learned from a Tissue Engineered 3D Model of the Glial Scar.* Front. Cell. Neurosci., 2015. **9:377**.
10. Wang Y, et al., *Astrocytes from the contused spinal cord inhibit oligodendrocyte differentiation of adult oligodendrocyte precursor cells by increasing the expression of bone morphogenetic proteins.* J Neurosci. , 2011. **31**(16): p. 6053-8.
11. Su Z, et al., *Reactive astrocytes inhibit the survival and differentiation of oligodendrocyte precursor cells by secreted TNF-α.* J Neurotrauma, 2011. **28**(6): p. 1089-100.
12. García-Álvarez I, et al., *Inhibition of glial proliferation, promotion of axonal growth and myelin production by synthetic glycolipid: A new approach for spinal cord injury treatment.* Restor Neurol Neurosci., 2015.
13. RJ, F., *Why does remyelination fail in multiple sclerosis? .* Nat Rev Neurosci, 2002. **3**: p. 705-714.
14. Williams, A., G. Piaton, and C. Lubetzki, *Astrocytes--friends or foes in multiple sclerosis?* Glia, 2007. **55**(13): p. 1300-12.
15. Lee, K.Y. and D.J. Mooney, *Alginate: properties and biomedical applications.* Progress in polymer science, 2012. **37**(1): p. 106-126.
16. Rowley, J.A., G. Madlambayan, and D.J. Mooney, *Alginate hydrogels as synthetic extracellular matrix materials.* Biomaterials, 1999. **20**(1): p. 45-53.
17. Banerjee, A., et al., *The Influence of Hydrogel Modulus on the Proliferation and Differentiation of Encapsulated Neural Stem Cells.* Biomaterials, 2009. **30**(27): p. 4695-4699.
18. Bhardwaj, N. and S.C. Kundu, *Electrospinning: a fascinating fiber fabrication technique.* Biotechnol Adv, 2010. **28**(3): p. 325-47.
19. Pires, L.R., et al., *Ibuprofen-loaded poly(trimethylene carbonate-co-epsilon-caprolactone) electrospun fibres for nerve regeneration.* J Tissue Eng Regen Med, 2013.
20. Perge, J.A., et al., *Why do axons differ in caliber?* J Neurosci, 2012. **32**(2): p. 626-38.
21. Howe, C.L., *Coated glass and vicryl microfibers as artificial axons.* Cells Tissues Organs, 2006. **183**(4): p. 180-94.

22. Lee, S., et al., *A culture system to study oligodendrocyte myelination-processes using engineered nanofibers.* Nature methods, 2012. **9**(9): p. 917-922.
23. Fukushima, K., *Poly(trimethylene carbonate)-based polymers engineered for biodegradable functional biomaterials.* Biomater Sci, 2016. **4**(1): p. 9-24.
24. Pêgo, A.P., et al., *Copolymers of trimethylene carbonate and ε-caprolactone for porous nerve guides: Synthesis and properties.* Journal of Biomaterials Science, Polymer Edition, 2001. **12**(1): p. 35-53.
25. Pêgo, A.P., et al., *Influence of Catalyst and Polymerization Conditions on the Properties of 1,3-Trimethylene Carbonate and ε-Caprolactone Copolymers.* Macromolecular Chemistry and Physics, 2003. **204**(5-6): p. 747-754.
26. Pego, A.P., et al., *Adhesion and growth of human Schwann cells on trimethylene carbonate (co)polymers.* J Biomed Mater Res A, 2003. **67**(3): p. 876-85.
27. Rocha, D.N., *Impact of Mechanotrasduction in the Context of Central Nervous System Diseases (Unplublished doctoral thesis)*. 2015, University of Porto: Portugal.
28. McCarthy, K.D. and J. de Vellis, *Preparation of separate astroglial and oligodendroglial cell cultures from rat cerebral tissue.* The Journal of Cell Biology, 1980. **85**(3): p. 890-902.
29. Chen, Y., et al., *Isolation and culture of rat and mouse oligodendrocyte precursor cells.* Nat Protoc, 2007. **2**(5): p. 1044-51.
30. Maia, F.R., et al., *Matrix-driven formation of mesenchymal stem cell-extracellular matrix microtissues on soft alginate hydrogels.* Acta Biomater, 2014. **10**(7): p. 3197-208.
31. Bouvier, E.S.P. and S.M. Koza, *Advances in size-exclusion separations of proteins and polymers by UHPLC.* TrAC Trends in Analytical Chemistry, 2014. **63**: p. 85-94.
32. Duncan, D., *A relation between axon diameter and myelination determined by measurement of myelinated spinal root fibers.* The Journal of Comparative Neurology, 1934. **60**(3): p. 437-471.
33. Moskowitz, P.F., et al., *Expression of the class III beta-tubulin gene during axonal regeneration of rat dorsal root ganglion neurons.* J Neurosci Res, 1993. **34**(1): p. 129-34.
34. Ohsawa, K., et al., *Microglia/macrophage-specific protein Iba1 binds to fimbrin and enhances its actin-bundling activity.* J Neurochem, 2004. **88**(4): p. 844-56.
35. Lourenco, T., et al., *Modulation of oligodendrocyte differentiation and maturation by combined biochemical and mechanical cues.* Sci Rep, 2016. **6**: p. 21563.
36. Wood, P., E. Okada, and R. Bunge, *The use of networks of dissociated rat dorsal root ganglion neurons to induce myelination by oligodencrocytes in culture.* Brain Res, 1980. **196**(1): p. 247-52.
37. Pang, Y., et al., *Neuron-oligodendrocyte myelination co-culture derived from embryonic rat spinal cord and cerebral cortex.* Brain and Behavior, 2012. **2**(1): p. 53-67.
38. Barnett, S.C. and C. Linington, *Myelination: do astrocytes play a role?* Neuroscientist, 2013. **19**(5): p. 442-50.
39. Kawano, H., et al., *Role of the lesion scar in the response to damage and repair of the central nervous system.* Cell and Tissue Research, 2012. **349**(1): p. 169-180.
40. Kimura-Kuroda, J., et al., *An in vitro model of the inhibition of axon growth in the lesion scar formed after central nervous system injury.* Mol Cell Neurosci, 2010. **43**(2): p. 177-87.
41. Jang, E., et al., *Phenotypic polarization of activated astrocytes: the critical role of lipocalin-2 in the classical inflammatory activation of astrocytes.* J Immunol, 2013. **191**(10): p. 5204-19.
42. East, E., J.P. Golding, and J.B. Phillips, *A versatile 3D culture model facilitates monitoring of astrocytes undergoing reactive gliosis.* J Tissue Eng Regen Med, 2009. **3**(8): p. 634-46.
43. Domingues, H.S., et al., *Oligodendrocyte, Astrocyte, and Microglia Crosstalk in Myelin Development, Damage, and Repair.* Front Cell Dev Biol, 2016. **4**: p. 71.
44. Moore, C.S., et al., *How factors secreted from astrocytes impact myelin repair.* J Neurosci Res, 2011. **89**(1): p. 13-21.
45. Watkins, T.A., et al., *Distinct stages of myelination regulated by gamma-secretase and astrocytes in a rapidly myelinating CNS coculture system.* Neuron, 2008. **60**(4): p. 555-69.

46. Corley, S.M., et al., *Astrocytes attenuate oligodendrocyte death in vitro through an alpha(6) integrin-laminin-dependent mechanism.* Glia, 2001. **36**(3): p. 281-94.
47. Nair, A., T.J. Frederick, and S.D. Miller, *Astrocytes in Multiple Sclerosis: A Product of their Environment.* Cellular and molecular life sciences : CMLS, 2008. **65**(17): p. 2702-2720.
48. Rolls, A., R. Shechter, and M. Schwartz, *The bright side of the glial scar in CNS repair.* Nat Rev Neurosci, 2009. **10**(3): p. 235-41.
49. Talbott, J.F., et al., *Endogenous Nkx2.2+/Olig2+ oligodendrocyte precursor cells fail to remyelinate the demyelinated adult rat spinal cord in the absence of astrocytes.* Exp Neurol, 2005. **192**(1): p. 11-24.
50. Eng, L.F., R.S. Ghirnikar, and Y.L. Lee, *Glial fibrillary acidic protein: GFAP-thirty-one years (1969-2000).* Neurochem Res, 2000. **25**(9-10): p. 1439-51.
51. Fok-Seang, J., et al., *Migration of oligodendrocyte precursors on astrocytes and meningeal cells.* Dev Biol, 1995. **171**(1): p. 1-15.
52. Bannerman, P., et al., *Astrogliosis in EAE spinal cord: derivation from radial glia, and relationships to oligodendroglia.* Glia, 2007. **55**(1): p. 57-64.
53. Tan, A.M., W. Zhang, and J.M. Levine, *NG2: a component of the glial scar that inhibits axon growth.* Journal of Anatomy, 2005. **207**(6): p. 717-725.
54. Chandler, S., et al., *Matrix metalloproteinases degrade myelin basic protein.* Neurosci Lett, 1995. **201**(3): p. 223-6.
55. Gijbels, K., R.E. Galardy, and L. Steinman, *Reversal of experimental autoimmune encephalomyelitis with a hydroxamate inhibitor of matrix metalloproteases.* J Clin Invest, 1994. **94**(6): p. 2177-82.
56. Lindberg, R.L., et al., *The expression profile of matrix metalloproteinases (MMPs) and their inhibitors (TIMPs) in lesions and normal appearing white matter of multiple sclerosis.* Brain, 2001. **124**(Pt 9): p. 1743-53.
57. Seifert, G., K. Schilling, and C. Steinhauser, *Astrocyte dysfunction in neurological disorders: a molecular perspective.* Nat Rev Neurosci, 2006. **7**(3): p. 194-206.
58. Su, Z., et al., *Reactive astrocytes inhibit the survival and differentiation of oligodendrocyte precursor cells by secreted TNF-alpha.* J Neurotrauma, 2011. **28**(6): p. 1089-100.
59. Blakemore, W.F., J.M. Gilson, and A.J. Crang, *The presence of astrocytes in areas of demyelination influences remyelination following transplantation of oligodendrocyte progenitors.* Exp Neurol, 2003. **184**(2): p. 955-63.
60. Wang, Y., et al., *Astrocytes from the contused spinal cord inhibit oligodendrocyte differentiation of adult oligodendrocyte precursor cells by increasing the expression of bone morphogenetic proteins.* J Neurosci, 2011. **31**(16): p. 6053-8.
61. Nash, B., et al., *Functional duality of astrocytes in myelination.* J Neurosci, 2011. **31**(37): p. 13028-38.
62. Xing, B., et al., *RhoA-inhibiting NSAIDs promote axonal myelination after spinal cord injury.* Experimental Neurology, 2011. **231**(2): p. 247-260.
63. Vogel, C. and Marcotte, E.M, *Insights into the regulation of protein abundance from proteomic and transcriptomic analyses.* Nature reviews. Genetics, 2012. **13**(4): p. 227-232.

- This page was intentionally left blank. -

CHAPTER 4

MICROPILLAR ARRAY TO STUDY OLIGODENDROCYTE MYELINATION PROCESS

- This page was intentionally left blank. -

INTRODUCTION

The formation of myelin mainly occurs after birth [1]. Multipotent neuronal stem cells (NSCs) differentiate in oligodendrocyte precursor cells (OPCs) after induction by sonic hedgehog (SHH) and fibroblast growth factor (FGF) in oligodendrogliogenic niches [2]. Due to these local signals, OPCs are originated in diverse CNS zones and then diffuse through CNS before further differentiating into oligodendrocytes. Although the generated number of OPCs is vast and the needless cells are removed by apoptosis, this process does not influence the normal myelination of CNS [3]. CNS biogenesis of myelin sheaths is achieved by a highly regulated process in which oligodendroglial structures are enwrapped around axons in a tightly way. After that, oligodendrocytes send signals to myelinated axons to establish their dependency to myelin [4]. *In vivo* differentiation of OPCs into oligodendrocytes requires insulin growth factor-1 (IGF-1), ciliary neurotrophic factor (CNTF) and thyroid hormone T3 [2, 5, 6].

OPCs are found also found in the adult brain. However, some differences between the OPCs in the developmental and the adult brain are evident. In the adult brain OPCs have lower motility, capacity of proliferation and survival rate [7-9]. In the adult CNS, OPCs are not restricted to a specific zone, instead they are believed to be distributed all over the CNS [2].

The process of differentiation involves a series of consecutive morphological changes. Firstly, bipolar OPCs with high capacities of migration and proliferation, expressing A2B5 antigen, platelet-derived growth factor receptor-α (PDGFRα) and chondroitin sulphate proteoglycan neuron-glial antigen 2 (CSPG NG2) differentiate into immature oligodendrocytes with multiple processes and characterized by the expression of O4 antigen. Then the migration and proliferation capacities of oligodendrocytes ceases and a more mature state characterized by the existence of a myelin membrane sheath and the expression galactocerebroside and 2',3'cyclicl nucleotide 3'-phosphodiesterase (CNPase) is observed. Finally, oligodendrocytes produce a more complex morphology and terminally differentiate into myelinating oligodendrocytes capable of wrap neurons *in vivo*. MBP, MAG, MOG and PLP are myelin proteins highly expressed at this final stage (**Figure 4.1**) [10].

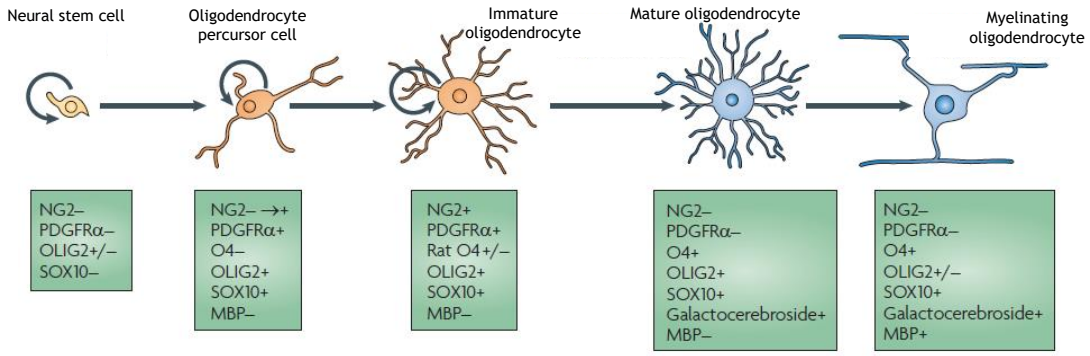

Figure 4.1 *Oligodendrocyte development.* Adapted from Nishiyama *et al* (2009) [11].

Myelin ensheathment around axons is one of the most complex plasma membrane transformations occurring in vertebrate nervous system. However, despite the clear advances in understanding the processes of OPC differentiation, a lack of knowledge is evident when thinking about the process of forming a compacted spiral structure around axons (myelin wrapping) [12]. This is explained by the difficulty in visualizing membrane formation and the dynamics of the process at the nanometer scale [13].

Some models trying to explain myelin sheath formation during development are continuously been proposed. In the “carpet crawler” model myelin is firstly extended along the whole axon before starts ensheathing it. This initial wrap then moves under the growing sheet to form the subsequent wrap – like a carpet rolling [14, 15]. However, some contradictory reports state that the number of wraps is not constant along the forming sheath (the number of wraps in the middle is higher than in the lateral zones), devaluating this first proposed model [16]. Pedraza *et al* suggested the “serpent model” that relies on a unidirectional spiralling of the myelin along the axon. When the sufficient thickness of myelin membrane is achieved, the wraps spread sideways into overlapping sheets [17]. However this model does not explain the paranodal loops that show the maximum thickness of the myelin in the centre of the internode and the outer myelin segment to be the closest to the node of Ranvier. A more recent model proposes that oligodendrocytes extend a triangular shaped process, attaching to the axon. Oligodendrocytes continue to pour out the process and myelin spreads sideward coordinated by axonal signals. This model is designated “liquid croissant” myelin forming model (**Figure 4.2**) [18].

Nevertheless, all these models lack significant concept proofs due to the gap in space resolution achieved by actual microscopy techniques, the inherent difficulties in culturing oligodendrocytes and neurons and the non-existence so far of an adequate myelin membrane labelling to facilitate oligodendrocyte processes visualization [19].

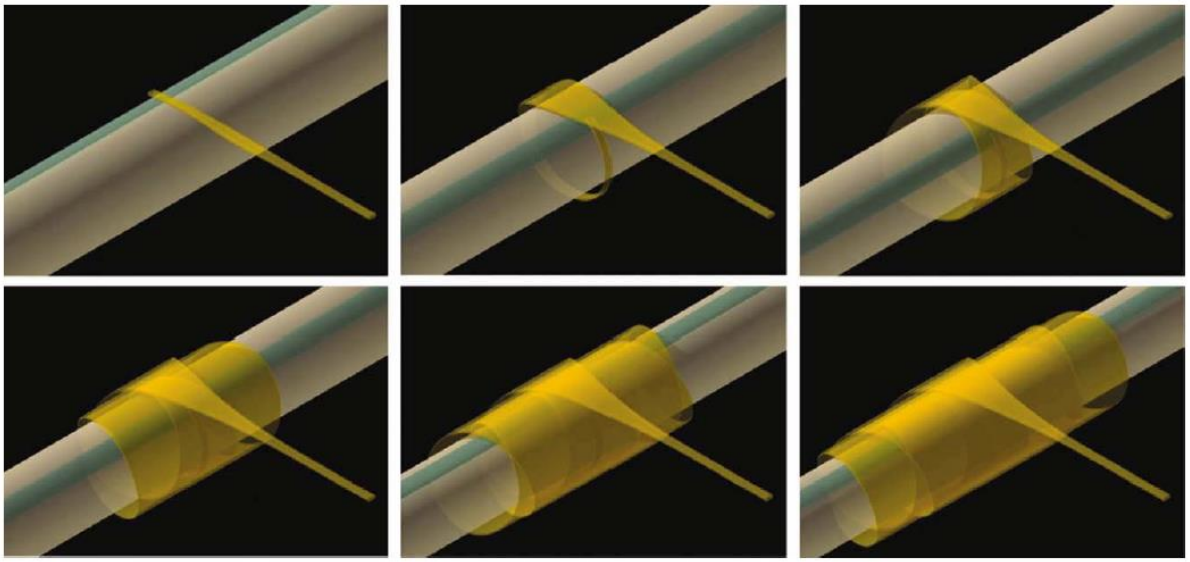

Figure 4.2 *Schematic representation of the "liquid croissant" model.* Adapted from Sobottka *et al* (2011) [18].

Taken together, the next big objective to the improvement of knowledge about these processes would be the creation of a suitable, biocompatible with CNS oligodendrocytes and optical transparent *in vitro* platform to follow the CNS myelination process

Polydimethylsiloxane (PDMS) as a tool to dissect myelin wrapping mechanisms

Polydimethylsiloxane (PDMS) is a silicone rubber composed of carbon, hydrogen and oxygen (**Figure 4.3**). Its structure is defined by a backbone of Si-O composed of repeated units of -$Si(CH_3)_2O$- which determines its molecular weight and, consequently its properties. In comparison with other polymers, PDMS has a low glass transition temperature (approximately -125ºC) and a unique flexibility. Besides, it is optical transparent, presents a low biological activity (low bioaccumulation and high biocompatibility) and can be used within a vast range of temperatures [20, 21]. Other features that makes PDMS an interesting polymer are its inert chemical characteristics and high permeability to gases.

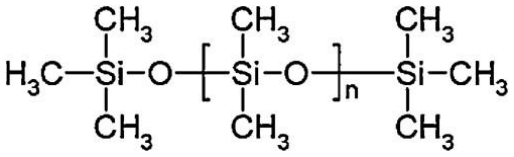

Figure 4.3 *Chemical structure of PDMS.*

The fabrication of PDMS devices is relatively easy and straightforward and it allows the design of surfaces with micron scale features that can be prepared in a very reproducible way. Beyond, PDMS preparation associated costs are low. Together, these characteristics make PDMS very attractive for many applications, and nowadays it is currently being used to produce

microelectromechanical systems (MEMs) or micro- and nano-fluidics devices, among others [22].

In this work, a PDMS micropillar array is proposed as a novel *in vitro* platform to mimic axons and to follow myelin formation and wrapping processes.

MATERIALS AND METHODS

Polydimethylsiloxane (PDMS) silicon mould fabrication and micropillar production

Polydimethylsiloxane silicon mould was designed by the group and its manufacture was conducted in TU Delf (Netherlands). The design of the micropillar array was based on axonal diameters dimensions. The mould consisted of a regular square with 6x6mm divided in four smaller quadrants with diameters of 2μm, 3μm, 4μm and 5μm, all of them with 10μm height and distancing 30μm from each other (**Figure 4.4**).

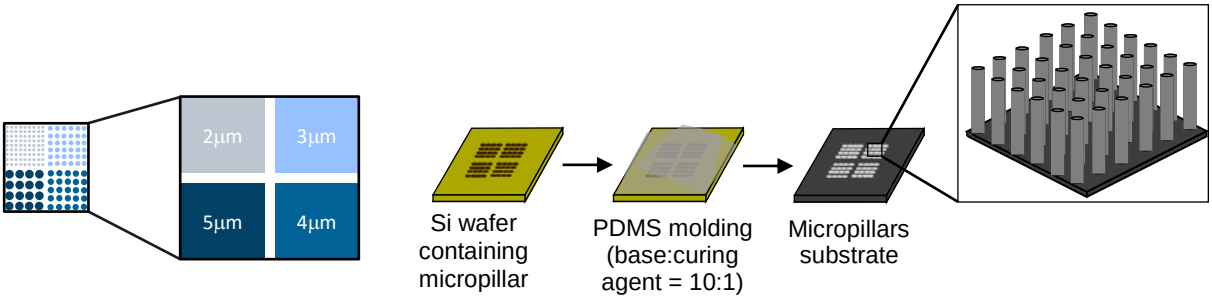

Figure 4.4 *Scheme of PDMS micropillars production*. PDMS moulds were sent from TU Delf (Delf University of Technology, Netherlands) and subsequent production of the micropillars was conducted in the context of this project. Adapted from [23].

In order to fabricate the PDMS micropillar array, PDMS base (Dow Corning) composed of dimethylsiloxane oligomers with vinyl-terminated end groups, platinum catalyst and silica filler and a curing agent (Dow Corning) constituted by a crosslinking agent (dimethylmethylhydrogen siloxane) and an inhibitor (tetramethyltetravinyl cyclotretrasiloxane) were vigorously mixed at a ratio of 10:1 (w/w%) between the base and the curing agent and, subsequently, degassed in a desiccator connected to a vacuum pump to remove air bubbles. The crosslinking reaction between the base and the curing agent occurred at temperatures ranging between 37ºC and 60ºC during 4h-12h. When the PDMS was solidified the micropillars were peeled off in the presence of isopropanol (Merk) and left in a Petri dish containing isopropanol until further use.

PDMS micropillar characterization

The morphology of the pillars was assessed by Scanning Electron Microscopy (SEM). Samples were prepared by removing isopropanol and subsequently substitute for water and leave in a vacuum pump desiccator for 30 min. The SEM exam was performed using a High resolution Scanning Electron Microscope with X-Ray Microanalysis: JEOL JSM 6301F/ Oxford

INCA Energy 350. Samples were coated with an Au/Pd thin film for 70s and with a 15mA current, by sputtering, using the SPI Module Sputter Coater equipment.

Primary cells

All experiments involving animals and their care were performed in agreement with institutional ethical guidelines (IBMC/INEB/i3S), the EU directive (2010/63/EU) and Portuguese law (DL 113/2013).
All described procedures had the approval of the Portuguese official authority on animal welfare and experimentation (*Direção Geral de Alimentação e Veterinária*). Animals had free access to food and water and were kept under a 12h light/12h dark cycle.

Cortex isolation
To obtain oligodendrocytes Wistar Han rat pups in post-natal day 2 (P2) were sacrificed by decapitation and brain was removed to further dissociate the cortex and the meningeal tissue. Approximately 8-16 pups were sacrificed every two weeks. Removal of brain was performed using straight micro-scissors and fine forceps previously cleaned and sterilized. The procedure was conducted under a magnifying glass in a Petri dish containing Hank's Balanced Salt Solution (HBSS, Gibbco) without calcium and magnesium supplemented with 2% (v/v) penicillin/streptomycin (P/S) (Gibco). Firstly, the skin of the head was cut until the nose with a sharper scissor with the other hand holding the head (from the ear) with a big forceps. The skin was opened to the corners in order to let the skull bones be visible. Then, with a straight microscissor, the skull bone was cut until the nose and to the sides. The bones were removed with a thinner forceps and a special care was taken to not damage the cortex. With the same forceps, the cortex was carefully removed (from the olfactive bulbs) and cut by the cerebellum. Subsequently, using thinner forceps, the two hemispheres were separated and the meningeal tissue was detached from the cortex. Cortex were maintained in ice-cold HBSS without calcium or magnesium with P/S to prevent cell dissociation and death.

Mixed glial cell (MGC) cultures
After cortex removal, the cortices were firstly mechanically digested with a 10 mL serological pipette and passed through a 25G needle to dissociate clusters. Cortices were then enzymatically digested with HBSS without calcium or magnesium supplemented with 0,0025% (w/v) trypsin (Sigma) and 0.001mg/mL DNase I (Applichem LifeSciences) for 15 min at 37ºC. The action of the trypsin was inhibited by the addition of Dulbecco's modified Eagle medium (DMEM) Glutamax High glucose (Gibco) supplemented with 10% (v/v) heat inactived Foetal Bovine Serum (FBS, Sigma F7524) and 1% (v/v) P/S and the homogeneized was then centrifuged at 500g during 10 min. The supernatant was poured off, the pellet re-suspended in serum containing DMEM and filtered through a 40 μm nylon cell strainer (BD Falcon) to

remove large cell clusters. Finally cells were distributed for T75 cell culture flasks, previously coated with 100 mg/mL poly-L-lysine (PLL, mol wt 30 000-70 000, Sigma) (30 min, 37ºC) at a density of cell suspension obtained from two brains per flask. Cells were cultured with serum containing DMEM at 37ºC, 5% CO_2 during 4 days to allow cell adhesion to the flask and then medium was changed every 2-3 days (changing ¼ of the medium at day 4; ½ at day 6 and all medium from day 8 on). Cells were maintained during 15 days until confluent, when the components of the MGC cultures where mechanically separated (see following section).

Oligodendrocyte progenitor cell (OPC) cultures

OPCs were mechanically isolated from MGC as previously described [24, 25]. At day 14 after plating, MGC were confluent with phase-dark OPCs appearing on top of phase-grey bed layers of astrocytes. On that day, a pre-shake was performed: the T75 lids were tightly sealed and transferred to an horizontal orbital shaker (Infors) during 2h at 210 RPM (37ºC) to remove the majority of loosely adherent microglia cells. After that, medium was replaced and cells were left at 37ºC for 2h to allow the normal metabolism stabilization. An overnight shake (18h-20h) at 230 RPM (37ºC) was then performed to further detach loosely attached microglia and OPCs. After shaking overnight, OPCs were further purified by differential selective adhesion. The cell suspension was transferred to non-treated polystyrene Petri dishes (10 cm of diameter) to allow microglia to adhere during 2h at 37ºC and unattached OPCs were collected, passed through a 40μm cell strainer to remove cell clusters and centrifuged at 450g during 10 min (RT). The cell pellet was then re-suspended, cells counted and seeded on PLL-coated (previously described) micropillar array. Cells were maintained during 24h-48h in proliferation medium (OPC SATO Medium): DMEM Glutamax High Glucose supplemented with 100μg/mL of transferrin (Sigma, T2036), 16μg/mL of putrescine (Sigma, P5780), 100μg/mL of Bovine Serum Albumin (BSA) (BioWest, P6154), 60ng/mL progesterone (Sigma, P8783, dissolved in pure ethanol), 40ng/mL of sodium selenite (Sigma, S5261, dissolved in 0.1M NaOH), 40ng/mL of thyroxine (Sigma, T1775, dissolved in 0.1M NaOH), 30ng/mL of triiodo-L-thyronine (Sigma, T6397, diluted in 0.1M NaOH), 0.01μg/mL of Platelet-derived growth factor-AA (PDGF-AA) (Peprotech, 100-13A), 0.01μg/mL of Fibroblast Growth Factor (FGF) (Peprotech, 100-18B), 5μg/mL of insulin (Sigma, 19278) and 1% (v/v) of P/S. After 24h-48h cells were cultured without FGF and PDGF-AA and 0.5% (v/v) of heat inactivated FBS (Sigma Aldrich, F7524) was added (OL SATO Medium).

The purity of OPC culture was estimated by immunocytochemistry.

Immunocytochemistry

For experiments involving immunocytochemistry analysis, before fixation, cells were washed twice with pre-warmed Phosphate Buffer Saline (PBS) (Gibco) solution for 10 min. Afterwards, cells were fixed with 4% (v/v) paraformaldehyde (PFA) (Merck Milipore) during 10/15min at

RT, washed twice with PBS and permeabilized and blocked in PBS containing 5% (v/v) normal goat serum (NGS) (Biosource) and 0.3% Triton X-100 (Sigma) for 1h at 4ºC. Primary antibodies were then diluted in PBS with 1% (v/v) NGS and 0.15% (v/v) Triton X-100 and incubated at 4ºC overnight. Following the primary antibody incubation, cells were washed three times with PBS to remove the excess of the primary antibodies and the secondary antibodies were diluted in PBS containing 1% (v/v) NGS and 0.15% (v/v) Triton X-100 and added to the cells. Secondary antibodies' incubation was conducted at 4ºC for 45min to 1h. Afterwards, cells were washed three times with PBS and incubated with Hoescht (ThermoFisher) diluted in PBS (1:1000) containing 1% (v/v) NGS and 0.15% (v/v) Triton X-100 for 15min at RT. Subsequently, cells were mounted using FluoroMount (Sigma) and observed under an inverted fluorescence microscope (AxioVert) or confocal microscope (SP5, Leica, Germany). The following primary antibodies were used: rat anti-MBP (1:100, Abd Serotec), rabbit anti-NG2 (1:250, Merk), rabbit anti-IBA1 (1:500, Wako), mouse anti-βIII tubulin (1:500, Promega) and rabbit anti-GFAP (1:500, Dako). Secondary antibodies used were 488 donkey anti-rat (1:1000, Invitrogen), 647 donkey anti-rabbit (1:1000, Invitrogen) and 488 donkey anti-mouse (1:1000, Invitrogen). For the evaluation of culture purities, the combination of the used primary antibodies is summarized in **Table 3**.

Live imaging

OPCs were seeded on micropillars at a density of $4.5x10^5$ viable cells/micropillar array (viable cells were determined by Trypan blue exclusion assay) pre-coated with PLL (37ºC, overnight). Cells were kept in OPC SATO medium overnight and after changed to imaging medium which was composed by SATO 10x diluted in Fluorobrite DMEM Medium (ThermoFisher Scientific) supplemented with 0.5% heat inactivated FBS (Sigma), 5μg/mL of insulin (Sigma), 1:100 GlutaMAX (Thermofisher Scientific) and 1:100 sodium pyruvate (Thermofisher Scientific). Micropillars were glued to μ-Dish Glass bottom (ibidi) and immediately imaged in a motorized inverted epi-fluorescence microscope (Zeiss AxioVert 200M, Carl Zeiss, Germany) during 48h. Images were acquired every 30 min and in multiple micropillar array positions.

Alternatively, a cell staining dye for plasmatic membrane was used to stain oligodendrocytes processes and facilitate image acquisition and visualization. CellMask Green plasma membrane stain (Life Technologies) was diluted in pre-warmed imaging medium (1μL to 1mL of medium) and added to cells during 10 min at 37ºC, 5% CO_2. Subsequently, cells were washed carefully three times with pre-warmed PBS and imaging medium was added immediately after. Images were taken in a confocal microscope (Confocal Leica SP5, Leica Systems, Germany).

Statistical analysis

Statistical analysis were performed using GraphPad Prism version 7.00 for Windows, GraphPad Software, La Jolla California USA, www.graphpad.com. Statistical differences between groups were calculated based on *t*-student test (two group comparison) ore two-way ANOVA when two factors affected the measurements, followed by Tukey's multiple comparisons test for multiple comparisons. Gaussian distributions were tested using D'Agostino and Pearson normality tests. When Gaussian distribution could not be tested due to the lack of measurements or failed in the above mentioned tests, non-parametric tests were performed. Mann-Whitney tests were used in the case of unpaired *t*-tests. A p-value below 0.05 was considered statistically significant and data are shown as mean ± standard deviation (SD).

RESULTS AND DISCUSSION

PDMS micropillar array can be sucessfully fabricated

PDMS micropillars were produced at a ratio of 10:1 between the base monomer and the curing agent. Nonetheless, a vast propensity for bending or collapsing during the steps of unmoulding and subsequent addition of cells was noticed. To overcome the instability of the pillars in keeping their straight structure, some approaches were tried and are summarized in **Table 4.1**.

Table 4.1 *Optimization process of the peeling off of the micropillars from the mold and storage until cell culture application.* × identifies that all pillars were bended, ± that only the 5μm pillars were standing and ✓ represents that all pillars were straight after the mentioned preparation steps. (IPA: isopropanol)

#	Step 1: peeling off		Step 2		Step 3		Step 4	
1	In dry state	×	Sonication/Vacuum application in a dessicator	×	-	-	-	-
2	PBS or H_2O	×	Sonication/Vacuum application in a dessicator	×	-	-	-	-
3	IPA	✓	Drying in the flow chamber	×	-	-	-	-
4	IPA	✓	CO_2 critical point drying	✓	Addition of complete cell culture medium	×	-	-
5	IPA	✓	Gradients of IPA/PBS	±	Coating with PLL	±	Addition of OPCs	±
6	IPA	✓	CO_2 critical point drying	✓	UV surface treatment (λ=365nm, 1h30, 6mm distance)	✓	Addition of PLL coating	×
7	IPA	✓	CO_2 critical point drying	✓	Plasma O_2 surface treatment (3min, 0.6mbar)	✓	Addition of PLL coating followed by complete cell culture medium	✓

Firstly, unmoulding the pillars was performed directly in the air, without the addition of any liquid (**Table 4.1, entry #1**). However, after observations under an optical microscope, all micropillars were collapsed or bended. This might have happened due to adhesive or capillary forces that may lead to the grounding or lateral collapse of the pillars [26].

Thereby, avoiding the collapsing during the peeling off of the mould and subsequent steps or trying to promote the unbending of the micropillars were the two different strategies subsequently followed to overcome this issue. For the latter case, it was realized that, after

peeling off the PDMS micropillars in the presence of water or PBS (**Table 4.1, entry #2**), the pillars from all quadrants immediately bended and even when sonication or vacuum was applied, the micropillars remained bended. For that reason, subsequent work was directed to try to avoid collapsing in the process of unmoulding. While removing the micropillars with PBS or water proved to be inefficient in promoting pillars to stand straight, the addition of isopropanol (IPA) during the unmoulding step was well succeeded. In fact, one important difference between the IPA and water or PBS, is their intrinsic viscosity values. IPA presents an estimated intrinsic viscosity of 2.1mPa.s at 25ºC [27] while water is reported to have viscosities around 0.89mPa.s at the same temperature [28]. The difference between the intrinsic viscosities of both liquids might be the reason why the peeling off with IPA was well succeeded contrarily to what happen with water and PBS. However, in order to use the pillars with cells, the IPA would have to be removed. The first attempt was to simply allow it to dry in the flow chamber (**Table 4.1, entry #3**). Nevertheless, the evaporation of the IPA caused the pillars to collapse again. Following the strategy of trying to dry IPA and having them stand, a CO_2 critical point dryer technique was employed. This technique relies on elevating wet samples to a critical point where the physical characteristics of the liquid and gaseous phases are not discernible. Hence, it is possible to change from liquid to gaseous phase without damaging the structures due to the inexistence of liquid capillary forces [26] provoked by surface tension [29]. Drying micropillars with the CO_2 critical point dryer resulted on straight standing pillars. However, immersing them in cell culture medium led to the collapse of pillars (**Table 4.1, entry #4**). Consequently, this strategy was discarded and liquid changes between IPA and other biological compatible liquids were tried (**Table 4.1, entry #5**). Changing progressively and carefully from IPA to PBS revealed to be successful in keeping the larger diameter pillars (5μm quadrant) straight and in a lesser extent the 4μm pillars quadrant. Nonetheless, the remaining quadrants did not resist and capillary forces induced the collapsing of all 2 and 3μm pillars. This may be partially explained by the aspect ratio values (ratio between pillar height and diameter [26]) that increases from 5μm to 2 μm pillars. Thereby, 2μm pillars show the highest propensity to collapse due to the increased surface to volume ratio that promotes a higher susceptibility to surface forces [26].

The question that was then raised was whether the hydrophobicity characteristic of the PDMS would have influence on the collapsing or bending of the micropillars. As it is reported, the immersion capillary forces depend on energy surface [30] therefore, promoting the hydrophilicity nature of the surface of the pillars seemed to be important to maintain their structure when put in contact with aqueous solutions. Since PDMS is highly hydrophobic, reverting this characteristic was subsequently attempted. Over the years, several PDMS surface modifications have been proposed [31]. The surface modification strategies like the UV or the plasma treatments are some of the easiest and fastest. Accordingly, the UV treatment was firstly tried by exposing PDMS micropillars to an ultraviolet (UV) lamp (VL-6LC,

6W) (**Table 4.1, entry #6**). The lamp was distanced from the pillars approximately 6mm and the samples were exposed to a 365nm wavelength radiation for 1h30. The wavelength was chosen based on the fact that exposing PDMS surfaces to long wavelengths causes the chain scission of the PDMS and the generation of free radicals in its structure, as stated elsewhere [32]. After the exposition, the micropillar array maintained the straight structure though the immediate coating with a PLL solution still caused the pillars to bend. Although an in depth study on the extent of the alteration of PDMS hydrophobicity was not conducted, some groups published that the hydrophilic nature of UV treated PDMS is not stable for long. UV exposure creates radicals in the surface that may react and rearrange themselves forming terminal groups that are mainly hydrophobic [33, 34]. A possible solution would be the exposition of the PDMS surface to UV/ozone treatment, which would allow the reaction of the radicals with oxygen, creating a more stable hydrophilic surface [33]. Nonetheless, this study was not performed.

Besides UV treatment, plasma treatment has also been described as a successful method to modify PDMS surfaces. In this methodology, some gases such as oxygen, nitrogen or hydrogen react with the surface of the sample after any energy is applied, creating functional groups. In the case of O_2 plasma treatment, an oxidization of the surface, substituting the methyl groups for the reactive oxygen happens [31]. Therefore, an O_2 plasma surface treatment was conducted in a plasma generator (Electronic Diener) (**Figure 4.5**) after drying samples in a CO_2 critical point dryer (**Table 4.1, entry #7**). The treatment took three minutes under an O_2 pressure of 0.6mbar and immediately after, micropillars were immersed in a PLL solution and observed under an optical microscope. All four quadrants were able to maintain their structure. Despite not having verified the extension of the modification, the fact that the structure was not disturbed after the addition of a liquid, indicated that the modification was well succeeded. When changing from PLL solution to complete cell culture medium the results obtained were similar. A preliminary test about the stability of the oxygen plasma-treated substrates indicated that PDMS micropillars can stand straight after long periods of storage at no humidity conditions (desiccator).

Figure 4.5 *Plasma Generator Equipment (Departamento de Química da Universidade de Coimbra).*

Once the appropriated structure of all micropillar quadrants could not be achieved in time for further cellular assays, studies on OPCs' behaviour in the developed platform were performed considering only the largest pillars (5μm diameter) as they were the ones that showed to resist to bending or collapsing after changing from the liquid of the peeling off (IPA) to PBS. Therefore, the data and conclusions presented in the following sections concern these surfaces.

SEM morphological characterization of the micropillars was conducted and **Figure 4.6** presents some representative photos of each quadrant. The micropillars showed the expected morphological features (height 10μm, distance between pillars 30 μm and diameters varying between 2 and 5 μm).

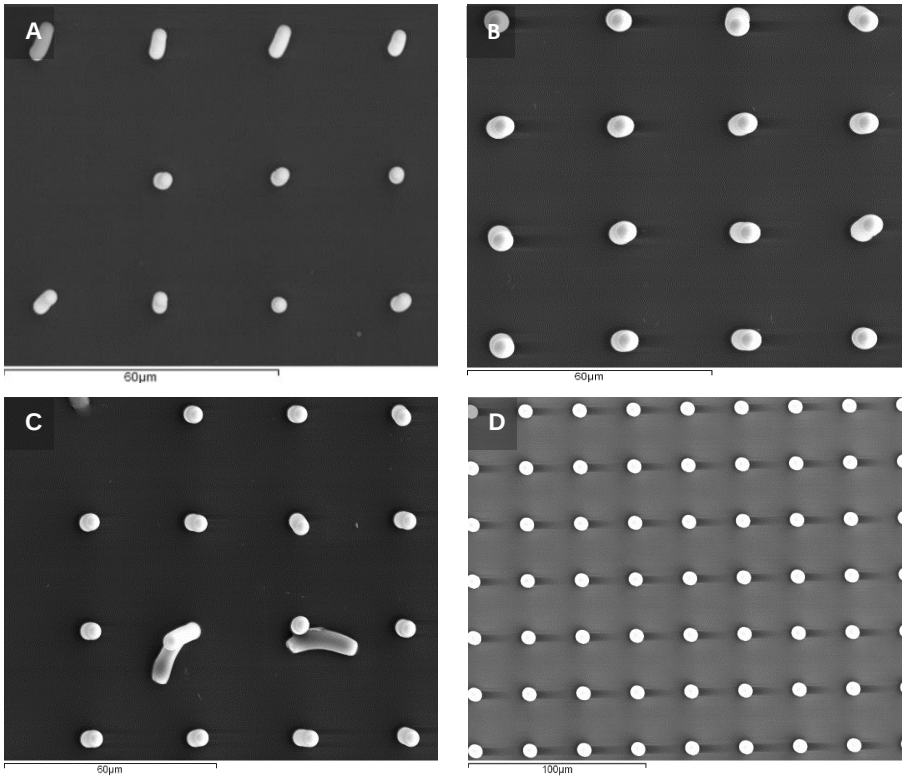

Figure 4.6 *Scanning electron microscopy images of the PDMS pillars.* From A to D: 2μm, 3μm, 4μm, 5μm diameter pillars. Scale bar is indicated in the images.

This *in vitro* multidiameter micropillar platform is intended to serve as a myelinating platform serving the pillars as surrogate axons. *In vivo* there is a tendency of oligodendrocytes to myelinate axons with larger diameter rather than those with diameters bellow 0,3 μm. Besides, augmenting the diameter of an unmyelinated axon was shown to be a trigger for myelination [35, 36]. Therefore, these previous findings show that axon diameter is crucial for the regulation of the myelination process and that the range of diameters chosen for micropillars (between 2 and 5μm) fit relevant CNS axons' characteristics.

Pure primary rat OPCs can be efficiently obtained

To investigate if OPCs cultures were free of any other cell type contaminant an immunocytochemistry test against neural cells' characteristic markers was performed. OPC cultures were evaluated for the presence of neurons (through expression of the characteristic marker βIII tubulin [37]), microglia (analysing cell expression of IBA1, a specific calcium binding protein [38]), and astrocytes (for the expression of GFAP, a hallmark of the astrocytes) (**Figure 4.7**). OPCs were seeded on PLL coated ϕ13 mm glass coverslips (50 000 cells per coverslip, respectively) and fixed at day 5 of culture. The number of cells that were not oligodendrocytes/OPCs was quantified and is shown in **Table 4.2**. Cell culture purity was found to be 92%**,** which indicates that oligodendrocytes were successfully isolated from rat pups' cortex. These results are in accordance with values usually obtained in this kind of primary cell isolation [39, 40].

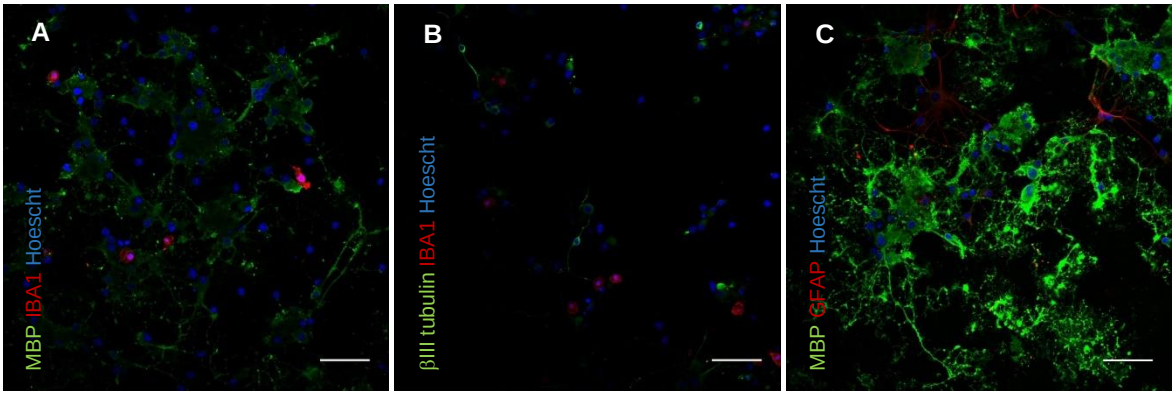

Figure 4.7 *Representative images of oligodendrocytes stained with neuronal and glial characteristic markers.* Staining was made for the presence of microglia (IBA1) (**A** and **B**), neurons (βIII tubulin) (**B**) and astrocytes (GFAP) (**C**). Scale bar indicates 50μm.

Table 4.2 *Quantification of the number of positive cells for non-oligodendroglial cells in oligodendrocytes cultures.* (n=1)

	Positive cells (%)
IBA1	1.8
βIII TUBULLIN	2.1
MBP	-
NG2	-
GFAP	3.4

OPCs are capable of adhere and survive in PLL-coated PDMS micropillars

In order to evaluate if oligodendrocytes were able to adhere on PDMS micropillars and the optimal density, different cell densities were seeded either on non-coated or on PLL-coated substrates (**Table 4.3**).

Table 4.3 *Conditions tested for the seeding of OPCs on PDMS micropillars.* A density between $1.5x10^5$ and $7.5x10^5$ was tested and for each density, the coating conditions were also verified (coated or non-coated with PLL).

Number of cells	Coating with PLL	No coating
$1.5x10^5$ cells	Poor adhesion and density	Non-adhesion of OPCs
$2.5x10^5$ cells	Relatively good adhesion and density	Non-adhesion of OPCs
$4.5x10^5$ cells	Optimal adhesion and density	Non-adhesion of OPCs
$6.0x10^5$ cells	Good adhesion and density	Non-adhesion of OPCs
$7.5x10^5$ cells	Good adhesion but excessive density	Non-adhesion of OPCs

After observing under an optical microscope the oligodendrocytes' behaviour and morphology in such conditions, a qualitative analysis was performed and some conclusions were able to be taken: oligodendrocytes preferentially adhered to PLL coated PDMS micropillars and higher densities promoted the aggregation of the cells while in lower densities cells tend to die. For that reason, the defined number of cells to be seeded was $4.5x10^5$ cells/micropillar array.

PDMS pillars are a suitable platform for the proliferation and differentiation of OPCs

Whether if PDMS micropillars would be a suitable platform for the proliferation and differentiation of OPCs in oligodendrocytes was the question that was subsequently raised. OPCs were seeded on PDMS micropillars and maintained in OL SATO for at least five days after being two days in OPC SATO and observed under an optical microscope (**Figure 4.8**). Cells were seen to proliferate extensively and differentiate in process-bearing cells.

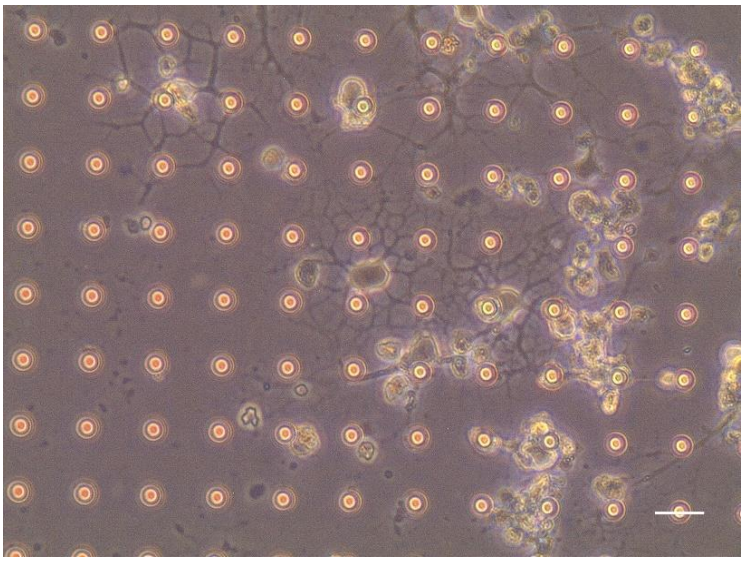

Figure 4.8 *Optical microscope image of oligodendrocytes adhered to PLL-coated PDMS micropillars (at a density of 4.5x10^5 cells/micropillar array in the day 5 of culture).* The arrow is indicating a micropillar. Due to their morphological characteristics, the process-bearing cells depicted in the figure are considered oligodendrocytes. Scale bar indicates 20μm.

For a deep analysis about the differentiation capacity of OPCs in PDMS micropillars, an immunocytochemistry assay was performed at days 1, 3 and 7 of culture. During this period cells were cultured in OL SATO medium to allow differentiation. It was clearly visible that cells differentiate over time and that the number of cells bearing the typical oligodendrocyte processes progressively increased (**Figure 4.9**). When comparing the number of cells expressing the characteristic progenitor marker (NG2) over the days, a significant decrease from day 1 to 7 was verified (**Figure 4.10, A**). Regarding the myelin marker, the number of MBP positive cells significantly increased over days of culture, as expected (**Figure 4.10, A**). Nevertheless, when asking whether the PDMS substrate would be a more permissive environment for cell differentiation rather the traditional used glass coverslips, no significant differences between both substrates was found (**Figure 4.10, B**). This conclusion was not expectable as PDMS micropillars mimic better the natural microenvironment OPCs normally face due to the pillars' cylindrical structure that resemble axons. Nevertheless, Teixeira *et al* [41] stated that after culturing and differentiating NSC into oligodendrocytes on PDMS substrates or on TCPS, the number of MBP positive cells was higher on TCPS rather than on PDMS. This may be explained by hydrophilicity effects since both TCPS and glass coverslips substrates are hydrophilic and PDMS is highly hydrophobic.

Interestingly, although the number of cells expressing MBP in PDMS micropillars at day 7 was significantly higher than in the other days of culture, the morphology of the oligodendrocytes was not the expected one. Accordingly to the literature, a complete oligodendrocyte

differentiation *in vitro* (glass) is normally achieved at day 7 of culture. On this day, oligodendrocytes are not extending many processes, but forming a myelin sheath [42].

It is known that the ECM plays a crucial role during oligodendrogenesis either by providing biochemical signals that induce the differentiation of OPCs (through their intrinsic proteins) or by its physical cues acting as a mechanical support for OPCs development. Accordingly, the ECM stiffness has been reported as determinant in modulating the survival of OPCs as well as their proliferation and differentiation capacities, making them mechanosensitive cells [43, 44].

Although a study on the influence of the mechanical properties of PDMS in the course of OPC differentiation was not conducted, it can be hypothesized that PDMS mechanical properties may influence the differentiation process of the OPCs.

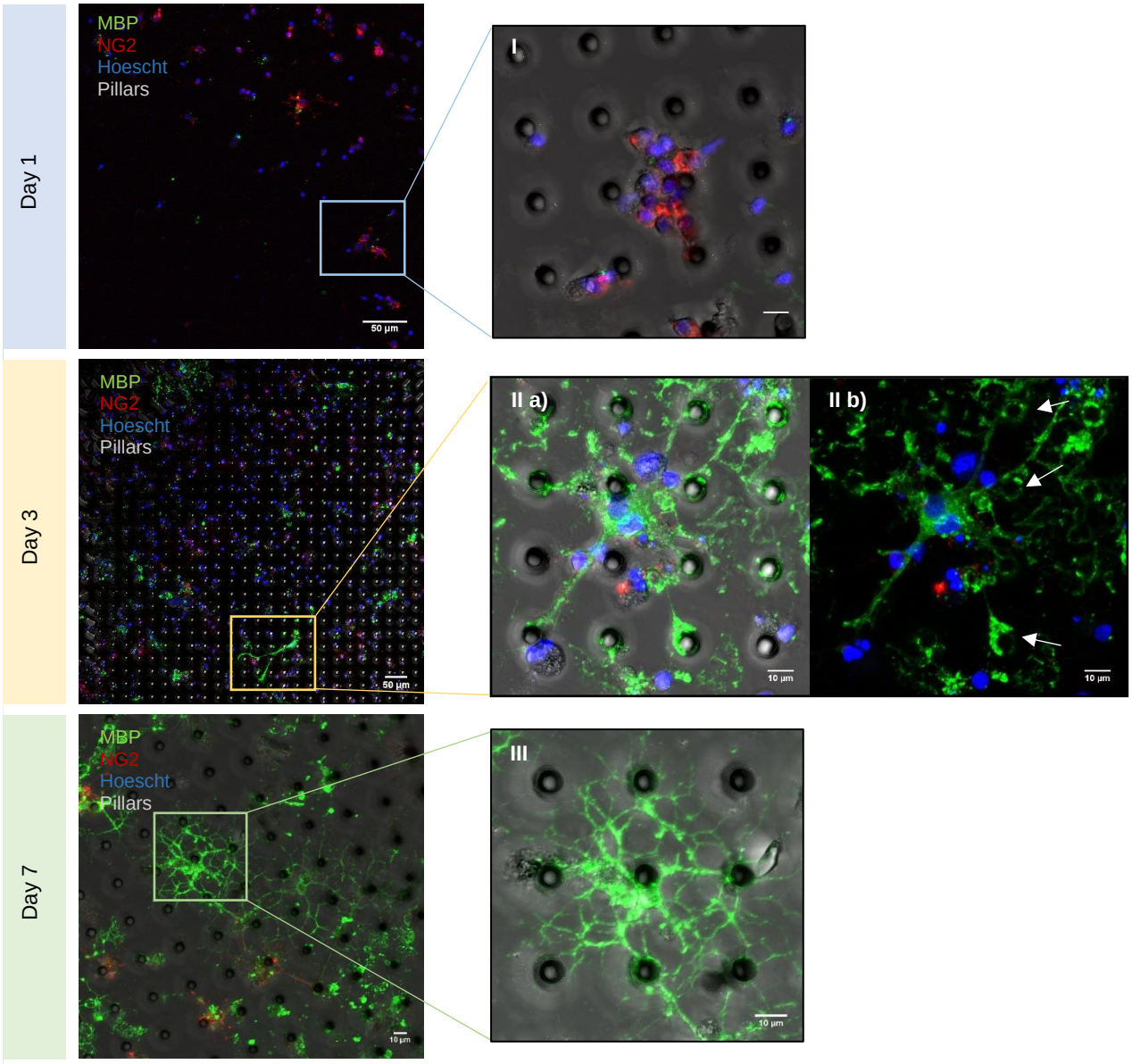

Figure 4.9 *OPC differentiation ability in PDMS micropillars.* Images I, II and III represent detailed views of the left images. Image IIb) is the same as IIa) but without showing the bright field channel (pillars). Arrows are pointing to processes wrapped around the pillars. Scale bar is indicated in the figures.

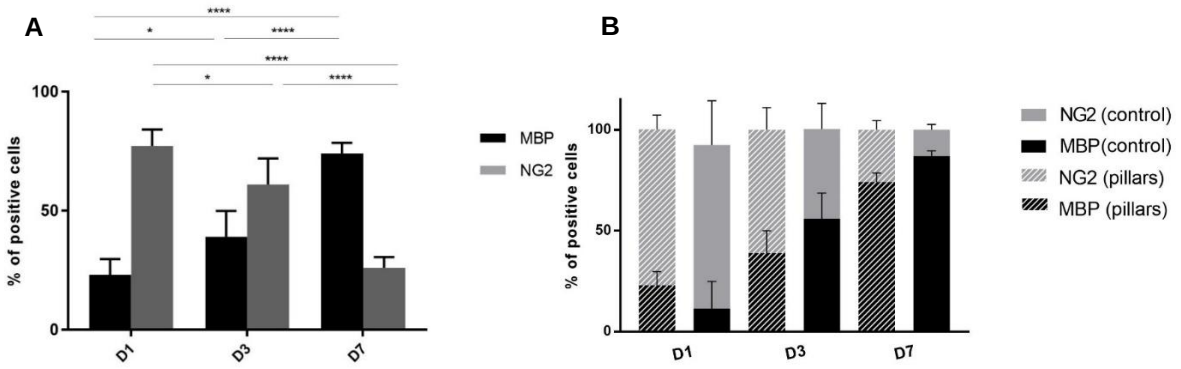

Figure 4.10 *Quantification of the number of cells expressing NG2 and MBP over days of culture.* **A**. Comparison between cells expressing MBP and NG2 in PDMS micropillars. A significant difference is noted in the expression of both markers over days. **B.** Comparison between the number of cells expressing the OPC or oligodendrocyte markers in PLL-coated glass coverslips and PLL-coated PDMS micropillars. No significant differences were found between glass and micropillars. Results show mean ± standard deviation (n=2 independent experiments), asterisks represents statistical significance (** $p < 0.01$, **** $p < 0.0001$). Statistical analysis was performed using two-way ANOVA and Tukey's multiple comparison test (B).

Besides, through the immunocytochemistry assay it was also clearly visible that either at day 3 (**Figure 4.9, IIb denoted by the arrows**) or at day 7 (**Figure 4.9, III**) many cells enwrapped pillars. Although the number of MBP positive cells was significantly higher at day 7, the morphology of the cells between those days was not considerably modified. This may have happened due to the insufficient factors provided by the PDMS platform to complete the myelination process of the oligodendrocytes.

Figure 4.11 shows a detailed overview of a confocal z-stack figure of one oligodendrocyte wrapping the pillars at day 7. The 3D reconstruction of the same image enabled a detailed visualization of the myelin wrapping around pillars (**Figure 4.12**).

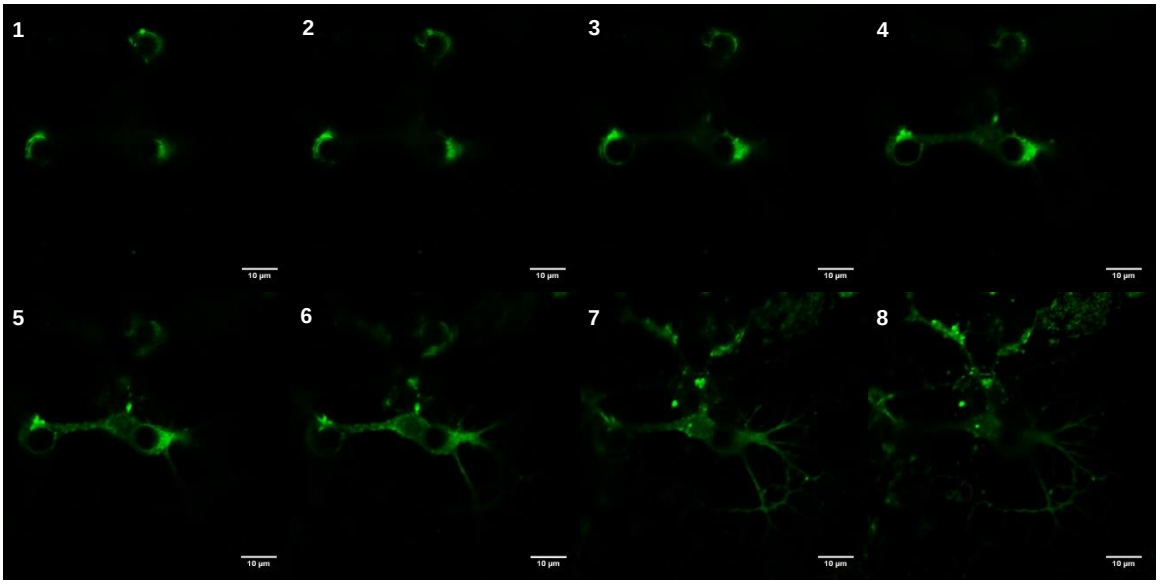

Figure 4.11 *Different planes of an oligodendrocyte around micropillars at day 7 of culture.* The green represents MBP staining. The images show from top to the bottom of the substrate (1-8). Scale bar is indicated in images.

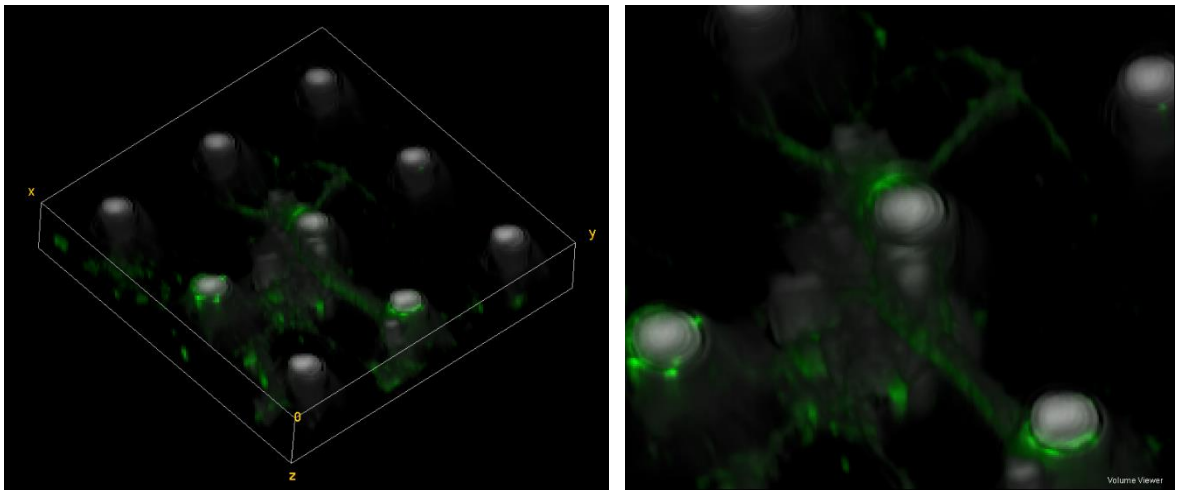

Figure 4.12 *3D view of a myelinated micropillar (day 7).* 3D reconstruction was performed in ImageJ using VolumeViewer plugin after subtracting the background in the bright field channel and add all z-stack images. Green indicates the stain for MBP.

Although the wrapping was proved to happen around the pillars, it was not possible to distinguish the formation of progressive myelin processes neither the formation of a compact myelin sheath. Besides, as an immunocytochemistry assay relies on analysing cells at a fixed time point and oligodendrocyte' extension of their processes is a highly motile process [36] some of observations could merely be OPCs surveying to pillars rather than wrapping them. Nevertheless, as cytoskeleton components are highly involved in the process of compact myelination (in immature oligodendrocyte, F actin is highly concentrated whereas in mature oligodendrocyte, the levels of acetylated α-actin are increased [45]), a study of their expression over days should also be done to facilitate the study of oligodendrocyte myelination in PDMS micropillars.

Physical cues are necessary but may be not sufficient to promote the oligodendrocyte compact wrapping process

Since the immunocytochemistry data was not conclusive regarding the process of oligodendrocyte wrapping around pillars, a live imaging assay of OPCs cultured in the PDMS micropillar array was then performed. Firstly, OPCs were followed between day 4 and 5 after inducing differentiation. However, as cells at these days presented multiple processes and the visualization was very difficult, following cells in an earlier stage of differentiation was found to produce more clear data. Images were taken every half hour from day 0 until day 2 after changing to differentiation medium (**Figure 4.13**).

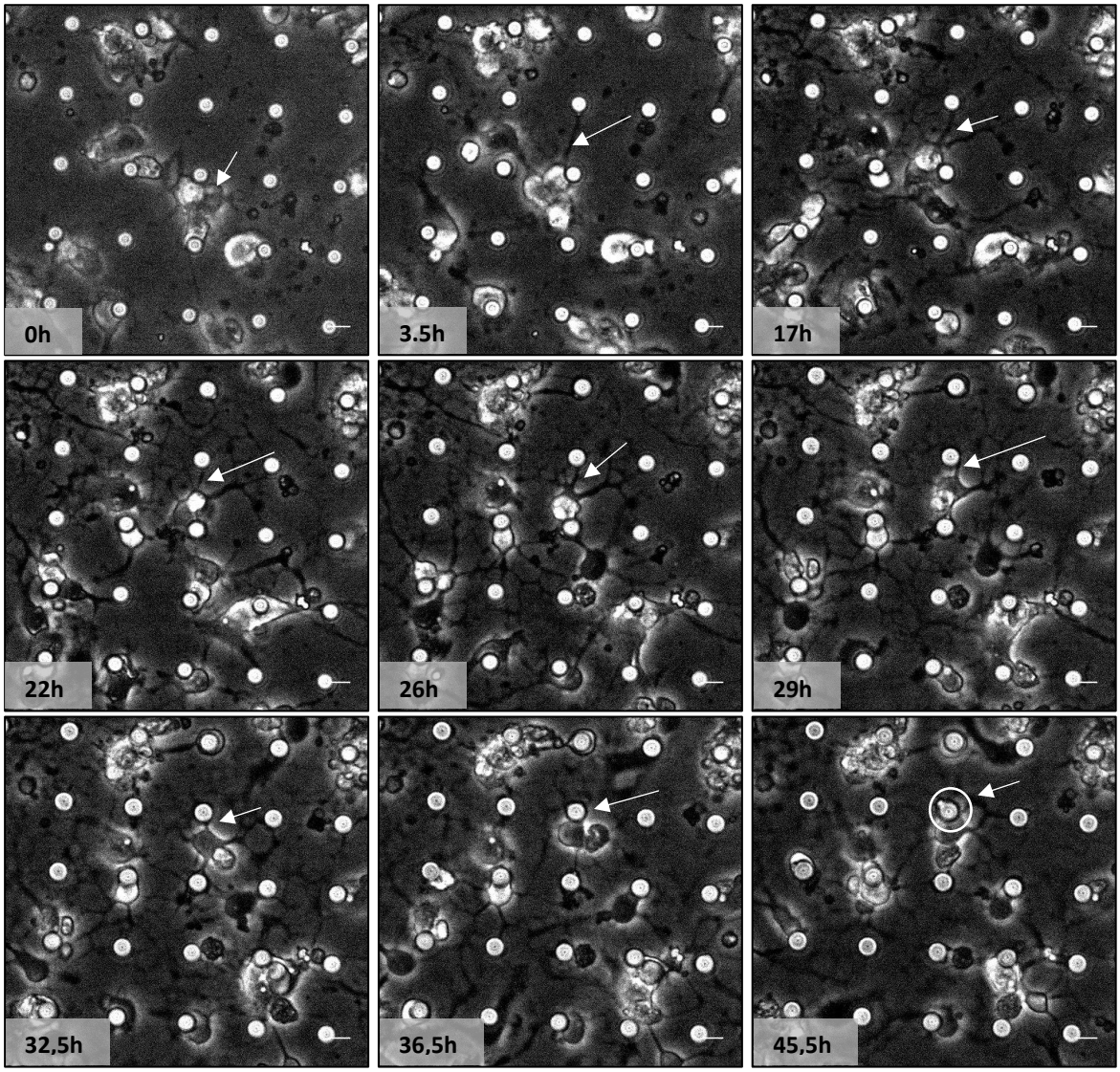

Figure 4.13 *Live imaging photos of oligodendrocytes in PDMS micropillars.* Cells at day 0 after changing to differentiation medium were followed during 48h. The arrows are pointing a cell extending a process and enwrapping a pillar. Scale bar indicates 10μm.

Firstly, it was possible to observe that after changing to differentiation medium, cells were already fixed in a certain place in the substrate and their migration capacity was reduced. During the time of acquisition of the images, OPCs remained stable in that point. Afterwards, OPCs start to extend and retract their processes in a continuous and slow process that could take many hours until stay fixed in a certain micropillar. As the time progresses, it was observed a tendency for the distance between the cell body of the OPC and the spreading processes to decrease (**Figure 4.13 between 26h and 29h**) and, surprisingly, the cell body gets progressively closer to the pillar until enwrapping it. The possible wrapping by the cell body is interesting once, so far researchers have assumed that once oligodendrocytes myelinate more than one axon at the same time, the cell body does not enwrap none of the axons [19]. Nevertheless, the timeframe of the acquisition of the images did not allow to distinguish if the

wrapping around the pillars was permanent or merely transient. For that reason, an increased time of acquisition would be of added value.
Furthermore, it was also realized that, one OPC myelinated more than one pillar, which was in accordance with expectations, as in the CNS one oligodendrocyte is responsible for the myelination of multiple neurons [19]. However there is a visible tendency of the same pillar to be myelinated by more than one oligodendrocyte. This fact, although being just an assumption due to the low resolution of the technique, is not unreasonable since the same axon along its extension is myelinated by more than one oligodendrocyte.

Interestingly, it was also clearly visible that, in the presence of oligodendrocytes micropillars did not collapse or bend, indicating that cellular forces are not enough to disturb the structure of the pillars. Therefore, PDMS rigidity may be adequate regarding this point, though more studies about pillars' deformation and the optimal conditions for pillars' fabrication can be explored in the future.

Although this technique enabled to visualize OPC myelination around pillars and to consolidate that these cells are capable of enwrapping pillars, not many conclusions could be taken whether the wrapping is organized or not and which are the underlying mechanisms responsible for the myelination process due to the low resolution of the microscopy technique implemented. Therefore, a more accurate and higher resolution technique should be considered in further studies. Moreover, a marker to the myelin membrane would be valuable to better distinguish the myelin bearing processes. For that reason, in the scope of this project, the live imaging was also attempted in a confocal microscope and using a cell stain for live imaging (CellMask Green). Despite not being specific for myelin membrane, this marker stains the cytoplasmatic membrane of cells and proved to be efficient in staining the myelin processes (**Figure 4.14**). However, the live imaging photos could not be taken due to unfavourable conditions associated with the confocal microscope (temperature variations caused defocus in the image).

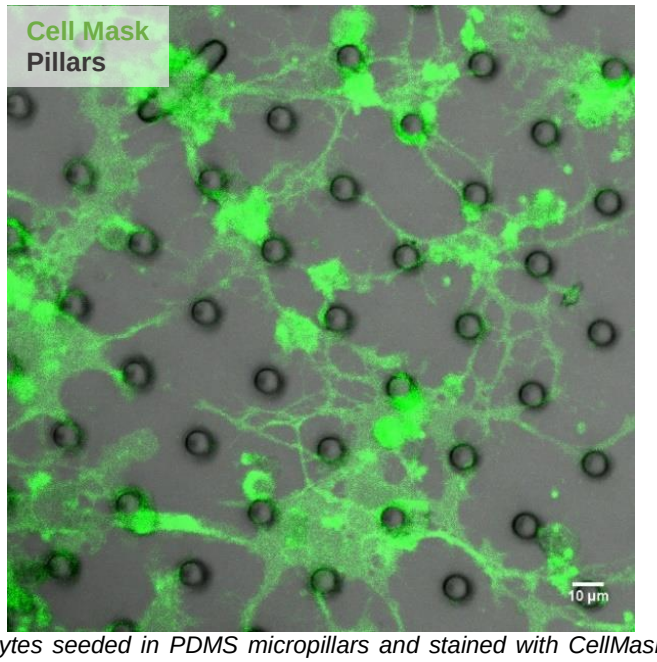

Figure 4.14 *Oligodendrocytes seeded in PDMS micropillars and stained with CellMask Green (ThermoFisher).* Oligodendrocytes' myelin processes are visible. Scale bar is depicted in the image.

Not many papers in the literature report the use of oligodendrocytes cultured *in vitro* for cell live imaging. The majority of reports involves *in vivo* or *ex vivo* live imaging. Important advances in the imaging technology field have been contributing to the progress of this field of knowledge, namely through the development of the two-photon imaging, single molecule imaging or exploration of photoswitchable fluorescent proteins [46-48]. For example, Hughes *et al* [49] generated a transgenic mice expressing the green fluorescent protein (GFP) in NG2 cells and used a two-photon imaging microscope to follow these cells. Moreover, Hill and Grutzendler reported that the fluorescent dye sulforhodamine 101 can be used to trace myelinating oligodendrocytes within the CNS [50]. Besides, studies using *ex vivo* cerebral models have become popular in this field. Harrer and co-workers explored an organotypic cerebellar slice culture where OPCs were expressing GFP. This model was used to study mechanisms of demyelination by adding demyelinating monoclonal antibodies to the slices. Recurring to confocal live imaging, the authors showed that these antibodies were able to promote the myelin degeneration and oligodendrocyte cell death [51]. Nonetheless, the field of the *in vitro* live imaging of oligodendrocytes is still in its infancy [46]. Recently, Ioannidou *et al* [52] used mixed CNS myelinating cultures from β-actin GFP mice spinal cord with an MBP mutation to which neurospheres expressing dsRed were added to allow the visualization either of oligodendrocytes' cytoplasm or the membranous processes distinguishable of these cells and followed myelination under an inverted fluorescent microscope. In this paper, the same events of oligodendrocytes' processes extension and retraction were also seen, strengthening the reliability of the presented PDMS micropillar array platform to study myelination.

Furthermore, this *in vitro* platform is advantageous regarding the existing neuron-oligodendrocyte co-culture models once its inherent simplicity allows to mimic axon-oligodendrocyte interactions. However, in this study, biochemical signals involved in the oligodendrocyte-neuron crosstalk were not considered although known to be key players in the myelination process. Namely, it has been proved that the myelin formation and OPC survival is influenced by the interaction of integrin molecules with axonal or substrate ECM proteins (for example, laminin-2) [53]. Signals sent by the axons are fundamental in modulating the proliferation and differentiation of oligodendrocytes as well as in defining the myelin thickness that surrounds a specific axon. On the other hand, oligodendrocytes also provide signals to axons that affect their intrinsic survival. Together this intimate crosstalk is responsible for correct signal propagation along the axons as well as for the adequate formation of molecular, structural and functional domains of the myelin sheath [54].

For that reason, a study involving the addition of axonal factors or ECM protein coatings to the micropillars would improve the knowledge about myelination and resemble better the *in vivo* CNS myelinating system. For example, using medium containing factors essential for neuronal growth (like nerve growth factor) would be valuable.

Although this platform lacks some important *in vivo* CNS features (for example, in the CNS the axons are not several micrometres apart, but this platform was constructed based on a micropillar distance of 30μm) using micropillars to act as surrogate axons is far from being an explored field. Only one research team has enrolled in this kind of strategy. Mei and co-workers have developed conical micropillars as a tool for high throughput screening of MS possible targets [55]. This platform was then implemented by Redmond *et al* [56] to conclude about possible molecules involved in the oligodendroglial wrapping.

CONCLUSIONS

This study shows that PDMS micropillars are a reliable and suitable *in vitro* platform for the study of CNS myelination processes. Their physical properties that resemble axons allow to understand the physical cues underlying the processes of OPC proliferation, differentiation and wrapping. With well-defined micropillars' diameters, the micropillar array enables the more controlled manipulation of the variables involved in the system of myelination.

Besides, as far as it is reported, the project presented here was the first attempt to follow oligodendrocyte differentiation and wrapping in real time using PDMS micropillars as surrogate axons

REFERENCES

1. Larsen, P.H., et al., *Myelin formation during development of the CNS is delayed in matrix metalloproteinase-9 and -12 null mice.* J Neurosci, 2006. **26**(8): p. 2207-14.
2. Miron, V.E., T. Kuhlmann, and J.P. Antel, *Cells of the oligodendroglial lineage, myelination, and remyelination.* Biochimica et Biophysica Acta (BBA) - Molecular Basis of Disease, 2011. **1812**(2): p. 184-193.
3. Caprariello, A.V., et al., *Apoptosis of Oligodendrocytes during Early Development Delays Myelination and Impairs Subsequent Responses to Demyelination.* J Neurosci, 2015. **35**(41): p. 14031-41.
4. Alizadeh, A., S.M. Dyck, and S. Karimi-Abdolrezaee, *Myelin Damage and Repair in Pathologic CNS: Challenges and Prospects.* Frontiers in Molecular Neuroscience, 2015. **8**.
5. Tosic, M., et al., *Triiodothyronine has diverse and multiple stimulating effects on expression of the major myelin protein genes.* J Neurochem, 1992. **59**(5): p. 1770-7.
6. Jones, S.A., et al., *Triiodothyronine is a survival factor for developing oligodendrocytes.* Mol Cell Endocrinol, 2003. **199**(1-2): p. 49-60.
7. Wren, D., G. Wolswijk, and M. Noble, *In vitro analysis of the origin and maintenance of O-2Aadult progenitor cells.* J Cell Biol, 1992. **116**(1): p. 167-76.
8. Tang, D.G., Y.M. Tokumoto, and M.C. Raff, *Long-term culture of purified postnatal oligodendrocyte precursor cells. Evidence for an intrinsic maturation program that plays out over months.* J Cell Biol, 2000. **148**(5): p. 971-84.
9. Ruffini, F., et al., *Distinctive properties of human adult brain-derived myelin progenitor cells.* Am J Pathol, 2004. **165**(6): p. 2167-75.
10. Zhang, S.C., *Defining glial cells during CNS development.* Nat Rev Neurosci, 2001. **2**(11): p. 840-3.
11. Nishiyama, A., et al., *Polydendrocytes (NG2 cells): multifunctional cells with lineage plasticity.* Nat Rev Neurosci, 2009. **10**(1): p. 9-22.
12. Franklin, R., *Why does remyelination fail in multiple sclerosis?* Nature Reviews Neuroscience, 2002. **3**(9): p. 705-714.
13. Snaidero, N., et al., *Myelin membrane wrapping of CNS axons by PI(3,4,5)P3-dependent polarized growth at the inner tongue.* Cell, 2014. **156**(1-2): p. 277-90.
14. Bunge, M.B., R.P. Bunge, and H. Ris, *Ultrastructural study of remyelination in an experimental lesion adult cat spinal cord.* The Journal of Biophysical and Biochemical Cytology, 1961. **10**(1): p. 67-94.
15. Bunge, R.P., M.B. Bunge, and M. Bates, *Movements of the Schwann cell nucleus implicate progression of the inner (axon-related) Schwann cell process during myelination.* J Cell Biol, 1989. **109**(1): p. 273-84.
16. Knobler, R.L., J.G. Stempak, and M. Laurencin, *Nonuniformity of the oligodendroglial ensheathment of axons during myelination in the developing rat central nervous system. A serial section electron microscopical study.* J Ultrastruct Res, 1976. **55**(3): p. 417-32.
17. Pedraza, L., J.K. Huang, and D. Colman, *Disposition of axonal caspr with respect to glial cell membranes: Implications for the process of myelination.* J Neurosci Res, 2009. **87**(15): p. 3480-91.
18. Sobottka, B., et al., *CNS live imaging reveals a new mechanism of myelination: the liquid croissant model.* Glia, 2011. **59**(12): p. 1841-9.
19. Chang, K.-J., S.A. Redmond, and J.R. Chan, *Remodeling myelination: implications for mechanisms of neural plasticity.* Nat Neurosci, 2016. **19**(2): p. 190-197.
20. Lötters, J.C., et al., *The mechanical properties of the rubber elastic polymer polydimethylsiloxane for sensor applications.* Journal of Micromechanics and Microengineering, 1997. **7**(3): p. 145.

21. Seethapathy, S. and T. Górecki, *Applications of polydimethylsiloxane in analytical chemistry: A review.* Analytica Chimica Acta, 2012. **750**: p. 48-62.
22. Slaughter, G. and B. Stevens, *A cost-effective two-step method for enhancing the hydrophilicity of PDMS surfaces.* BioChip Journal, 2014. **8**(1): p. 28-34.
23. Gupta, M., et al., *Micropillar substrates: a tool for studying cell mechanobiology.* Methods Cell Biol, 2015. **125**: p. 289-308.
24. McCarthy, K.D. and J. de Vellis, *Preparation of separate astroglial and oligodendroglial cell cultures from rat cerebral tissue.* The Journal of Cell Biology, 1980. **85**(3): p. 890-902.
25. Chen, Y., et al., *Isolation and culture of rat and mouse oligodendrocyte precursor cells.* Nat Protoc, 2007. **2**(5): p. 1044-51.
26. Chandra, D. and S. Yang, *Stability of High-Aspect-Ratio Micropillar Arrays against Adhesive and Capillary Forces.* Accounts of Chemical Research, 2010. **43**(8): p. 1080-1091.
27. Corning, D. *Isopropanol (Anhydrous) datasheet*. 2002 [cited 2016 10th September]; Available from: http://www.dow.com/assets/attachments/business/pcm/solvents/isopropanol/tds/isopropanol.pdf.
28. Korosi, A. and B.M. Fabuss, *Viscosity of liquid water from 25 to 150.degree. measurements in pressurized glass capillary viscometer.* Analytical Chemistry, 1968. **40**(1): p. 157-162.
29. Goldfarb, D.o.L., et al., *Aqueous-based photoresist drying using supercritical carbon dioxide to prevent pattern collapse.* Journal of Vacuum Science & Technology B, 2000. **18**(6): p. 3313-3317.
30. Aoun, L., et al., *Microdevice arrays of high aspect ratio poly(dimethylsiloxane) pillars for the investigation of multicellular tumour spheroid mechanical properties.* Lab Chip, 2014. **14**(13): p. 2344-53.
31. Zhou, J., A.V. Ellis, and N.H. Voelcker, *Recent developments in PDMS surface modification for microfluidic devices.* Electrophoresis, 2010. **31**(1): p. 2-16.
32. Ye, H., Z. Gu, and D.H. Gracias, *Kinetics of ultraviolet and plasma surface modification of poly(dimethylsiloxane) probed by sum frequency vibrational spectroscopy.* Langmuir, 2006. **22**(4): p. 1863-8.
33. Efimenko, K., W.E. Wallace, and J. Genzer, *Surface Modification of Sylgard-184 Poly(dimethyl siloxane) Networks by Ultraviolet and Ultraviolet/Ozone Treatment.* Journal of Colloid and Interface Science, 2002. **254**(2): p. 306-315.
34. Oláh, A., H. Hillborg, and G.J. Vancso, *Hydrophobic recovery of UV/ozone treated poly(dimethylsiloxane): adhesion studies by contact mechanics and mechanism of surface modification.* Applied Surface Science, 2005. **239**(3–4): p. 410-423.
35. Lee, S., et al., *A culture system to study oligodendrocyte myelination-processes using engineered nanofibers.* Nature methods, 2012. **9**(9): p. 917-922.
36. Káradóttir, R.T. and J.H. Stockley, *Deconstructing myelination: it all comes down to size.* Nature methods, 2012. **9**(9): p. 883-884.
37. Moskowitz, P.F., et al., *Expression of the class III beta-tubulin gene during axonal regeneration of rat dorsal root ganglion neurons.* J Neurosci Res, 1993. **34**(1): p. 129-34.
38. Ohsawa, K., et al., *Microglia/macrophage-specific protein Iba1 binds to fimbrin and enhances its actin-bundling activity.* J Neurochem, 2004. **88**(4): p. 844-56.
39. Rocha, D.N., *Impact of Mechanotrasduction in the Context of Central Nervous System Diseases (Unplublished doctoral thesis)*. 2015, University of Porto: Portugal.
40. Rocha, D.N., et al., *Extracellular Environment Contribution to Astrogliosis – Lessons learned from a Tissue Engineered 3D Model of the Glial Scar.* Front. Cell. Neurosci., 2015. **9:377**.
41. Teixeira, A.I., et al., *The promotion of neuronal maturation on soft substrates.* Biomaterials, 2009. **30**(27): p. 4567-4572.

42. Barateiro, A. and A. Fernandes, *Temporal oligodendrocyte lineage progression: In vitro models of proliferation, differentiation and myelination.* Biochimica et Biophysica Acta (BBA) - Molecular Cell Research, 2014. **1843**(9): p. 1917-1929.
43. Jagielska, A., et al., *Mechanical environment modulates biological properties of oligodendrocyte progenitor cells.* Stem Cells Dev, 2012. **21**(16): p. 2905-14.
44. Lourenco, T., et al., *Modulation of oligodendrocyte differentiation and maturation by combined biochemical and mechanical cues.* Sci Rep, 2016. **6**: p. 21563.
45. Michalski, J.-P. and R. Kothary, *Oligodendrocytes in a Nutshell.* Frontiers in Cellular Neuroscience, 2015. **9**: p. 340.
46. Rassul, S.M., R.K. Neely, and D. Fulton, *Live-imaging in the CNS: New insights on oligodendrocytes, myelination, and their responses to inflammation.* Neuropharmacology, 2015.
47. Richert, S., et al., *In vivo labeling of peroxisomes by photoconvertible mEos2 in myelinating glia of mice.* Biochimie, 2014. **98**: p. 127-134.
48. Shibata, S., et al., *Sox10-Venus mice: a new tool for real-time labeling of neural crest lineage cells and oligodendrocytes.* Mol Brain, 2010. **3**: p. 31.
49. Hughes, E.G., et al., *Oligodendrocyte progenitors balance growth with self-repulsion to achieve homeostasis in the adult brain.* Nat Neurosci, 2013. **16**(6): p. 668-676.
50. Hill, R.A. and J. Grutzendler, *In vivo imaging of oligodendrocytes with sulforhodamine 101.* Nat Methods, 2014. **11**(11): p. 1081-2.
51. Harrer, M.D., et al., *Live imaging of remyelination after antibody-mediated demyelination in an ex-vivo model for immune mediated CNS damage.* Experimental Neurology, 2009. **216**(2): p. 431-438.
52. Ioannidou, K., et al., *Time-Lapse Imaging of the Dynamics of CNS Glial-Axonal Interactions In Vitro and Ex Vivo.* PLoS ONE, 2012. **7**(1): p. e30775.
53. Camara, J., et al., *Integrin-mediated axoglial interactions initiate myelination in the central nervous system.* J Cell Biol, 2009. **185**(4): p. 699-712.
54. Poliak, S. and E. Peles, *The local differentiation of myelinated axons at nodes of Ranvier.* Nat Rev Neurosci, 2003. **4**(12): p. 968-980.
55. Mei, F., et al., *Micropillar arrays as a high-throughput screening platform for therapeutics in multiple sclerosis.* Nat Med, 2014. **20**(8): p. 954-60.
56. Redmond, S.A., et al., *Somatodendritic Expression of JAM2 Inhibits Oligodendrocyte Myelination.* Neuron, 2016. **91**(4): p. 824-36.

- This page was intentionally left blank. -

CHAPTER 5

GENERAL CONCLUSIONS AND FUTURE PERSPECTIVES

- This page was intentionally left blank. -

The central nervous system is complex and the interactions between all components (neurons and glia) are of extreme importance for its normal functionality. However, when an insult disrupts this homeostasis scenario this communication is massively disturbed. Specifically, the loss of myelin (which is a protective membrane that unsheathes axons and facilitates the electrical signal propagation between neurons) is the reason of many neurodegenerative diseases.

Currently, there is no effective treatment for demyelinating diseases because the biological features of these diseases are not totally understood. Scientists are eagerly seeking for better models to mimic in the laboratory, as far as possible, the biological features of these diseases. However, so far no model can truly replicate the *in vivo* CNS interactions either in pathological contexts or in homeostasis scenarios. For that reason, there is an unmet need to develop new models that can contribute to the understanding of the biological mechanisms of injured CNS and to the search for new therapeutical targets for these diseases.

Consequently, the work here presented aimed to explore two *in vitro* novel engineered models that can contribute to our current knowledge of the processes that mediate myelination.

Firstly, a previously described 3D axonal myelination *in vitro* platform coupled with a tissue engineered model of astrogliosis was further explored to study the crosstalk between astrocytes and oligodendrocytes, specifically their interaction in the context of astrogliosis. It was shown that the activation of astrocytes (a hallmark of astrogliosis) significantly impaired the course of oligodendrocytes' differentiation, corroborating the preliminary studies already advanced by the group. Besides, our date further confirmed the reliability of the use of electrospinning nanofibers to act as surrogate axons, allowing the uncoupling the study of the crosstalk between astrocytes and oligodendrocytes from axonal processes' interaction.
However, future studies to explore the impact of the activated astrocytes on oligodendrocyte differentiation should be done, namely through the quantitative evaluation of the expression of more myelin related markers (like proteolipid protein, PLP or myelin oligodendrocyte glicoprotein, MOG) and progenitor markers (as NG2). Besides, a deeper study to unveil the mechanisms of MBP expression decrease in OPCs when in the presence of activated astrocytes would be of added value. Understanding if the decrease of MBP is the result of a reduction of the number of live OPCs or the incapacity of live OPCs to differentiate is crucial. For that purpose, the assessment of apoptotic markers should be conducted to understand the related causes of this phenomenon.
Moreover, the effects of other characteristic astrocyte phenotypes on OPC development were not studied. Namely, inducing astrocytes to a quiescent state (for example, by adding factors responsible for the maintenance of their quiescence like tenascin-C [1]) would be important to understand the impact of the homeostasis characteristic astrocytes on OPC myelination. In

addition, improving the glial scar model by adding cell adhesion motifs to the alginate to allow astrocytes to acquire a morphology closer to the one observed in vivo would be also valuable. Once the morphology of activated astrocytes did not resemble the well-described elongated and hypertrophic astrocytes within the glial scar, the extent of the astrocytes activation could not be fully confirmed. Furthermore, to assess the similarity of the 3D axonal myelination platform with the *in vivo* situation, in the future, the results obtained with the engineered nanofibers should be confirmed with results obtained when the OPCs are cultured in the presence of neurons (like DRG neurons) since the majority of myelination platforms established in the literature are the co-cultures between DRG neurons and OPCs.

A study about the influence of fiber diameter on the course of OPC differentiation after inducing an astrogliosis scenario would be interesting. Specifically, producing aligned nanofibers with well-controlled diameters by electrospinning techniques is a possible future achievement. Although few studies have described the influence of fiber diameter for myelination [2, 3] none have reported this influence in the context of remyelination processes.

Finally, the ultimate aim of this platform would be to apply it to the screenning of biological relevant therapeutical targets or molecules and the study of their impact on the communication of these two types of cells. Although ibuprofen was the preliminary tested drug, a deeper study on its effects on astrocyte-oligodendrocyte crosstalk is needed.

Additionally, in this work, for the first time an *in vitro* micropillar array platform was explored with the aim of studying the process of OPC myelination. We have observed that the PDMS micropillars promote the OPC differentiation and wrapping in a reproducible manner. However, data presented here is just preliminary and further studies still need to be performed. Firstly, the mechanical properties of the PDMS platform should be characterized and varied. The effect of mechanical properties on OPC differentiation and myelination should be described once OPCs are reported to be mechanosensitive [4, 5]. Achieving an elastic modulus near the brain's ECM should be the objective in order to mimic as far as possible the *in vivo* CNS tissue. In addition, the biochemical cues of the axons-oligodendrocytes crosstalk were not considered in this study. For that reason, improving the complexity of the system by adding neuronal factors or ECM proteins to serve as coatings for the micropillars could significantly change the differentiation observed without any external factor.

Besides, the oligodendrocytes' wrapping should be studied with a better resolution microscopy technique, either with fixed cells (for example, SEM) or in real time. Regarding the live imaging in the micropillars, a better myelin processes' marker should be explored to facilitate the accurate understanding of the process of OPC myelination.

Furthermore, the study of OPC differentiation in the platform with pillars with different diameters is now possible to be done once the issues regarding pillar stability were overcome. The effects of micropillars diameter can also be determined.

Finally, using a conductor polymer to which electrodes can be attached to transmit electrical signals instead of PDMS polymer would also be extremely attractive to closely mimic the CNS *in vivo* signal transmission between neurons and their effects on myelination.

Importantly, both studies highlight the relevance of the microenvironment in which neural cells are grown. Although the traditional *in vitro* 2D platforms allow the well-controlled analysis of individual variables, the intrinsic complexity arising from the three-dimensionality of the CNS is not achieved. Both *in vitro* platforms developed in the scope of this project show that cells in 3D microenvironments behave more closely to those *in vivo*.

Overall, this project adds important steps towards the development of relevant biological *in vitro* CNS models, expanding the knowledge about biological fundamentals of the CNS cells' interactions either in pathological contexts or in homeostasis scenarios, improving the clinical relevance of these platforms.

REFERENCES

1. Nash, B., et al., *Functional duality of astrocytes in myelination.* J Neurosci, 2011. **31**(37): p. 13028-38.
2. Lee, S., et al., *A culture system to study oligodendrocyte myelination-processes using engineered nanofibers.* Nature methods, 2012. **9**(9): p. 917-922.
3. Lee, S., et al., *A rapid and reproducible assay for modeling myelination by oligodendrocytes using engineered nanofibers.* Nat Protoc, 2013. **8**(4): p. 771-82.
4. Jagielska, A., et al., *Mechanical environment modulates biological properties of oligodendrocyte progenitor cells.* Stem Cells Dev, 2012. **21**(16): p. 2905-14.
5. Lourenco, T., et al., *Modulation of oligodendrocyte differentiation and maturation by combined biochemical and mechanical cues.* Sci Rep, 2016. **6**: p. 21563.

- This page was intentionally left blank. -

APPENDIX

- This page was intentionally left blank. -

APPENDIX A: REVIEW "HIGH THROUGHPUT PLATFORMS FOR THE SCREENING OF NEW THERAPEUTIC TARGETS FOR NEURODEGENERATIVE DISEASES"

Rocha, DN, Carvalho, ED, Pêgo, AP

Drug Discov Today. 2016 May 10. pii: S1359-6446(16)30155-6. doi: 10.1016/j.drudis.2016.05.005.

- This page was intentionally left blank. -

Several cell-based platforms are being explored as central nervous system tissue mimics, in health and in disease, for the high-throughput screening of new therapeutic targets and drugs to address the challenging management of neurodegenerative disorders.

High-throughput platforms for the screening of new therapeutic targets for neurodegenerative diseases

Daniela N. Rocha[1,2,3], **Eva D. Carvalho**[1,2,3,4] and **Ana Paula Pêgo**[1,2,3,4]

[1] INEB – Instituto de Engenharia Biomédica, Universidade do Porto, Porto, Portugal
[2] i3S – Instituto de Investigação e Inovação em Saúde, Universidade do Porto, Porto, Portugal
[3] Faculdade de Engenharia, Universidade do Porto, Porto, Portugal
[4] Instituto de Ciências Biomédicas Abel Salazar, Universidade do Porto, Porto, Portugal

Despite the recent progress in the understanding of neurodegenerative disorders, a lack of solid fundamental knowledge on the etiology of many of the major neurodegenerative diseases has made it difficult to obtain effective therapies to treat these conditions. Scientists have been looking to carry out more-human-relevant studies, with strong statistical power, to overcome the limitations of preclinical animal models that have contributed to the failure of numerous therapeutics in clinical trials. Here, we identify currently existing platforms to mimic central nervous system tissues, healthy and diseased, mainly focusing on cell-based platforms and discussing their strengths and limitations in the context of the high-throughput screening of new therapeutic targets and drugs.

Introduction

Neurodegenerative diseases (see Glossary) are incurable and highly debilitating conditions that can lead to impaired cognitive and sensorial functions and/or problems in movement (ataxia). These include Alzheimer's disease (AD), Parkinson's disease (PD), Huntington's disease (HD) and multiple sclerosis (MS), among others. Some central nervous system (CNS) neurodegenerative diseases are known to have a genetic/familiar component, whereas others are highly multifactorial [1].

Neurodegenerative diseases were initially investigated using anatomical studies followed by biochemical analysis. Currently, a common practice is the study of familial genes that could be involved in these diseases or identification of major pathways involved in the mechanisms of the disease, recurring to mutation integration (knock-in and knockout) in animal models. This enabled the massive progress seen recently in the knowledge of these diseases. Nevertheless, these conditions remain untreatable, and several important mechanisms of neurodegeneration are still to be fully understood. In 2010, the annual costs of mental and neurological pathologies in Europe were €798 billion. Owing to the nature of these diseases, 40% of these costs were related to

Corresponding author: Pêgo, A.P. (apego@ineb.up.pt)

Daniela N. Rocha is currently the Deputy R&D Manager at Blueclinical (Porto), and worked at INEB (Biomedical Engineering Institute), before her current post, under the supervision of Ana Paula Pêgo. In 2015, she received her PhD degree in biomedical engineering from the University of Porto and her MBA from Porto Business School. She has eight years of experience in research within the biomaterials for neuroscience field, including polymers and hydrogels. Her expertise includes primary cell isolation, 3D cell culture techniques, mechanotransduction events and related signalling pathways.

Eva D. Carvalho is an MSc bioengineering student from University of Porto (Portugal) and is currently developing a master's thesis in Ana Paula Pêgo's group on platforms to study demyelinating diseases. In 2013, Eva enrolled a research project at IBMC (Portugal) in which the TGF-β signalling pathway in *Drosophila melanogaster* was studied. In 2015, at REMEDI (Ireland), Eva was focused on developing iPSC from *Retinitis pigmentosa* patients. Her main research interests are on neurodegenerative diseases and neuroregeneration.

Ana Paula Pêgo (PhD) is the Coordinator of the nBTT: nanoBiomaterials for Targeted Therapies Group at INEB|i3S. By using nanomedicine strategies her team aims at providing *in situ* and in a targeted manner the required signals to promote nervous tissue regeneration. The research on new biomaterials for application in neurosciences includes the development of new polymers for the design of alternative vectors to viruses for efficient nucleic acid delivery to neuronal cells and preparation of nerve grafts for spinal cord injury treatment. Her team recently developed a tissue-engineered astroglial scar to serve as a platform for the identification of glial scar features or elements that might represent therapeutic targets to treat central nervous system lesions.

1359-6446/
http://dx.doi.org/10.1016/j.drudis.2016.05.005

Please cite this article in press as: Rocha, D.N. et al. High-throughput platforms for the screening of new therapeutic targets for neurodegenerative diseases, Drug Discov Today (2016), http://dx.doi.org/10.1016/j.drudis.2016.05.005

GLOSSARY

Biolistic transfection A physical method of transfection in which the target tissue is bombarded with DNA-coated gold particles.
Bioprinting The process of generating spatially controlled cell patterns or constructs using 3D printing technologies – typically it involves dispensing cells in an injectable biomaterial, like hydrogels.
Electrospinning A fibre production method that uses electric force to draw charged threads of polymer solutions or melts up to fibre diameters in the nano- to micro-metre range. It is used in the biomaterials field because of close resemblance between electrospun polymer fibres and the extracellular matrix fibrillar components.
High-throughput screening A process in which large numbers of conditions (chemicals, biological agents, etc.) are tested with high efficiency, to identify biologically active molecules and/or cellular targets as candidates for further validation in additional experiments.
Mechanotransduction The process by which a cell translates mechanical stimulus into biochemical signals – the transduced signals can vary in properties, being electrical (i.e. the ones involved in the depolarisation of cellular membranes), chemical (i.e. those producing a second messenger) or transcriptional (i.e. in the activation of gene expression), among others.
Microelectrode arrays or multielectrode arrays (MEAs) Devices that contain multiple microelectrodes through which neural signals are obtained and/or delivered, essentially serving as neural interfaces that connect neurons to electronic circuitry – MEAs can be used in vivo or in vitro, neuronal cultures on MEAs can survive for over a year in vitro.
Microfluidics The behaviour, precise control and manipulation of fluids that are typically geometrically constrained to a submillimeter scale.
Multicellular spheroids Microscale, spherical cell clusters–spheroids can be monoculture or multiculture.
Neurodegenerative diseases A disease group characterised by progressive nervous system dysfunction, being associated with atrophy of affected structures of the nervous system.
Tissue engineering Generally involves the use of materials (scaffolds), cells and bioactive molecules to prepare de novo tissues in vitro or in vivo with the goal of trying to understand tissue function or as part of tissue regenerative or repair strategies.

loss of productivity of the affected people [2]. Costs are probably higher today because these pathologies usually have a long-term impact and the population is aging. Taking all this into consideration, it is clear that there is the need to increase our understanding of CNS neurodegenerative disorders to address them effectively.

Over time, scientists have been looking forward to making more-human-relevant studies mainly because of the difficulty in translating the obtained results in preclinical animal models to humans, the costs associated with animal models, as well as all the ethical issues raised with the use of the latter. As such, there is a growing need for biologically and clinically relevant *in vitro* models to be used to increase the knowledge of CNS function, define disease biomarkers, study and test new therapeutic targets and drug candidates before the start of clinical trials, as well as enable the discovery of new interesting applications for known therapeutic molecules.

In vitro screening systems need to recreate an environment that is as representative as possible to the one found *in vivo* in the target tissue or system unit of interest. Although simple *in vitro* systems are appealing, there is a need to find equilibrium between model simplicity and physiological relevancy for data understanding and interpretation to be possible and relevant. Ideally a platform must allow the full control of system complexity and existing variables. Additionally, it should enable the researcher to start with a simple platform that, in time, with the increasing understanding of the system, can become more and more complex, giving rise not only to a higher understanding of the system but also to more-relevant results and knowledge. Moreover, with the increasing need to test as many variables as possible at once, high-throughput screening (HTS) assays have been evolving. Here, we identify the existing platforms to mimic the healthy and diseased CNS, mainly focusing on cell-based platforms, discussing their strengths and limitations in the context of the HTS of new therapeutic targets and drugs for the treatment of neurodegenerative diseases.

Considerations for HTS platforms

Typically, in the context of biomedicine, HTS is applied in the design of chemical structures to be used in drug discovery and further testing in a therapeutic setting or to test compounds and/or conditions to address biological questions in fundamental research [3]. The need for HTS platforms is increasing among industry and academic researchers, because they can solve the problem of lengthy, resource-intensive procedures that can, sometimes, make the screening of the required large number of conditions impossible. One of the main causes of failure during clinical trials is the lack of efficacy of the existing *in vitro* systems to test drug toxicity, which ends up being revealed only at late stages of the research [4].

HTS assays are usually divided into two categories: biochemical assays, studies of protein–protein interactions, proteases, enzymatic activity, among others; and cell-based assays. Biochemical assays usually assume a starting knowledge of a molecular target; by contrast cell-based assays often aim to identify modulators of a pathway of interest.

There are several published studies that focus on the considerable potential of HTS-based biochemical assays. Pedro *et al.* [5] developed a method in which the activity of the leucine-rich repeat kinase 2 (LRRK2) was measured, because increased LRRK2 activity was proved to be related to PD. The group used the AlphaScreen® assay which relies on the emission of fluorescence if there is a biomolecular interaction between the donor and the acceptor (the kinase and a moesin which is its putative physiological substrate). This HTS platform has been proposed to test the capacity of small molecules in inhibiting the activity of LRRK2. Crowe *et al.* [6] carried out another interesting study, screening almost 30,000 compounds to assess their influence on tau protein assembly. Formation of toxic tau oligomers in the brain is one of the main observed pathologic events of AD. With this in mind, using an HTS assay based on complementary thioflavin T fluorescence and fluorescence polarisation methods, the authors were able to observe the effects of inhibitors of tau oligomerisation and found that aminothienopyridazines (ATPZs) caused inhibition of

Please cite this article in press as: Rocha, D.N. et al. High-throughput platforms for the screening of new therapeutic targets for neurodegenerative diseases, Drug Discov Today (2016), http://dx.doi.org/10.1016/j.drudis.2016.05.005

fibril assembly as well as fibrillisation of tau. Because the normal ability of tau to stabilise microtubules was not affected, ATPZs were shown to be promising drugs to treat AD. In addition, Wang *et al.* [7] developed a study focused on the process of hydrolysis of acetylcholine by acetylcholinesterase, which is a central mechanism in the control of neural response. In AD the levels of acetylcholine are low, making it an interesting therapeutic target. The authors measured acetylcholinesterase activity and screened acetylcholinesterase inhibitors thus proving the feasibility of the assay that has the potential to be, in the future, used as an HTS platform for screening inhibitors of acetylcholinesterase. Further evidence supporting the relevance of biochemical-based assays in the context of neurodegenerative diseases was conducted by Shu and co-workers [8] who devised an HTS assay based on a novel reporter substrate of autophagin-1 composed of a natural substrate (LC3B) fused to an assayable enzyme (PLA2) that becomes active upon cleavage by this cysteine protease. This platform can serve for identification and characterisation of autophagin-1 inhibitors – inferring the role of autophagy, because its regulation could be the cause of many diseases, including neurodegenerative ones. More recently, Kashem *et al.* [9] studied the inhibition of sphingosine-1-phosphate (S1P), a sphingolipid whose degradation by S1P phosphatases and sphingosine-1-phosphate lyase (SPL) is involved in AD and MS pathologies. Briefly, the group created a scintillation proximity assay able to screen possible inhibitors in 384-well microplates in a rapid way. By testing a library of 10^6 compounds the team identified several classes of SPL inhibitors amenable to be used as a new class of immunosuppressive drugs.

With cell-based assays, entire pathways can be subjected to questions creating multiple potential points of interest, in contrast to the study of single predetermined steps as in the biochemical assays. Furthermore, cell-based assays can provide information that a biochemical assay cannot, such as the nature of the pharmacological activity of the screened compound at a specific receptor or intracellular target. Furthermore, there are also some targets that cannot be properly reconstituted in a biochemical assay [10–14], such as complex interactions between receptors or cellular factors that are not easily reproducible outside the cell. Consequently, cell-based platforms are particularly promising because they can be powerful tools in the study of cell growth and differentiation, to investigate the influence of small molecules and cell growth conditions on cell function and physiology, and also to understand signalling pathways in mammalian cells. These have also proven to be very useful in some CNS studies [15–25]. In this context, Thid and co-workers [15] designed a new neural cell culture substrate based on the phospholipid bilayer as a biomimetic platform for cell behaviour studies, which was shown to support cellular adhesion and growth. Kang *et al.* [19] have established a microelectrode array to measure neuronal network activity in a platform that could constitute an interesting drug screening platform. In fact, HTS has also been used to ease and standardise manual methods for the measurement of neurites [24]. There are many important factors that need to be considered when planning a cell-based platform. These include choosing the biological system (primary cells, cell line or explants), choosing the assay approach (functional, phenotypic or reporter gene) [26] and another crucial factor is the assay readout.

Primary cells of human origin are possibly the most physiologically relevant model system and, although primary cells can sometimes be difficult to obtain, several primary cell types from humans and other species are already commercially available [27]. Nevertheless, transformed cell lines of human origin are currently the most commonly used systems. Many of these lines preserve a highly differentiated phenotype being good platforms to screen complex physiological responses. Additionally, cell lines can be engineered to express a specific target [27], which can increase their interest as models for certain studies. Diverse transformed and primary mammalian cells have been exploited to study diseases, including diabetes, cancer and neurodegenerative diseases [3,28,29]. More recently, the development of induced pluripotent stem cell (iPSC) technology provided a new powerful tool for drug screening, allowing the use of cells with the same genetic background of the patients without certain cell type constraints associated with the use of the patient primary cells, as in the case of CNS cells [30].

Issues such as cell viability, doubling time (when applicable) and recovery from freeze–thaw cycles must all be considered [31]. Additionally, cell seeding density and passage number can significantly affect the output and, consequently, the size of the cell bank needed [27]. Differences in cell growth across the plate that can occur with long incubation periods also need to be taken into account, being easily prevented by careful regulation of the humidity and temperature of the incubator and by an even distribution of the plates in the incubator.

When using a cell-based assay focused on a signalling pathway there is flexibility on the choice of the readout. Particularly, if an antibody is available, possible readouts can be any step in which a protein is modified (e.g. phosphorylated), translocated or its abundance changed [32]. When talking about HTS applications, the most applied detection method seems to be fluorescence-based assays. This is mainly because of high sensitivity, diverse selection of fluorophores and a variety of readouts based on different environment-sensitive fluorescence properties [33] that, altogether, allow miniaturisation, flexibility in assay design, ease of manipulation and even the possibility to monitor multiple events simultaneously [33]. Fluorescence readouts are also appealing because fluorescence microscopy techniques have significantly evolved in the past decades with increasing sensitivity, image definition and automatisation features.

Cell-based 2D platforms

Glass coverslips and tissue-culture polystyrene (TCPS) are the most frequently used substrates to culture cells. These can be adequate and convenient substrates for 2D cell cultures and have been widely used for toxicity assays, for example. Malik and co-workers [34] recently reported a 2D model to assess neurotoxicity profiles of several drugs. The authors have used pluripotent stem cells to develop a highly reproducible HTS system and identified cardiac glycosides as potential drugs to target glioblastomas, as a result of their toxicity for human neural stem cells. Although several cell culture models have been successfully established using glass or TCPS substrates, it is well known that these offer cells a very different mechanical environment compared with the one experienced in physiological conditions *in vivo* [35–38]. With this in mind, the biomaterial engineering field has been contributing to

Please cite this article in press as: Rocha, D.N. et al. High-throughput platforms for the screening of new therapeutic targets for neurodegenerative diseases, Drug Discov Today (2016), http://dx.doi.org/10.1016/j.drudis.2016.05.005

the development of physiologically relevant *in vitro* assays by the use of 2D materials that can better mimic *in vivo* mechanical properties. These substrates include polymeric substrates [39] or hydrogels [40–44]. In fact we have recently shown that substrate mechanical properties can influence neuronal morphology and intracellular signalling pathways [39]. In this section, relevant 2D platforms within the context of CNS disorders are discussed.

Disease models

Neurons can exist in the body over a lifetime and neurodegenerative diseases are progressive conditions that affect neurons in time. Consequently, to mimic the physiological conditions *in vitro*, long-term culture systems are necessary. Lesuisse and Martin developed a long-term system using cortical neurons to study mechanisms of neuronal maturation, aging and death and concluded the appearance of an age-related biochemical phenotype in the culture [45]. Interestingly, long-term neuronal cultures were later used to study AD progression by Bertrand *et al.* [46], in this case using cultures of hippocampal neurons. More recently, Todd and co-workers established a method for long-term high-density culturing of hippocampal neurons [47]. The authors claim that their organoid system can serve as a model for AD and in other neurodegeneration studies, because these cultures can provide distinct advantages when testing the effects of long-term therapeutic strategies.

Envisaging AD therapies, Seyb *et al.* [16] developed a cell-based HTS to screen molecules for their ability to inhibit calpain, because this has been correlated with beta-amyloid (Aβ) cytotoxicity. Here the authors explored differentiated Sh-SY5Y cells (a commercially available cell line established by subsequent cloning of the neuroblastoma cell line SK-N-SH, which was established from a metastatic bone tumour). Although this appears to be an interesting screening platform, no direct inhibitors of calpain were found in this study.

Recently, several studies with stem cells have been directed towards the identification of novel therapeutic approaches to understand and ultimately cure neurodegenerative diseases [48–50]. Using cell models of mouse and rat neural stem cells treated with hydrogen peroxide to induce oxidative stress, Wang *et al.* achieved interesting insights regarding the action mechanism of Tecfidera™ (dimethyl fumarate) [51]. This drug, which has been approved in Europe and is already available on the market, shows an ability to reduce relapse rates in MS patients. The team saw an increase in the survival of stem cells through regulation of *Nrf2* and the extracellular-signal-regulated kinase (ERK)1/2/mitogen-activated protein kinase (MAPK) signalling pathway. Zhang *et al.* [52] used a HD-specific iPSC line to develop an *in vitro* HD cell model. Being a cell model based on human cells makes it potentially more clinically relevant and, consequently, useful for the screening of therapeutic drugs.

Salvador and co-workers developed an *in vitro* model of traumatic brain injury (TBI) [53] based on cultures of murine brain microvascular endothelial cells from the cerebral cortex conducted on collagen-coated flexible-bottomed culture plates, in the presence or absence of astrocytic factors. By using these substrates which can be easily subjected to stretch, simulating the primary mechanical disruption typically occurring in TBI, together with oxygen and glucose deprivation, the authors achieved a closer to reality replication of the events occurring in TBI.

Co-cultures have also been widely studied and used as cell models to understand neurodegeneration. Several co-culture models have been proposed to address myelination in the CNS context [54–56]. For instance, Howe and co-workers published the effects of the Fc portion of human IgM (Fcμ) in CNS cells. To achieve this, the group used a mixed culture of oligodendrocytes, microglia and astrocytes and found that, under treatment of Fcμ, the microglia changed to a phenotypic activated state and started to release cytokines such as interleukin (IL)-1β. The authors hypothesised that molecules produced in response to IL-1β kill the leukocytes that trigger inflammation in diseases such as MS. Thus, Fcμ could be an interesting target to explore against demyelination in MS [57].

Microfluidic platforms

Molecular gradients are important regulatory components of tissue processes. Numerous molecular gradients can be found in the majority of tissues, and to mimic such milieu authors have elegantly used microfluidics technology in 2D environments [20,21,58–60]. Although microfluidics chambers were initially used in the context of neurosciences to force the physical isolation of axons from each other and from their respective cell bodies, these systems are now useful for several applications on CNS (co-)culture studies [61–63] because they introduced an easy and feasible way of studying neurobiology, as a result of the precise control of the microenvironment of the cells; for a review, see [64]. Molecular and cellular interactions are both easily achieved with this methodology.

Microfluidic-based neuronal circuits

There are several good examples of *in vitro* neuronal cell cultures grown and manipulated in microfluidic devices and their value as a tool to study fundamental physiological changes that occur in the CNS. In 2009, Park *et al.* produced a multicompartment co-culture microfluidic platform to study mammalian CNS axon–glia interactions for the screening of growth factors and potential myelin repair drug candidates [20]. In the same year, the same researchers [21] showed that a multicompartment microfluidic neuron culture platform could be used for biochemical analysis of the proteic axonal fraction allowing the simultaneous use of multiple experimental conditions in parallel on a single platform (Fig. 1a). Park *et al.* also [63] developed a multicompartment microfluidic platform where oligodendrocyte progenitor cells (OPCs) were directly seeded on top of isolated axons. OPCs were shown to differentiate successfully into myelin-producing oligodendrocytes. This platform was used to study the localised effects of chondroitin sulfate proteolgycans (CSPG), coming to the conclusion that CSPG at concentrations lower than 250 ng/ml did not cause the retraction of pre-established axons.

Hosie *et al.* explored microfluidic platforms to study glutamate excitotoxicity, which is a pathogenic condition in several neurodegenerative diseases. The authors isolated distal axons from cell bodies in a microfluidic device and concluded that the most susceptible part of the neuron to excitotoxicity is the distal axon [65]. More recently, Roberston *et al.* [66] developed a high-throughput platform to monitor neuronal synaptic communication for drug screening purposes. The authors have combined a microfluidic system with a calcium-imaging array to study primary hippocampal cultured networks. This system can overcome

Please cite this article in press as: Rocha, D.N. et al. High-throughput platforms for the screening of new therapeutic targets for neurodegenerative diseases, Drug Discov Today (2016), http://dx.doi.org/10.1016/j.drudis.2016.05.005

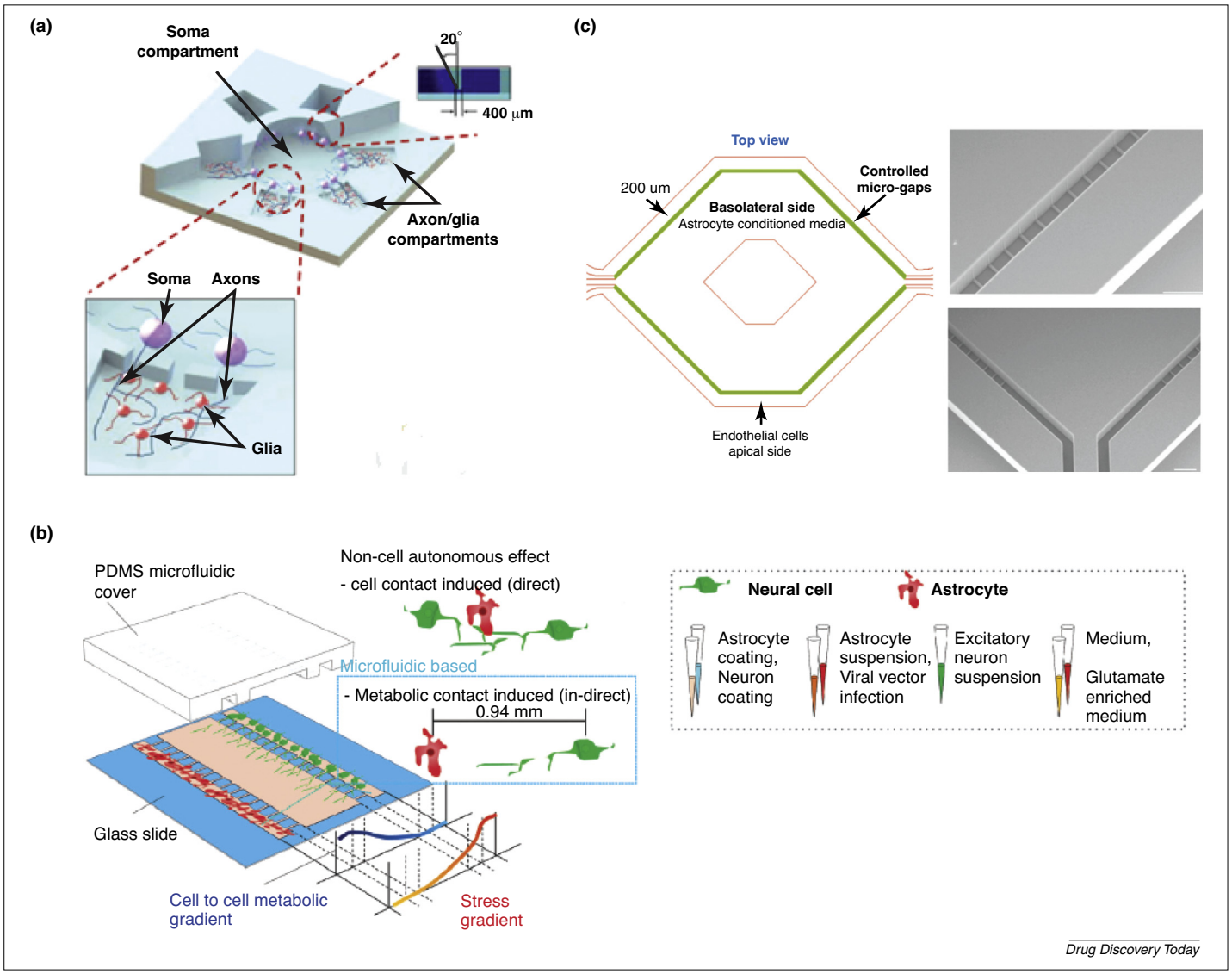

FIGURE 1

Schematic representations of 2D cell-based platforms. **(a)** Multicompartment neuron–glia co-culture system, which enables multiple localised axon treatments in parallel. Reproduced, with permission, from [21]. **(b)** Microfluidic platform that allows the co-culture of astrocytes and cortical neurons to address non-cell autonomous effects in amyotrophic lateral sclerosis (ALS) disease, induced through the metabolic communication between neurons and astrocytes over a distance of 0.94 mm. Reproduced, with permission, from [69]. **(c)** Microfluidic blood–brain barrier (BBB) model that comprises a microcirculation two-compartment chamber – top view of the basolateral chamber which is supported in the centre by a support structure to prevent the collapse of the top of the microfabricated chamber. Scanning electron microscopy (SEM) images of the 3 μm gaps and apical and basolateral fluidic chamber. Reproduced, with permission, from [66].

some limitations of microelectrode arrays such as the lack of interface between some electrodes and cells as a result of random distribution of cells, assuring the quality of the signal and data collected.

Kang and co-workers [19] used an agarose hydrogel to build a multi-well neuronal microcircuit microelectrode array platform, which enables the reduction of data collection times. This tool could prove to be powerful for neurobiological assays assuring the statistical power needed for data analysis in a short period of time and it would be interesting to combine it with a microfluidic system.

Microfluidic-based disease models

Microfluidic platforms have also been widely explored as disease models. Cho *et al.* [67] developed a microfluidic chemotaxis platform to mimic the AD brain, namely creating gradients of soluble Aβ to study microglial behaviour and unravel the reason behind microglial accumulation near Aβ plaques. This microfluidic platform, which contains a central Aβ reservoir and Aβ gradients in the cellular compartments, could be used for other migration studies in the framework of other neurodegenerative diseases such as the study of OPC migration in demyelinating diseases such as MS. Lee and Park [68] also developed an AD model. The formation of Aβ aggregates is known to be influenced by several external factors of the surrounding microenvironment. High concentrations of metal ions such as Fe^{2+} are present within and peripheral to the senile plaques, and in AD patient neutrophils. The authors address the issue of Aβ deposition by immobilising monomers on a polydimethylsiloxane microgrooved surface, and then comparing the clearance effects of several chelators on Fe^{3+}-induced formation of Aβ aggregates.

Please cite this article in press as: Rocha, D.N. et al. High-throughput platforms for the screening of new therapeutic targets for neurodegenerative diseases, Drug Discov Today (2016), http://dx.doi.org/10.1016/j.drudis.2016.05.005

Kunze *et al.* [69] developed a microfluidic cell culture platform to improve the understanding of astrocyte–neuron interactions in amyotrophic lateral sclerosis (ALS) pathology by co-culturing neurons with super oxide dismutase (SOD)-mutant astrocytes: astrocytes genetically modified to overexpress a mutated form of SOD1, a mutation known to occur in ALS. This microfluidic device prevents the direct contact between cultured cells enabling the study of metabolic communication between the cultured cell types (Fig. 1b).

Microfluidic-based BBB models

The blood–brain barrier (BBB) is known to be a highly selective barrier between the brain vasculature and brain tissue, composed of endothelial cells (ECs) of the cerebral microvasculature, which are interconnected by tight junctions. Although the BBB is absolutely essential for the normal function of the brain, preventing the entry of pathogens and unwanted substances, it also constitutes the main impediment for drug entry into the brain when drugs are intravenously administered. Therefore, a large number of systems have been proposed and used to investigate the cellular and molecular mechanisms underlying BBB establishment, to test new drugs, evaluate conditions and mechanisms that cause the barrier disruption, among others [70]. *In vitro* models of the BBB have been traditionally achieved using cell culture trans-wells but microfluidic systems have enabled the establishment of dynamic and more physiologically relevant *in vitro* BBB models. The use of microfluidic platforms has enabled the application of shear stress to the cultured ECs via fluid flow, which was shown to increase the barrier properties of the BBB in *in vitro* models [71–73] – better mimicking the physiological conditions.

Prabhakarpandian *et al.* [74] have recently developed an innovative microfluidic BBB model that comprises a microcirculation two-compartment chamber (Fig. 1c). In this study, ECs were cultured in the presence of astrocyte-conditioned medium. The authors focused on the permeability of the BBB *in vitro* model and have not really addressed trans-endothelial electrical resistance (TEER) measurements. BBB integrity alteration can be routinely assessed *in vitro* by determining cell monolayer permeability to different solutes and measuring the TEER.

The presence of astrocytes *in vitro* was shown to increase TEER values significantly in BBB models [75–77]. Xue and co-workers [78] have gone further in the pursuit of a clinically relevant culture model and established a platform comprising a tri-culture of astrocytes, neurons and ECs achieving TEER values significantly higher than those obtained in other models. Another study using a tri-culture of astrocytes, pericytes and endothelial cells also showed increased TEER values [75]. Although these studies suggest that the presence of more cell types that are present in the *in vivo* scenario is extremely important to obtain increased TEER they also suggest that the presence of the different cell types might not be as relevant for permeability issues [75,79]. As such, it is important to consider both factors when considering a model to test new drugs for CNS applications.

Cell-based 3D platforms

Whereas 2D approaches allow a well-controlled analysis of the impact of individual components on cells, our tissues have additional layers of complexity that arise from the three-dimensionality that strongly conditions cell function. To achieve a more native-like environment many researchers have started to work in 3D environments. By comparing cell culture systems with 2D and 3D architectures several authors observed significant differences in cell behaviour that suggest that neural cells cultured in 3D behave more closely to those *in vivo*. Therefore, the more physiologically relevant microenvironment of a 3D culture could enhance the quality and biological relevance of the obtained data. In the following subsections 3D models of increasing complexity will be approached; namely spheroid cultures, tissue slices and biomaterial-based platforms.

Spheroid culture models

In vitro multicellular spheroids have begun to bridge the complexity gap between monolayer cell culture and *in vivo* tissue structure and have become valuable *in vitro* models for developmental and drug resistance studies. These can also be very useful when studying a neurodevelopmental disease. To promote cell assembly while preventing spheroid aggregation, culture systems developed for cell spheroid formation such as hanging drops and microwells could be used to obtain uniform neurospheres [80]. There is currently a commercially available 3D spheroid culture platform named Perfecta3D® hanging drop plates (3D Biomatrix), which is a high-throughput 3D cell culture device that aims to simplify spheroid formation, culture and subsequent testing of the achieved 3D constructs. However, static suspension cultures also present limitations, such as the ones observed in the case of cultures with large-diameter aggregates, in which limited supply of oxygen, nutrients and/or growth factors to the centre of the aggregates could lead to the development of necrotic cores, and alter culture dynamics. In this case, dynamic culture systems are more appropriate [81].

Lancaster *et al.* settled a human pluripotent stem cell derived cerebral 3D organoid culture system in which various cerebral zones were represented. The authors maintained neuroectoderm from embryoid bodies in 3D Matrigel® droplets. The structure was then moved to a bioreactor, rapidly evolved, recreating different brain tissue areas [82]. Moreover, Tieng *et al.* generated neurospheres that differentiated in dopaminergic neurons and studied the influence of gamma secretase inhibitors (compound E and DAPT) on neuronal differentiation and maturation and concluded that these molecules could control maturation and induction of neural precursors. This model is of distinct interest for PD and demyelinating diseases [83].

Seidel and co-workers [84] developed a 3D model of tauopathy that recapitulates pathological processes known to occur in AD. This culture model is based on a spheroid culture of a human cell line and promises to provide an efficient system for the screening of new therapeutic drugs. This work further shows the relevance of 3D models and it is of added value when compared with 2D systems because the authors found increased neuronal differentiation and interesting levels of degeneration being achieved *in vitro*. Also aiming to recreate the AD environment *in vitro*, Park *et al.* [85] developed a 3D neurospheroid culture-based microfluidic system as an *in vitro* brain model (Fig. 2a). The cultured cells were then treated with Aβ to simulate the AD environment. The combination of spheroid cultures with microfluidic technology enabled the recreation of the 3D architecture and the interstitial fluid flow simultaneously, which could be of added value because the

Please cite this article in press as: Rocha, D.N. et al. High-throughput platforms for the screening of new therapeutic targets for neurodegenerative diseases, Drug Discov Today (2016), http://dx.doi.org/10.1016/j.drudis.2016.05.005

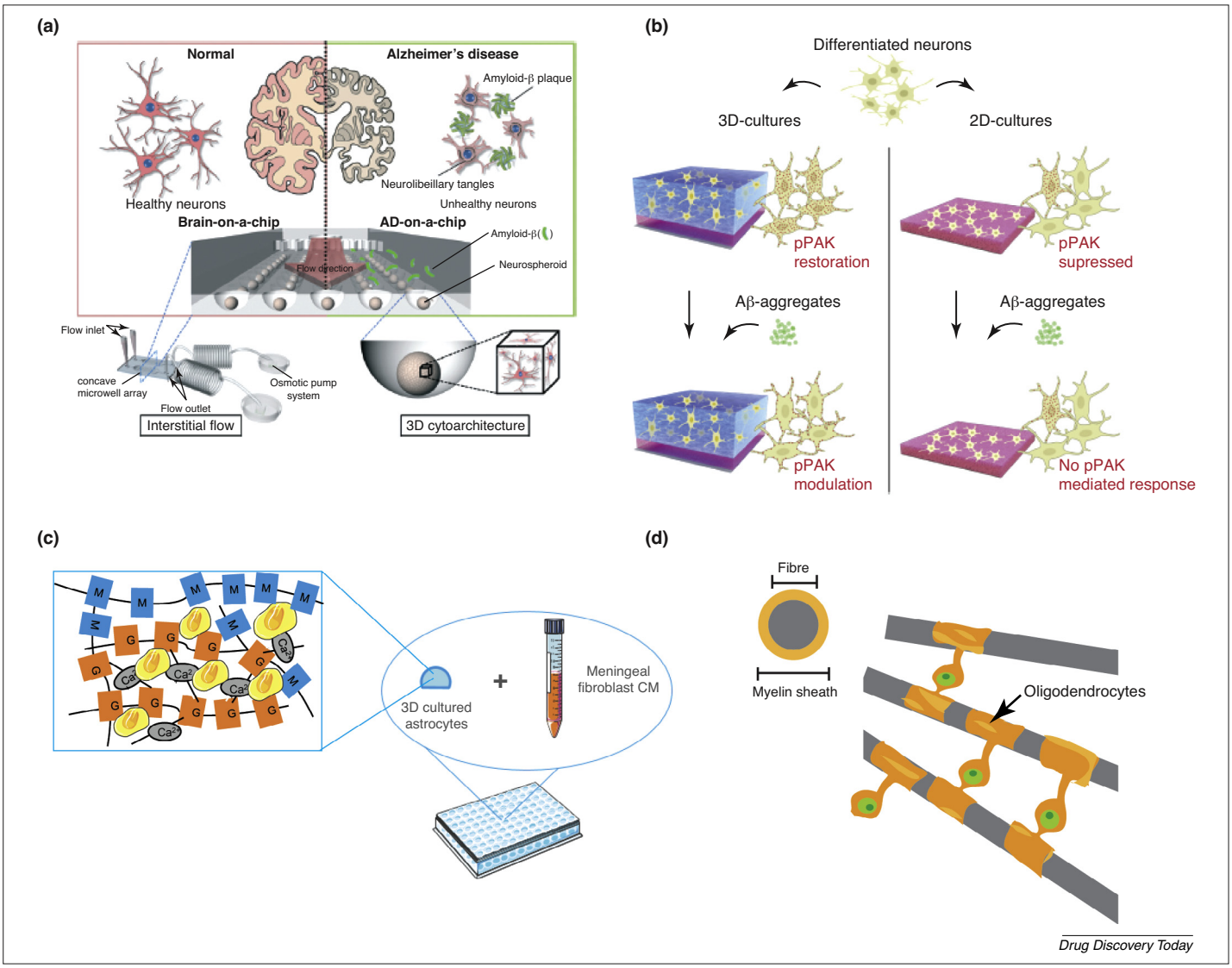

FIGURE 2

Schematic representations of 3D cell-based platforms. **(a)** 3D brain-on-a-chip with an interstitial level of flow. Reproduced, with permission, from [85]. **(b)** The impact of a 3D microenvironment. Differences in phosphorylated P21-activated kinases (pPAK) expression and responses to beta amyloid (Aβ) oligomers in 2D cultures and 3D self-assembling peptide (SAP) matrix cultures. Reprinted, with permission, from [112]. **(c)** Alginate-based *in vitro* tissue engineered glial scar. **(d)** Artificial axon system for myelination studies. Adapted, with permission, from [108].

authors have shown that Aβ toxicity in dynamic culture conditions is significantly higher than the one seen in static conditions. This *in vitro* brain model constitutes an interesting model for the *in vitro* study of neurodegenerative disorders in the brain.

Tissue-explant-based models

The use of tissue explants is also a strategy followed by several authors to achieve 3D cultures where tissue architecture, cellular and molecular content must be preserved. Because these closely recreate the *in vivo* environment, keeping cell-matrix composition and relative content similar to the ones in native tissue can be of added value when the aim is to create a model of a pathology that involves several cell types or even brain regions, and/or where tissue architecture and composition are key factors.

Reinhart *et al.* [86] have used rat brain tissue explants to which Huntingtin clones where delivered through biolistic transfection. Using a library of 74 compounds known to be involved in processes of cell death and inflammation, the authors concluded that IκB kinase complex compounds (WAY-717 and WAY-781), CXCR3 chemokine receptors (compounds 6c and T487), a c-Jun N-terminal kinase inhibitor (SP600125) and an adenosine 2A receptor agonist (CGS21680) and antagonist (KW-6002) showed neuroprotective features in the disease explant model. This platform was developed to study HD but it can be useful to establish other disease models for other pathologies that have a known genetic profile. Zhang *et al.* [87] have also used *ex vivo* tissue explant cultures of brain and spinal cord tissues to establish an MS *in vitro* model (Fig. 2b). The proposed system has been shown to constitute a good platform for the study of myelination and remyelination mechanisms. In this report, the authors used image stacks obtained from confocal microscopy and, through image software, quantified the myelin. An automated myelin quantification method is of added value for the screening of remyelination-promoting drugs. To test potential neuroprotective agents, Ravikumar *et al.*

Please cite this article in press as: Rocha, D.N. et al. High-throughput platforms for the screening of new therapeutic targets for neurodegenerative diseases, Drug Discov Today (2016), http://dx.doi.org/10.1016/j.drudis.2016.05.005

[88] established a protocol where spinal cord slice cultures were treated with lipopolysaccharide (an antigen used to induce neurodegeneration) and co-cultured in trans-wells in the presence of microglia cells seeded on poly(L-lysine)-coated glass coverslips. Polystyrene beads were used to activate the phagocytic capacity of the microglia. As bead concentration increased the axonal disruption also increased. Resveratrol was then tested as a neuroprotective agent and this treatment led to reduced levels of neurodegeneration when compared with controls.

More recently, Hutter-Schmid *et al.* [89] developed a model to study the relationship between damaged brain vessels and neurodegeneration. In the neurovascular unit vascular cells closely interact with astrocytes. Hence, understanding angiogenesis mechanisms in the brain, as well as simulating its reaction to growth factors and drugs, is of extreme importance. In this model, tissue slices were cultured in membrane inserts and shown to maintain the normal structural vessel network of the brain. This is relevant once alterations in the vascular system can contribute to the development of degenerative diseases such as AD [90]. As such, this model can be further used to screen new drugs to improve vascular function or also to study responses of the vascular cells to some common neurodegenerative drugs.

TBI incidence is rapidly increasing because of recent military conflicts. Miller and co-workers [91] developed a model of blast-induced TBI, in which mouse brain slices and a shockwave tube were used to mimic shockwave overpressure. Cell death and effects of the injury in neuron cells were assessed. The authors concluded that neuronal death was prominent. Besides, astrocytes and microglia were activated in the model, thus showing the feasibility of the model to mimic blast TBI. To screen neuroprotective compounds to be used in ischemic stroke, Beraki and co-workers [92] created a two-step robust screen methodology. Firstly, the authors used primary cortical neurons and subjected them to oxygen glucose privation for 2 hours. The compounds were then added to the culture and cell death, viability and toxicity were measured. Remaining compounds were then tested in a mouse brain organotypic slice culture and, among them, Carbenoxolone® proved to be the most efficient. This added a great therapeutic value for the treatment of this disease.

Biomaterial-based models

In the past decades, the fields of biomaterials and tissue engineering have been paramount to the developments observed in HTS platforms, helping the recreation of physiologically relevant *in vitro* systems. Nevertheless, adapting 3D assay systems to high-throughput testing brings additional challenges because miniaturisation might not be as straightforward as one would desire, however such platforms are emerging [93,94].

Lai and Kisaalita [95] have developed a 3D culture system for human neural stem cells. The authors have transformed the regular polystyrene 2D culture wells into 3D culture wells by building a porous polystyrene scaffold into standard 96-well plates. Although this solution has the added value of being cheaper than any of the previously mentioned commercial solutions, polystyrene might not present the ideal mechanical properties for many CNS cell-culture-based studies. Hydrogels have been more frequently explored, mainly because of their biological properties, because these more closely resemble the natural extracellular matrix and, consequently, positively impact cell behaviour. Neurons in a 2D microenvironment have been shown to have high Ca^{2+} dynamics in comparison with neurons cultured in 3D hydrogels [17,96–98] showing that the 3D environment is more relevant for electrophysiology studies. Irons *et al.* [17] have shown that neurons and astrocytes cultured in a 3D environment acquire a complex 3D morphology and are able to maintain cellular viability for several weeks. Additionally, network properties (pore size, mechanical properties, etc.) and degradation rate are tunable through changes in the cross-linking degree and gel chemistry [99]. Currently, different hydrogels have been explored for neural cell culture, either from natural mammalian extracellular-matrix-derived sources such as Matrigel® and collagen or synthetic or chemically defined hydrogels. Among the latter, several systems are already commercially available that have also been tested for culture of neural cells (most commonly for glioblastoma cell culture). These include: the HyStem™ (Advanced Biomatrix), a chemically defined hydrogel rich in hyaluronic acid; AlgiMatrix®, an alginate-based 3D culture system (ThermoScientific); the synthetic peptide nanofibre scaffold HydroMatrix™ Peptide Hydrogel (Sigma-Aldrich); and the QGel assay system (QGel). The gel-forming method will vary for each case, but nowadays photopolymerisation and chemical polymerisation also represent good approaches because mild reaction conditions can currently be applied, which can be performed at physiological pH and temperature, allowing even cell encapsulation at little or no cost to cell viability.

Choi and co-workers [100] have used a Matrigel®-based platform to culture human neural cells to recapitulate AD tauopathy and Aβ pathologies. The results of this study support the idea that 3D models better recreate clinically relevant environments and the hypothesis that Aβ deposition leads to tauopathy.

We have developed a 3D *in vitro* tissue engineered glial scar [101] by culturing primary astrocytes within alginate hydrogels, in the presence of meningeal-fibroblast-conditioned medium. Hydrogel mechanical properties were shown to influence cell behaviour significantly with intermediate stiffness gels promoting astrogliosis. This platform enabled the identification of RhoA as a pivotal mediator of astrocyte reactivity and, as such, identified it as a potential therapeutic target (Fig. 2c). Ibuprofen and chondroitinase ABC were shown to reduce RhoA levels and recover the astrocytic phenotype. These 3D cultures were shown to recapitulate many biological features of glial scars and could be useful in the future for the screening of therapeutic drugs to target astrogliosis.

Bioprinting is another appealing advancement because it can answer some problems of cell distribution throughout the 3D environment, particularly significant in the case of multiple-cell-type cultures, because cells and biomaterials can be deposited layer-by-layer in a controlled fashion [102,103]. Lee [103] used such a strategy to pattern embryonic neurons and astrocytes in a collagen 3D environment.

Polymeric materials have also been used as artificial axons for *in vitro* testing of rapid myelinating systems. These have been used as neuron-free models to study oligodendrocytes and the myelination process (Fig. 2d). Studies with artificial axons go back to 1990 when Bullock and Rome [104] used glass microfibres to study the behaviour of OPC differentiation and myelination. Although this

Please cite this article in press as: Rocha, D.N. et al. High-throughput platforms for the screening of new therapeutic targets for neurodegenerative diseases, Drug Discov Today (2016), http://dx.doi.org/10.1016/j.drudis.2016.05.005

was shown to be a suitable system to study oligodendrocytes, the authors did not find oligodendrocytes consistently wrapped around the glass fibres. More recently, Li *et al.* [105] produced electrospun poly(ε-caprolactone) and gelatin co-polymer fibres as artificial axons, which were shown to support growth and differentiation of OPCs. In this work, the authors claim that cells wrap the fibres but their data are not sufficient to fully assess the existence of myelin sheath all around the polymeric fibres. Lee *et al.* [106] also used electrospinning techniques to produce polystyrene and poly(L-lactic acid) nanofibers coated with poly(L-lysine). The authors produced fibres with different diameters and showed that OPCs react to this physical stimulus, because they were shown only to myelinate fibres with a diameter higher than 0.4 μm. This result is not extraordinarily surprising because *in vivo* CNS axons are known to present diameters that range from 0.3 to 2 μm [107] but it stresses the importance of the physical stimulus for myelination processes. This work was further able to show the existence of concentric wrapping of the polymeric fibres. All together, these studies have shown that axonal signals are not needed for OPC differentiation and myelination to occur. Because these systems allow the myelination process to occur in the absence of neurons, they may be particularly interesting to discriminate the cross-talk between myelinating oligodendrocytes and other CNS cells besides neurons.

TABLE 1

Illustrative examples of 2D and 3D platforms proposed in the context of CNS *in vitro* cellular models

Study focus	Dimensionality	Type of platform	Added value	Limitations	Refs
Neurotoxicity	2D	Human and rat monocultures	Scale up potential Human neural cells Possibility to achieve multiple neural cell types differentiated from the NSCs	Difficulty of access to large quantities of human neural cell types	[34]
Myelination	2D	Microfluidic co-culture	Possibility of testing six different culture conditions in parallel Ability to manipulate local physical and chemical environment	Inability to achieve robust myelination	[21]
Neuronal connectivity	2D	Microfluidic co-culture	Combination of calcium imaging with microfluidics technology	Inability to distinguish synapse formation origin Reduced volumes of aqueous solutions could lead to evaporation and extensive changes in imaging	[66]
BBB	2D	Microfluidic co-culture	Ability to reproduce a triple co-culture system using primary cells. BBB function and resemblance to *in vivo* events	Time-consuming readout	[78]
Dopaminergic nervous tissue	3D	Spheroid culture	Spontaneous electrical activity Controlled induction and maturation of neural precursors	No spatially organised structures	[83]
Alzheimer's disease	3D	Microfluidic and spheroid culture	Combination of 3D and microfluidics technology	Time-consuming readout	[85]
Multiple sclerosis	3D	Slice culture	Readout method – myelination, demyelination and re-myelination were reproduced and automatically quantified in a rapid and precise way	No recreation of the inflammatory component of the disease	[52]
Neurotoxicity	3D	Slice culture	Semi-automated readout method Tissue architecture is conserved	LPS-induced degeneration	[88]
Stroke	3D	Slice culture	Readout method Easiness to study a target pathway	Platform potential needs to be further confirmed with other drugs	[92]
Astrogliosis	3D	Biomaterials	System simplicity Resemblance of *in vivo* features Ability to tune mechanical properties	Time-consuming readout method	[101]

Abbreviations: BBB, blood–brain barrier; CNS, central nervous system; LPS, lipopolysaccharide; NSCs, neural stem cells.

Please cite this article in press as: Rocha, D.N. et al. High-throughput platforms for the screening of new therapeutic targets for neurodegenerative diseases, Drug Discov Today (2016), http://dx.doi.org/10.1016/j.drudis.2016.05.005

Concluding remarks and future perspectives for HTS platforms

Here we reviewed the current state-of-the-art of existing platforms for the study of CNS function in homeostasis and disease. Some already comply with the requirements to serve as an HTS platform; others can easily be extrapolated to such systems. In Table 1, a summary of the added value and limitations of illustrative examples is presented, in the framework of the development of such screening platforms.

When discussing HTS in the context of the CNS one must not forget the particularities of this intricate system. Neurons and glia establish complex and orchestrated cellular networks that are difficult to reproduce in simple culture systems. The CNS is one of the most densely cellularised tissues of our body, and the extracellular matrix, which occupies 20% of the CNS space, is an extremely important constituent and adds an extra layer of complexity to the system. Mechanotransduction is also becoming a relevant player in CNS disease. Consequently, the further exploration of extracellular-matrix-derived and biomaterial-based matrices to support 3D neural cultures is expected to improve the advanced models greatly. Nevertheless, future progress will not solely rely on biomaterial science but also on the adaptation of many of the commonly used readout techniques to the 3D culturing setting; namely the challenge of recovering or accessing cells from the matrices for further analysis and the necessity of using microscopic techniques that allow evaluation of multiple focal planes. Miniaturisation and automated handling of 3D cultures can also be defiant. The combination of microfluidics technology with 3D architectures is rapidly evolving [108–111] and, once 3D culture hurdles are overcome, work in this field will progress and afterwards microfluidics and co-culture systems can be combined.

In fact, a major obstacle for the advancement of the strategies discussed here has been the lack of solid fundamental knowledge on the etiology of many of the major neurodegenerative diseases. Many neurodegenerative disorders are multifactorial, with several players involved in the process. iPSC technology will open new avenues to the development of patient-specific models and personalised medicine. More recently, researchers have also developed platforms to mimic multi-organ interaction that are not present in the conventional tissue culture plate, by using microfluidics with a co-culture system with the aim of studying pharmacokinetics of drugs [59] or cell-based drug metabolism [60]. Although not yet applied to the CNS, 'quasi-all-body' model systems can bring new key information to the field.

Finally, new algorithms for image analysis and large dataset processing will also need to emerge to handle the terabytes of information generated, sometimes even in one experiment. Therefore, a truly multidisciplinary approach will be vital for the evolution of the field. Ultimately, this will translate into new drug targets, biomarkers, biomolecule-based therapies and novel and more-efficient disease treatment or management approaches.

Acknowledgements

This work had the financial support of *Fundação para a Ciência e Tecnologia* (FCT) through National Funds and, when applicable, co-financed by the FEDER through the PT2020 Partnership Agreement under the 4293 Unit I&D. D.N. Rocha acknowledges FCT for her PhD grant.

References

1 Bürli, R. *et al.* (2010) The role of histone deacetylases in neurodegenerative diseases and small-molecule inhibitors as a potential therapeutic approach. In *Neurodegenerative Diseases* (Dominguez, C., ed.), pp. 1–56, Springer Berlin Heidelberg
2 Nutt, D.J. (2011) The full cost and burden of disorders of the brain in Europe exposed for the first time. *Eur. Neuropsychopharmacol.* 21, 715–717
3 An, W.F. and Tolliday, N.J. (2009) Introduction: cell-based assays for high-throughput screening. In *Cell-Based Assays for High-Throughput Screening* (Clemons, P.A. *et al.* eds), pp. 1–12
4 Bleicher, K. *et al.* (2003) Hit and lead generation: beyond high-throughput screening. *Nat. Rev. Drug Discov.* 2, 369–378
5 Pedro, L. *et al.* (2010) Development of a high-throughput AlphaScreen assay measuring full-length LRRK2(G2019S) kinase activity using moesin protein substrate. *Anal. Biochem.* 404, 45–51
6 Crowe, A. *et al.* (2009) Identification of aminothienopyridazine inhibitors of tau assembly by quantitative high-throughput screening. *Biochemistry* 48, 7732–7745
7 Wang, M. *et al.* (2009) Convenient and continuous fluorometric assay method for acetylcholinesterase and inhibitor screening based on the aggregation-induced emission. *Anal. Chem.* 81, 4444–4449
8 Shu, C.W. *et al.* (2011) High-throughput fluorescence assay for small-molecule inhibitors of autophagins/Atg4. *J. Biomol. Screen.* 16, 174–182
9 Kashem, M.A. *et al.* (2014) A high-throughput scintillation proximity assay for sphingosine-1-phosphate lyase. *Assay Drug Dev. Technol.* 12, 293–302
10 Moore, K. and Rees, S. (2001) Cell-based versus isolated target screening: how lucky do you feel? *J. Biomol. Screen.* 6, 69–74
11 Johnston, P. (2002) Cellular assays in HTS. In *High Throughput Screening: Methods and Protocols* (Janzen, W.P., ed.), pp. 107–116, Humana Press
12 Denyer, J. (1998) HTS approaches to voltage-gated ion channel drug discovery. *Drug Discov. Today* 3, 323–332
13 Taylor, D.L. (2001) Real-time molecular and cellular analysis: the new frontier in drug discovery. *Curr. Opin. Biotechnol.* 12, 75–81
14 Conway, B.R. (1999) Quantification of G-protein coupled receptor internalization using G-protein coupled receptor-green fluorescent protein conjugates with the Arrayscan high-content screening system. *J. Biomol. Screen.* 4, 75–86
15 Thid, D. *et al.* (2007) Supported phospholipid bilayers as a platform for neural progenitor cell culture. *J. Biomed. Mater. Res. A* 84, 940–953
16 Seyb, K.I. *et al.* (2009) Identification of small molecule inhibitors of beta-amyloid cytotoxicity through a cell-based high-throughput screening platform. *J. Biomol. Screen.* 13, 870–878
17 Irons, H.R. *et al.* (2008) Three-dimensional neural constructs: a novel platform for neurophysiological investigation. *J. Neural Eng.* 5, 333–341
18 Freudenberg, U. *et al.* (2009) A star-PEg-heparin hydrogel platform to aid cell replacement therapies for neurodegenerative diseases. *Biomaterials* 30, 5049–5060
19 Kang, G. *et al.* (2009) Agarose microwell based neuronal micro-circuit arrays on microelectrode arrays for high throughput drug testing. *Lab Chip* 9, 3236–3242
20 Park, J. *et al.* (2009) A multi-compartment CNS neuron-glia co-culture microfluidic platform. *J. Vis. Exp.* http://dx.doi.org/10.3791/1399
21 Park, J.W. *et al.* (2009) Novel microfluidic platform for culturing neurons: culturing and biochemical analysis of neuronal components. *Biotechnol. J.* 4, 1573–1577
22 Valensi-Kurtz, M. *et al.* (2010) Enriched population of PNS neurons derived from human embryonic stem cells as a platform for studying peripheral neuropathies. *PLoS ONE* 52, e9290
23 Jundi, B. *et al.* (2010) The locust standard brain: a 3D standard of the central complex as a platform for neural network analysis. *Front. Syst. Neurosci.* 3, 21
24 Frimat, J.P. *et al.* (2010) The network formation assay: a spatially standardized neurite outgrowth analytical display for neurotoxicity screening. *Lab Chip* 10, 701–709
25 Johnstone, A.F.M. *et al.* (2010) Microelectrode arrays: a physiologically based neurotoxicity testing platform for the 21st century. *Neurotoxicology* 31, 331–350
26 An, W.F. and Tolliday, N. (2010) Cell-based assays for high-throughput screening. *Mol. Biotechnol.* 45, 180–186

Please cite this article in press as: Rocha, D.N. et al. High-throughput platforms for the screening of new therapeutic targets for neurodegenerative diseases, Drug Discov Today (2016), http://dx.doi.org/10.1016/j.drudis.2016.05.005

27 Johnston, P.A. and Johnston, P.A. (2002) Cellular platforms for HTS: three case studies. *Drug Discov. Today* 7, 353–363
28 Geller, H.M. *et al.* (1991) Applications of immortalized cells in basic and clinical neurology. *J. Cell. Biochem.* 45, 279–283
29 Ulrich, A.B. *et al.* (2002) Pancreatic cell lines: a review. *Pancreas* 24, 111–120
30 Xu, X.H. and Zhong, Z. (2013) Disease modeling and drug screening for neurological diseases using human induced pluripotent stem cells. *Acta Pharmacol. Sin.* 34, 755–764
31 Maddox, C.B. *et al.* (2009) Adapting cell-based assays to the high throughput screening platform: problems encountered and lessons learned. *JALA* 13, 168–173
32 Wyler, M.R. *et al.* (2009) Cell-based assays to probe the ERK MAP kinase pathway in endothelial cells. In *Cell-Based Assays for High-Throughput Screening* (Clemons, P.A. *et al.* eds), pp. 29–41
33 An, W.F. (2009) Fluorescence-based assays. In *Cell-Based Assays for High-Throughput Screening* (Clemons, P.A. *et al.* eds), pp. 97–107
34 Malik, N. *et al.* (2014) Compounds with species and cell type specific toxicity identified in a 2000 compound drug screen of neural stem cells and rat mixed cortical neurons. *Neurotoxicology* 45, 192–200
35 Agrawal, A.A. *et al.* (2010) Porous nanocrystalline silicon membranes as highly permeable and molecularly thin substrates for cell culture. *Biomaterials* 31, 5408–5417
36 Hiebl, B. *et al.* (2010) Cytocompatibility testing of cell culture modules fabricated from specific candidate biomaterials using injection molding. *J. Biotechnol.* 148, 76–82
37 Hu, W. *et al.* (2005) Effects of nanoimprinted patterns in tissue-culture polystyrene on cell behavior. *J. Vac. Sci. Technol. A* 23, 2984–2989
38 Palmgrén, J.J. *et al.* (2006) Drug adsorption to plastic containers and retention of drugs in cultured cells under *in vitro* conditions. *Eur. J. Pharm. Biopharm.* 64, 369–378
39 Rocha, D.N. *et al.* (2014) Poly(trimethylene carbonate-co-epsilon-caprolactone) promotes axonal growth. *PLOS ONE* 9, e88593
40 Lutolf, M.P. (2009) Biomaterials: spotlight on hydrogels. *Nat. Mater.* 8, 451–453
41 Geckil, H. *et al.* (2010) Engineering hydrogels as extracellular matrix mimics. *Nanomedicine* 5, 469–484
42 Zhu, J. (2010) Bioactive modification of poly(ethylene glycol) hydrogels for tissue engineering. *Biomaterials* 31, 4639–4656
43 Wang, Q.G. *et al.* (2010) The composition of hydrogels for cartilage tissue engineering can influence glycosaminoglycan profile. *Eur. Cell Mater.* 26, 86–95
44 Jo, Y.S. *et al.* (2010) Biomimetic PEG hydrogels crosslinked with minimal plasmin-sensitive tri-amino acid peptides. *J. Biomed. Mater. Res. A* 93, 870–877
45 Lesuisse, C. and Martin, L.J. (2002) Long-term culture of mouse cortical neurons as a model for neuronal development, aging, and death. *J. Neurobiol.* 51, 9–23
46 Bertrand, S.J. *et al.* (2011) Endogenous amyloidogenesis in long-term rat hippocampal cell cultures. *BMC Neurosci.* 12, 1–11
47 Todd, G.K. *et al.* (2013) Towards neuronal organoids: a method for long-term culturing of high-density hippocampal neurons. *PLOS ONE* 8, e58996
48 Mozafari, S. *et al.* (2015) Skin-derived neural precursors competitively generate functional myelin in adult demyelinated mice. *J. Clin. Invest.* 125, 3642–3656
49 Yagi, T. *et al.* (2011) Modeling familial Alzheimer's disease with induced pluripotent stem cells. *Hum. Mol. Genet.* 20, 4530–4539
50 Israel, M.A. *et al.* (2012) Probing sporadic and familial Alzheimer's disease using induced pluripotent stem cells. *Nature* 482, 216–220
51 Wang, Q. *et al.* (2015) Dimethyl fumarate protects neural stem/progenitor cells and neurons from oxidative damage through Nrf2-ERK1/2 MAPK pathway. *Int. J. Mol. Sci.* 16, 13885–13907
52 Zhang, N. *et al.* (2010) Characterization of human Huntington's disease cell model from induced pluripotent stem cells. *PLoS Curr.* 2, RRN1193
53 Salvador, E. *et al.* (2015) Stretch and/or oxygen glucose deprivation (OGD) in an *in vitro* traumatic brain injury (TBI) model induces calcium alteration and inflammatory cascade. *Front. Cell. Neurosci.* 9, 323
54 Diemel, L.T. *et al.* (2004) Remyelination of cytokine- or antibody-demyelinated CNS aggregate cultures is inhibited by macrophage supplementation. *Glia* 45, 278–286
55 Sorensen, A. *et al.* (2008) Astrocytes, but not olfactory ensheathing cells or Schwann cells, promote myelination of CNS axons *in vitro*. *Glia* 56, 750–763
56 Haastert, K. *et al.* (2005) Rat embryonic motoneurons in long-term co-culture with Schwann cells – a system to investigate motoneuron diseases on a cellular level *in vitro*. *J. Neurosci. Methods* 142, 275–284
57 Howe, C.L. *et al.* (2006) Activated microglia stimulate transcriptional changes in primary oligodendrocytes via IL-1beta. *Neurobiol. Dis.* 23, 731–739
58 Chung, B.G. *et al.* (2005) Human neural stem cell growth and differentiation in a gradient-generating microfluidic device. *Lab Chip* 5, 401–406
59 Sung, J.H. *et al.* (2010) A microfluidic device for pharmacokinetic-pharmacodynamic (PK-PD) model on a chip. *Lab Chip* 10, 446–455
60 Novik, E. *et al.* (2010) A microfluidic hepatic coculture platform for cell-based drug metabolism studies. *Biochem. Pharmacol.* 79, 1036–1044
61 Majumdar, D. *et al.* (2011) Co-culture of neurons and glia in a novel microfluidic platform. *J. Neurosci. Methods* 196, 38–44
62 Park, J. *et al.* (2009) A multi-compartment CNS neuron–glia co-culture microfluidic platform. *J. Vis. Exp.* http://dx.doi.org/10.3791/1399
63 Park, J. *et al.* (2012) Multi-compartment neuron–glia co-culture platform for localized CNS axon-glia interaction study. *Lab Chip* 12, 3296–3304
64 Park, J.W. *et al.* (2013) Advances in microfluidics-based experimental methods for neuroscience research. *Lab Chip* 13, 509–521
65 Hosie, K.A. *et al.* (2012) Chronic excitotoxin-induced axon degeneration in a compartmented neuronal culture model. *ASN Neuro* 4 pii:e00076
66 Robertson, G. *et al.* (2014) Chemically induced synaptic activity between mixed primary hippocampal co-cultures in a microfluidic system. *Integr. Biol.* 6, 636–644
67 Cho, H. *et al.* (2013) Microfluidic chemotaxis platform for differentiating the roles of soluble and bound amyloid-beta on microglial accumulation. *Sci. Rep.* 3, 1823
68 Lee, J.S. and Park, C.B. (2010) Microfluidic dissociation and clearance of Alzheimer's beta-amyloid aggregates. *Biomaterials* 31, 6789–6795
69 Kunze, A. *et al.* (2013) Astrocyte-neuron co-culture on microchips based on the model of SOD mutation to mimic ALS. *Integr. Biol.* 5, 964–975
70 Czupalla, C.J. *et al.* (2014) *In vitro* models of the blood–brain barrier. *Methods Mol. Biol.* 1135, 415–437
71 Siddharthan, V. *et al.* (2007) Human astrocytes/astrocyte-conditioned medium and shear stress enhance the barrier properties of human brain microvascular endothelial cells. *Brain Res.* 1147, 39–50
72 Griep, L.M. *et al.* (2013) BBB on chip: microfluidic platform to mechanically and biochemically modulate blood–brain barrier function. *Biomed. Microdevices* 15, 145–150
73 Cucullo, L. *et al.* (2008) Immortalized human brain endothelial cells and flow-based vascular modeling: a marriage of convenience for rational neurovascular studies. *J. Cereb. Blood Flow Metab.* 28, 312–328
74 Prabhakarpandian, B. *et al.* (2013) SyM-BBB: a microfluidic blood brain barrier model. *Lab Chip* 13, 1093–1101
75 Nakagawa, S. *et al.* (2009) A new blood–brain barrier model using primary rat brain endothelial cells, pericytes and astrocytes. *Neurochem. Int.* 54, 253–263
76 Jeliazkova-Mecheva, V.V. and Bobilya, D.J. (2003) A porcine astrocyte/endothelial cell co-culture model of the blood–brain barrier. *Brain Res. Brain Res. Protoc.* 12, 91–98
77 Gaillard, P.J. *et al.* (2001) Establishment and functional characterization of an *in vitro* model of the blood–brain barrier, comprising a co-culture of brain capillary endothelial cells and astrocytes. *Eur. J. Pharm. Sci.* 12, 215–222
78 Xue, Q. *et al.* (2013) A novel brain neurovascular unit model with neurons, astrocytes and microvascular endothelial cells of rat. *Int. J. Biol. Sci.* 9, 174–189
79 Gaillard, P.J. and de Boer, A.G. (2000) Relationship between permeability status of the blood–brain barrier and *in vitro* permeability coefficient of a drug. *Eur. J. Pharm. Sci.* 12, 95–102
80 Mori, H. *et al.* (2006) Effect of neurosphere size on the growth rate of human neural stem/progenitor cells. *J. Neurosci. Res.* 84, 1682–1691
81 Santos, T.L. *et al.* (2016) Culture of embryonic stem cell-derived neural stem/progenitors under rotary orbital suspension culture: impact of the hydrodynamic culture system on aggregate yield, morphology, and cell behavior. *J. Tissue Eng. Regen. Med.* http://dx.doi.org/10.1002/term.2121
82 Lancaster, M.A. *et al.* (2013) Cerebral organoids model human brain development and microcephaly. *Nature* 501, 373–379
83 Tieng, V. *et al.* (2014) Engineering of midbrain organoids containing long-lived dopaminergic neurons. *Stem Cells Dev.* 23, 1535–1547
84 Seidel, D. *et al.* (2012) Induced tauopathy in a novel 3D-culture model mediates neurodegenerative processes: a real-time study on biochips. *PLoS ONE* 7, e49150
85 Park, J. *et al.* (2015) Three-dimensional brain-on-a-chip with an interstitial level of flow and its application as an *in vitro* model of Alzheimer's disease. *Lab Chip* 15, 141–150
86 Reinhart, P.H. *et al.* (2011) Identification of anti-inflammatory targets for Huntington's disease using a brain slice-based screening assay. *Neurobiol. Dis.* 43, 248–256
87 Zhang, H. *et al.* (2011) Central nervous system remyelination in culture – a tool for multiple sclerosis research. *Exp. Neurol.* 230, 138–148
88 Ravikumar, M. *et al.* (2012) An organotypic spinal cord slice culture model to quantify neurodegeneration. *J. Neurosci. Methods* 211, 280–288
89 Hutter-Schmid, B. *et al.* (2015) Organotypic brain slice cultures as a model to study angiogenesis of brain vessels. *Front. Cell Dev. Biol.* 3, 52
90 Nelson, A.R. *et al.* (2016) Neurovascular dysfunction and neurodegeneration in dementia and Alzheimer's disease. *Biochim. Biophys. Acta* 1862, 887–900

Please cite this article in press as: Rocha, D.N. et al. High-throughput platforms for the screening of new therapeutic targets for neurodegenerative diseases, Drug Discov Today (2016), http://dx.doi.org/10.1016/j.drudis.2016.05.005

91 Miller, A.P. *et al.* (2015) Effects of blast overpressure on neurons and glial cells in rat organotypic hippocampal slice cultures. *Front. Neurol.* 6, 20
92 Beraki, S. *et al.* (2013) A pharmacological screening approach for discovery of neuroprotective compounds in ischemic stroke. *PLOS ONE* 8, e69233
93 Cheng, K. *et al.* (2008) Three-dimensional polymer scaffolds for high throughput cell-based assay systems. *Biomaterials* 29, 2802–2812
94 Moraes, C. *et al.* (2010) A microfabricated platform for high-throughput unconfined compression of micropatterned biomaterial arrays. *Biomaterials* 31, 577–584
95 Lai, Y. and Kisaalita, W.S. (2012) Performance evaluation of 3D polystyrene 96-well plates with human neural stem cells in a calcium assay. *J. Lab. Autom.* 17, 284–292
96 Desai, A. *et al.* (2006) Human neuroblastoma cell culture and differentiation in 3D collagen hydrogels for cell-based biosensing. *Biosens. Bioelectron.* 21, 1483–1492
97 Mao, C. and Kisaalita, W.S. (2004) Characterization of 3D collagen hydrogels for functional cell-based biosensing. *Biosens. Bioelectron.* 19, 1075–1088
98 Xu, T. *et al.* (2006) Viability and electrophysiology of neural cell structures generated by the inkjet printing method. *Biomaterials* 27, 3580–3588
99 Bryant, S.J. *et al.* (2008) Designing 3D photopolymer hydrogels to regulate biomechanical cues and tissue growth for cartilage tissue engineering. *Pharm. Res.* 25, 2379–2386
100 Choi, S.H. *et al.* (2014) A three-dimensional human neural cell culture model of Alzheimer's disease. *Nature* 515, 274–278
101 Rocha, D.N. *et al.* (2015) Extracellular environment contribution to astrogliosis-lessons learned from a tissue engineered 3D model of the glial scar. *Front. Cell. Neurosci.* 9, 377
102 Guillemot, F. *et al.* (2010) High-throughput laser printing of cells and biomaterials for tissue engineering. *Acta Biomater.* 6, 2494–2500
103 Lee, W. (2009) Three-dimensional bioprinting of rat embryonic neural cells. *Neuroreport* 20, 798–803
104 Bullock, P.N. and Rome, L.H. (1990) Glass micro-fibers: a model system for study of early events in myelination. *J. Neurosci. Res.* 27, 383–393
105 Li, Y. *et al.* (2014) Nanofibers support oligodendrocyte precursor cell growth and function as a neuron-free model for myelination study. *Biomacromolecules* 15, 319–326
106 Lee, S. *et al.* (2012) A culture system to study oligodendrocyte myelination processes using engineered nanofibers. *Nat. Methods* 9, 917–922
107 Remahl, S. and Hildebrand, C. (1982) Changing relation between onset of myelination and axon diameter range in developing feline white matter. *J. Neurol. Sci.* 54, 33–45
108 Choi, N.W. (2007) Microfluidic scaffolds for tissue engineering. *Nat. Mater.* 6, 908–915
109 Peret, B.J. and Murphy, W.L. (2008) Controllable soluble protein concentration gradients in hydrogel networks. *Adv. Funct. Mater.* 18, 3410–3417
110 Sailon, A.M. *et al.* (2009) A novel flow-perfusion bioreactor supports 3D dynamic cell culture. *J. Biomed. Biotechnol.* 2009, 873816
111 Hirschhaeuser, F. *et al.* (2010) Multicellular tumor spheroids: an underestimated tool is catching up again. *J. Biotechnol.* 148, 3–15
112 Zhang, D. *et al.* (2014) A 3D Alzheimer's disease culture model and the induction of P21-activated kinase mediated sensing in iPSC derived neurons. *Biomaterials* 35, 1420–1428

Please cite this article in press as: Rocha, D.N. et al. High-throughput platforms for the screening of new therapeutic targets for neurodegenerative diseases, Drug Discov Today (2016), http://dx.doi.org/10.1016/j.drudis.2016.05.005

APPENDIX B: OPTIMIZATION OF THE P(TMC-CL) ELECTROSPINNING NANOFIBERS PRODUCTION

- This page was intentionally left blank. -

Table 1 *Electrospinning parameters tested for P(TMC-CL) nanofiber production.*

	Polymer concentration (%)	Solvent ratio (DCM:DMF)	Distance (cm)	Voltage (kV)	Syringe needle (G)	Flow rate (mL/h)
1	10	3:1	14	14	18	1
			14	14	21	
			14	14	21	0.9
			14	14		0.8
			14	13		0.9
			15.5	14		0.9
			14	14		0.8
			14	16		0.9
			14	13		1
			15	14		1
2	10	1:0	14	14	21	1
			12	14		1
			14	15		1
			16	14		1
			16	14		1.2
			10	14		1
			10	10		1
3	10	6:1	14	14	21	1
			16	14		
			16	15		
			16	15		0.9
			16	15		0.8
			16	16		0.9
4	10	1:1	14	10	21	1
			14	12		
			14	13		
			14	16		
			10	14		

5	12.5	4:1	14	14	21	1
			20	14		
6	12.5	4:1	14	14	21	1
			14	15		
			20	14		
			10	14		
			14	14		
7	9	3:1	14	14	21	1
			14	15		
			20	14		
			20	15		
			20	16		
			20	17		
			10	14		
			10	12		
8	9	4:1	14	14	21	1
			15	14		
			13	14		
9	11	3:1	14	14	21	1
			20	14		
			20	15		
			20	13		
10	11	6:1	14	14	21	1
			16	14		1
			15	14		1
			13	14		0.9

Table 2 *SEM images of P(TMC-CL) nanofibers.* The conditions that are not here presented were excluded by optical microscopy analysis.

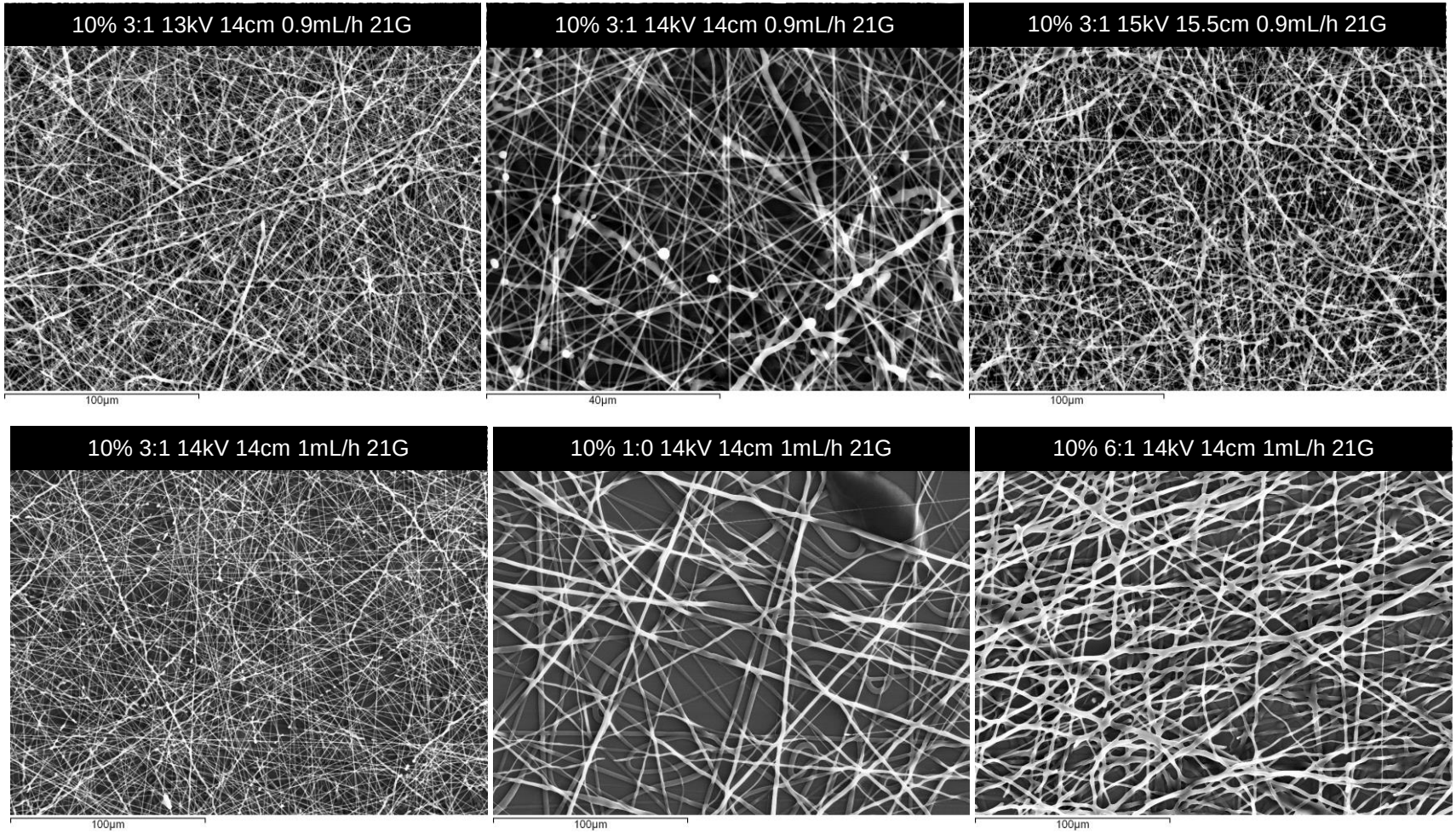

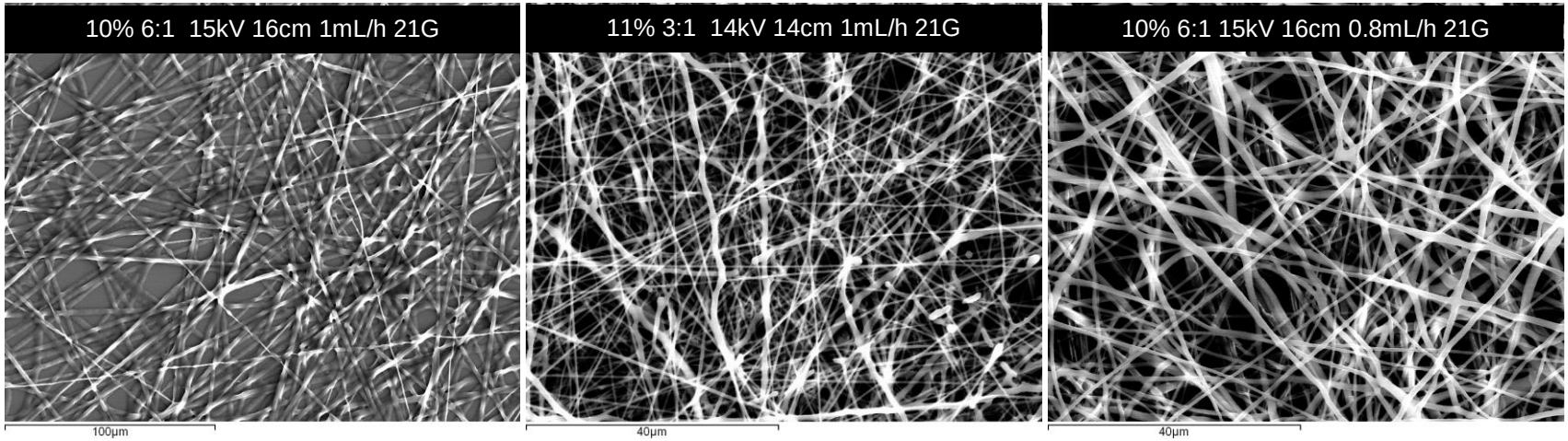
10% 6:1 15kV 16cm 1mL/h 21G
100µm
11% 3:1 14kV 14cm 1mL/h 21G
40µm
10% 6:1 15kV 16cm 0.8mL/h 21G
40µm

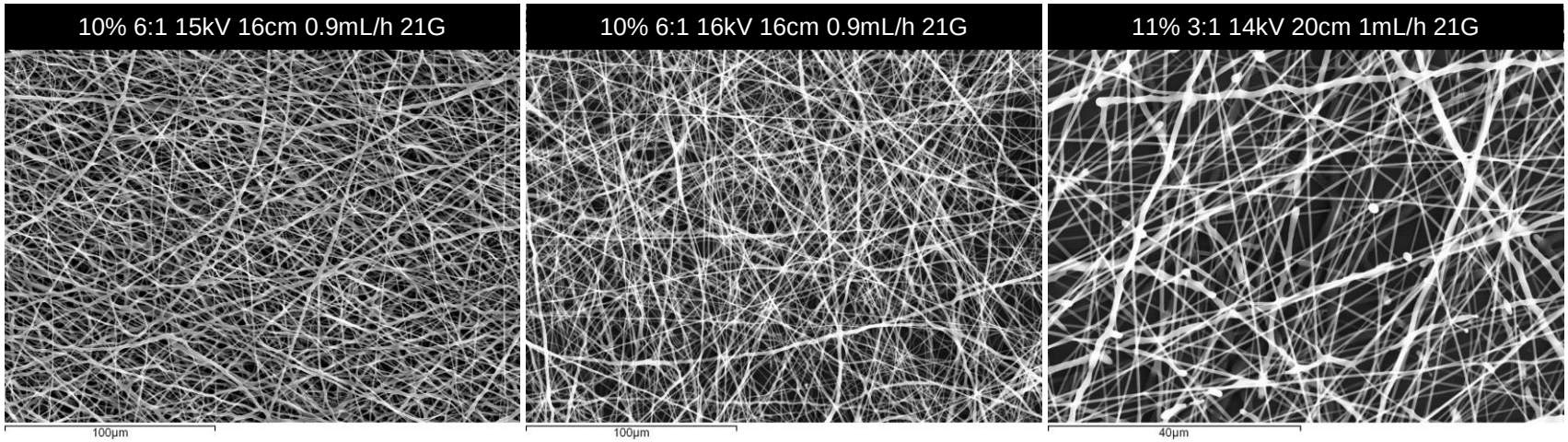
10% 6:1 15kV 16cm 0.9mL/h 21G
100µm
10% 6:1 16kV 16cm 0.9mL/h 21G
100µm
11% 3:1 14kV 20cm 1mL/h 21G
40µm

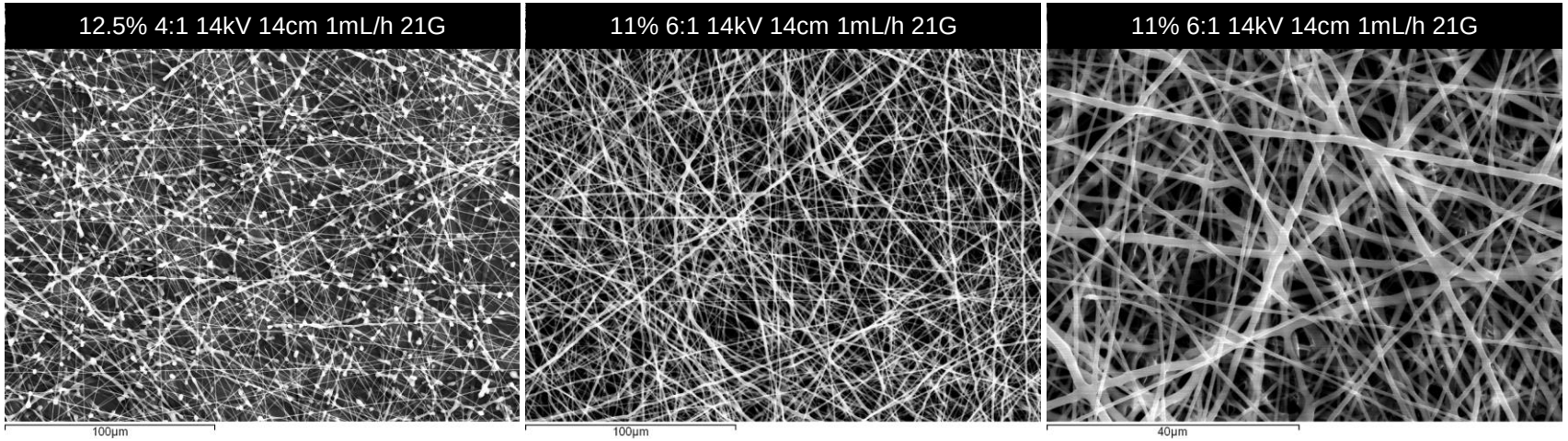
12.5% 4:1 14kV 14cm 1mL/h 21G
100µm
11% 6:1 14kV 14cm 1mL/h 21G
100µm
11% 6:1 14kV 14cm 1mL/h 21G
40µm

- This page was intentionally left blank. -

APPENDIX C: ANIMAL TUTORIAL COURSE FINAL REPORT

- This page was intentionally left blank.

Tutorial Report

All fields must be filled.

Final report must be submitted with tutor feedback and signature.

Tutorial plan description must **focus on the animal model used**, describing animals strain, conditions of animal maintenance, special animal requirements, techniques and procedures, animal welfare, euthanasia, and others relevant aspects considered during tutorial training. The participant must reflect in the report that has developed the capacity to work responsibly with animals, as expected after the introductory training conclusion.

PARTICIPANT DETAILS

Name Eva Daniela de Sousa Maia Carvalho

Group nBTT - nanoBiomaterials for Targeted Therapies

Email bio11042@fe.up.pt

TUTOR DETAILS

Name Sofia Santos

Group nBTT - nanoBiomaterials for Targeted Therapies

Email sasantos@ineb.up.pt

TUTORIAL TRAINING DETAILS

Project title Astrocyte – OPC crosstalk in the context of astrogliosis

Duration (minimum 10h) 10h

Place / Lab Animal Facility

Enumerate by topics specific procedures learned or consolidated[1]:

Rat pups sacrifice;

Rat pups brain removal and cortex and meninges dissection;Mice handling and restrain;

Mice intravenous and intraperitoneal injection;

Mice Intranasal drug administration

---

[1] Focus on the procedures performed on the animals, Ex: mouse restrain, mouse intraperitoneal administration, etc.

Mice anesthesia;

Mice perfusion;

Mice brain, kidney, liver and lung collection.

REPORT[2]:

1. Wistar Han rat pups cortex/meninges dissection

Wistar rats are currently one of the gold standard animal models used in laboratorial research. Originally, they were established in the beginning of the 20th century in Wistar Institute (Philadelphia) which created an inbred strain derived from Rattus norvegicus. Since then a lot of different Wistar lines have been produced and commercialized. Namely, Wistar Han® which is an albino model widely used for many different purposes such as, for surgery, to study aging, oncology, safety and efficacy [1].
To obtain different neuronal cell types, Wistar Han rat pups were used. Rats in post-natal day 2 (P2) were sacrificed and brain was removed to further dissociate the cortex and the meningeal tissue. At all times, this procedure was conducted in the euthanasia room of the animal facility. However, in order to maintain the minimal conditions of sterility during the entire process, using a flow hood would be the ideal scenario. Pups were taken out progenitor's cage and, as all were not sacrificed at the same time, the remaining ones were kept in a warming pad under infrared light to avoid hypothermia. Besides, pups were kept apart from the local of sacrifice to avoid distress in siblings provoked by odour release and vocalizations.
Decapitation was the euthanasia methodology chosen for sacrifice pups. Prior to death, animals were not anesthetized once pups (until P10) do not have sensors of hypoxia, thus volatile anaesthesia (such as isoflurane) would not be well succeeded. Besides, using injectable anaesthesia such as pentobarbital or ketamine is not effective at lower doses and when given in high doses tend to be toxic to neonates [2]. It has been reported that provoking hypothermia by burying pups in ice (1-5min) is the best method to provide immobilization and mild analgesia in rats in the first days of age. This methodology is comparable to local anaesthesia as it stops nerve transmission. The fact that pups have a small surface area and body size enables a progressive, quick and easy cool down [3]. However, hypothermia is only applicable for short time procedures (between 5-15min). In the context of this project, brain removal and dissection needs to be the fastest possible to avoid extensive cell death, hence, anaesthesia was not performed.
After decapitation, heads were sprayed with 70% ethanol to disinfect the area of dissection and also to avoid drying the tissue. Removal of brain was performed using straight micro-scissors and fine forceps previously cleaned and sterilized with ethanol 70%. The choice of the scissors and forceps was a critical point as pups have a very soft skull. The procedure was conducted under a magnifying glass in a Petri dish containing HBSS (Hank's Balanced Salt Solution) supplemented with antibiotics to avoid contamination.
Firstly, the skin of the head was cut until the nose with a sharper scissor with the other hand holding the head (from the ear) with a big forceps. The skin was opened to the corners in order to let the skull bones be visible. Then, with a straight microscissor, the skull bone was cut until the nose and to the sides. The

---

[2] Please provide an outline of how the tutorial time was used, including which procedures, which animal model and an estimate time spent on different procedures. Tutorial report must always focus on the animal model and the procedures applied. References to literature must be used to justify and/or support the procedures' choice.

bones were removed with a thinner forceps and a special care was taken to not damage the cortex. With the same forceps, the cortex was carefully removed (from the olfactive bulbs) and cut by the cerebellum. Lately, using a thinner forceps the two hemispheres were separated. Meningeal tissue was detached from the cortex with a thinner forceps. Cortex and meningeal tissue were maintained in an ice-cold solution to prevent cell dissociation and death.

2. Analysis of brain delivery capacity of dyes in C57BL/6 mice

C57BL/6 mice is an inbred mouse strain widely famous in the research community mainly due to the easiness of creating congenic and mutant mice. For that reason, different lines with different phenotypes derived from C57BL/6 have been developed.
Adult C57BL/6 mice were used as a model to study nanoparticle release to the brain. For that purpose, first experiments conducted involved injections of a dye via intravenous (IV) and intranasal (IN) routes to evaluate dye's capacity to reach the brain.
IN administration is a non-invasive methodology that allow the target directly to the brain via olfactory bulb and trigeminal neural pathways without crossing the blood brain barrier. This administration is considered safer for the mice once it specific targets the brain and the systemic exposure is reduced. The brain is exposed to the substances injected by intranasal route in a faster way (some minutes).
In order to administrate the dye via IN route, mice were firstly anesthetized with an injectable anaesthetic (mixture of ketamidine – 75mg/kg and medetomidine – 1mg/kg) intraperitoneally. The volume of the anaesthetic administrated is dependent on animal weight. Therefore, as mice used in this procedure had a weight around 27g (mean between three animals used), the volume injected was about 200uL. This value was obtained by multiplying the animal weight with the drug dosage for the specie and dividing this product by the drug concentration. As the solutions were maintained in a cold environment (4ºC) before administration, they were pre-warmed to a temperature close to animal's body temperature to minimize the discomfort to mice. A 25G needle and a 1mL syringe were used to perform intraperitoneal (IP) administrations.
In order to correctly administrate a solution by IP injection, mice should be firstly restrained in a proper way. Consequently, mice were removed from their cage by holding them through their tails and placing in the top of the cage without never leaving them. The nape of the mice was then grasped in order to do not allow mice head moving but at the same time, allowing normal breathing of the animals. After being firmly held, mice were slightly inclined to allow the abdomen to be in a high greater than the head. In that position, IP injection was able to be accomplished.
The right position to administrate the IP injection was found by bending the right leg of the animals and the needle was inserted above the knees in the top quadrant left. It is very important to note that this administration should always be done in the right side of the animal (left side of the user) to avoid cecum damaging. The bevel was turned up and the needle was inserted in an angle between the mice and the needle of about 45º. Prior to administration, a test reflux was done: if blood comes out, it means that the area chosen was not the appropriated, hence injection was not completed.
To assure that the mice were appropriately anaesthetized and to control the depth of anaesthesia some test reflexes were done. Firstly, the tail pinch reflex was conducted as loss of reflex in the tail is one of the first reflexes to be lost, following by the pedal withdrawal reflex, which is the most suitable and sensitive test to be sure that the animal is anaesthetized. Breathing was also controlled. Mice were kept under a warming pad to avoid hyperthermia.
It is worth noting that mice were always evaluated regarding their physical appearance and condition. Anaesthesia and further procedures were only conducted if animals were in an healthy condition.
Following anaesthesia, IN administrations of a dye were conducted using a polyurethane catheter (24G) inserted directly into the nares (10mm depth to enable the administration through the roof of the nasal

cavity) attached to a syringe. Mice were restrained and the head of the animals was assure to be elevated and in that position the catheter was inserted. The dye used was not toxic to the animals, thus this procedure caused minimal pain to mice. The amount of dye administrated was not very high (around 200uL). If blood was observed following the injection, it means that the catheter perforated veins, thus the administration was not correctly achieved. In those cases, mice were immediately sacrificed by cervical dislocation to minimize the pain.
Regarding IV administration, this route is also considered when the aim is to target the brain. For the IV injection, mice were restrained with a restraining device. The syringe was filled with the dye and a special care was taken regarding the air bubbles (having no bubbles is crucial for correct administration and safety of the mice). Administrations were done in the lateral veins. Once these veins are not easily seen, an infrared lamp was used to warm the tail which, in turn, caused vein dilatation. A 25G needle was use which was held in a very narrow angle. Prior to administration, a reflux was done and if the syringe was filled with blood the vein was achieved.
After injections via IN and IV routes mice were transferred to their cage to allow them to recover from the anaesthetics effects.
It is worth noting that animals were kept 12h light/12 dark with free access to food and water and maintained in filtered cages.

3. Time distribution

Wistar rats P2 decapitation: 1h
Wistar Rats pups' cortex and meningeal tissue dissociation: 5h
IP injection: 2h
IV injection: 1h
IN injection: 1h

Bibliography:

1. Goepfrich, AA, et al, Behavioral differences in three Wistar Han rat lines for emotional reactivity, cognitive processing and ethanol intake. Physiology & Behavior, 2013. 110–111: p. 102-108.
2. Gannon, WL et al, Guidelines of the American Society of Mammalogists for the use of wild mammals in research. Journal of Mammalogy, 2007. 88(3): p. 809-823.
3.Danneman, PJ et al, Evaluation of five agents/methods for anesthesia of neonatal rats. Lab Anim Sci, 1997. 47(4):p.386-95

Student: _____ Date: 2016/04/24

TUTORIAL FEEDBACK - To be filled by the supervisor

- Did the student complete the tutorial plan?
  Yes☒ No ☐

- Is the student competent (according FELASA B recommendations) to start working with animals without supervision after this tutorial?

yes ☒ No ☐

- I evaluate the work developed for this student during the tutorial plan as:

Excellent ☒ Very Good ☐ Good ☐ Average ☐ Poor ☐ Very Poor ☐

- Tutor Observations(optional):

Tutor: Sofia Alexandra Dixie Santos Date: 25/04/2016

To be filled by organization:

Received at: _____

APPENDIX D: RNA EXTRACTION FROM OPCS SEEDED ON P(TMC-CL) FIBERS OPTIMIZATION PROCESS

- This page was intentionally left blank.

Table 1 *RNA concentration and absorbance at 260nm, 280nm and 230nm values.*

#1						
Lysis buffer time	**PBS washing**	**Nanodrop results**				
			Conc. ng/µL	**A260**	**A280**	**260/280**	**260/230**
Add and remove immediately	No	**Glass**	28,5	0,571	0,287	1,99	2,18
		Fibers	12,6	0,251	0,145	1,74	1,09

#2						
Lysis buffer time	**PBS washing**	**Nanodrop results**				
			Conc. ng/µL	**A260**	**A280**	**260/280**	**260/230**
5 min	No	**Glass**	21,2	0,529	0,237	2,23	2,20
		Fibers	13,2	0,33	0,153	2,16	1,97

#3						
Lysis buffer time	**PBS washing**	**Nanodrop results**				
			Conc. ng/µL	**A260**	**A280**	**260/280**	**260/230**
10 min	No	**Glass**	17,9	0,447	0,219	2,04	2,18
		Fibers	12	0,300	0,182	1,67	2,21

#4						
Lysis buffer time	**PBS washing**	**Nanodrop results**				
			Conc. ng/µL	**A260**	**A280**	**260/280**	**260/230**
15 min	No	**Glass**	57,2	1,436	0,682	2,10	2,06
		Fibers	26,2	0,654	0,353	1,85	1,74

#5						
Lysis buffer time	**PBS washing**	**Nanodrop results**				
			Conc. ng/µL	**A260**	**A280**	**260/280**	**260/230**
10 min	Yes	**Glass**	33,8	0,860	0,390	2,17	1,95
		Fibers	36,0	0,899	0,550	1,63	0,90

Table 2 *Example of a RNA integrity measurement (Experion analysis)*. The RQI Classification is obtained by comparing the electrophorogram of the samples with RNA degraded standardized samples. RQI values vary between 1 (for highly degraded samples) and 10 (intact samples). Samples with RQI lower than 5 were not used in this study.

Well ID	Sample Name	RNA Area	RNA Concentration (ng/µl)	Ratio [28S:18S]	RQI	RQI Classification	RQI Alert
L	Ladder	296.69	160.00				
1	1 eva	6.57	3.54	1.63	N/A		Critical Anomaly
2	2 eva	85.40	46.05	1.62	8.5		
3	3 eva	73.02	39.38	1.90	7.9		
4	4 eva	15.57	8.40	1.83	N/A		RNA conc. too low
5	5 eva	40.70	21.95	1.88	N/A		Critical Anomaly
6	6 eva	50.74	27.36	0.01	5.0		
7	7 eva	64.30	34.67	0.04	N/A		Critical Anomaly
8	8 eva	116.32	62.73	0.00	5.1		
9	9 eva	57.15	30.82	0.07	3.8		
10	10 eva	59.53	32.10	0.03	3.5		
11	Sample 11	14.31	7.72	1.08	N/A		RNA conc. too low

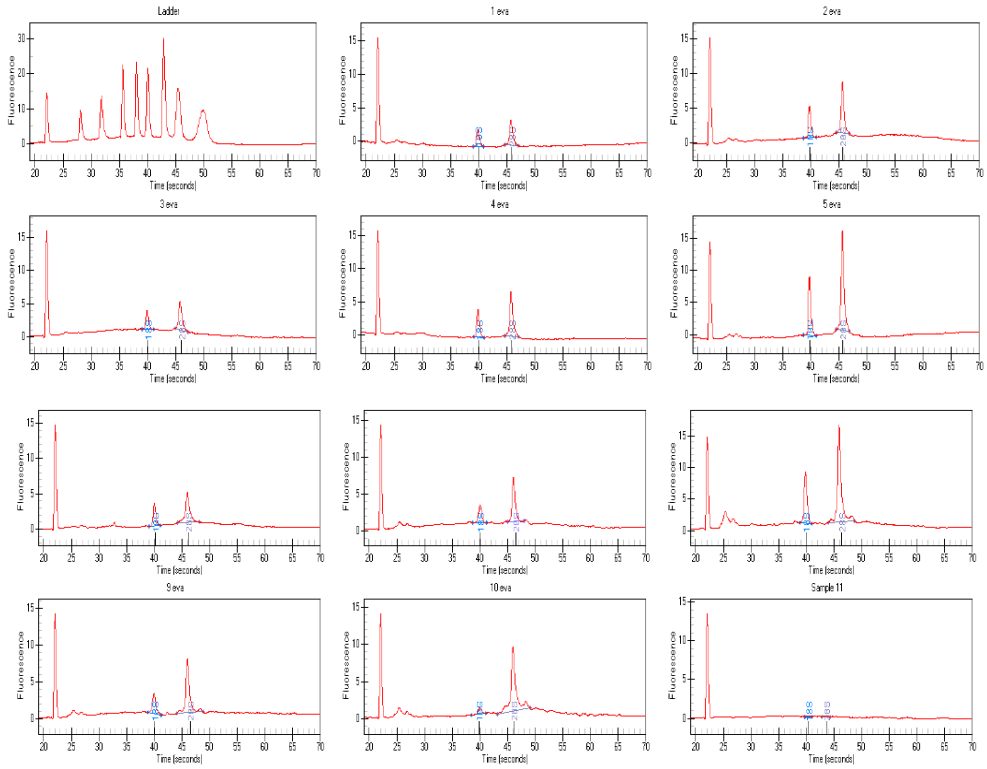

Figure 1 *Example of electrophorogram for RNA samples from OPCs seeded on P(TMC-CL) fibers.*

APPENDIX E: EFFICIENCY PROFILE OF PRIMERS FOR QRT-PCR

- This page was intentionally left blank.

Tested primers

Table 1 *Tested primers for qRT-PCR.*

HPRT Rat	Sense	5’ ATG GAC TGA TTA TGG ACA GGA CTG 3’
	Anti-sense	5’ GCA GGT CAG CAA AGA ACT TAT AGC 3’
YHAWZ Rat	Sense	5’ ACG ACG TAC TGT CTC TTT TGG 3’
	Anti-sense	5’ GTA TGC TTG CTG TGA CTG GT 3’
TBP Rat	Sense	5’ TGG GAT TGT ACC ACA GCT CCA 3’
	Anti-sense	5’ CTC ATG ACT GCA GCA AAC C 3’
MBP Rat	Sense	5’ TGT CAC AAT GTT CTT GAA GAA 3’
	Anti-sense	5’ GCT CCC TGC CCC AGA AGT 3’

Efficiency profiles for the primers

A - HPRT

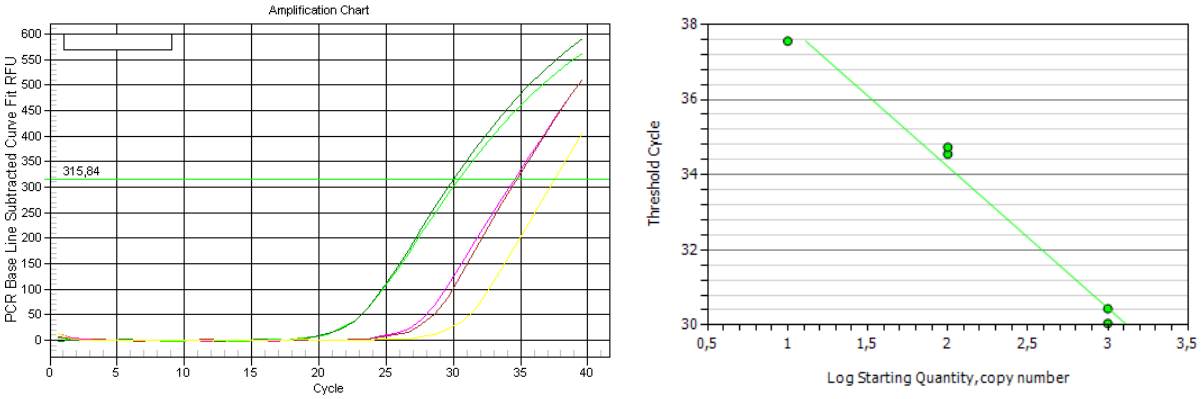

B - YWHAZ

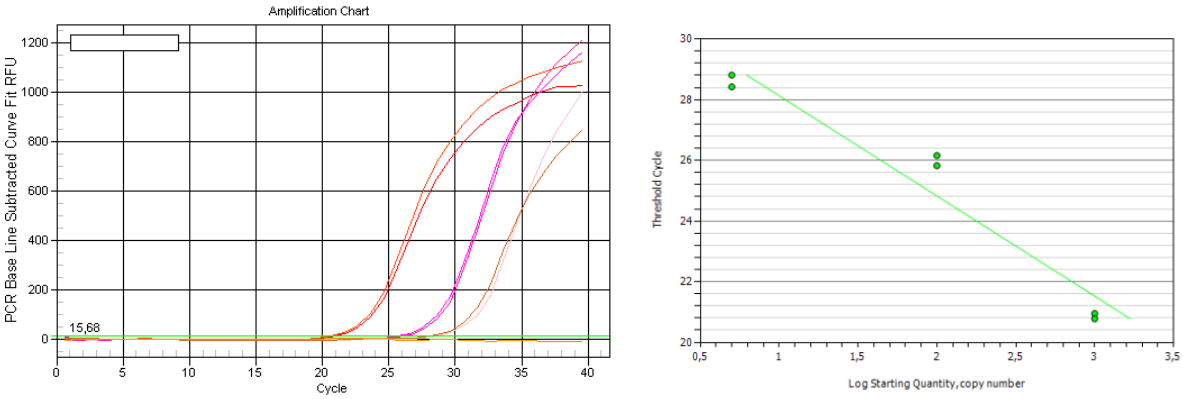

C - TBP

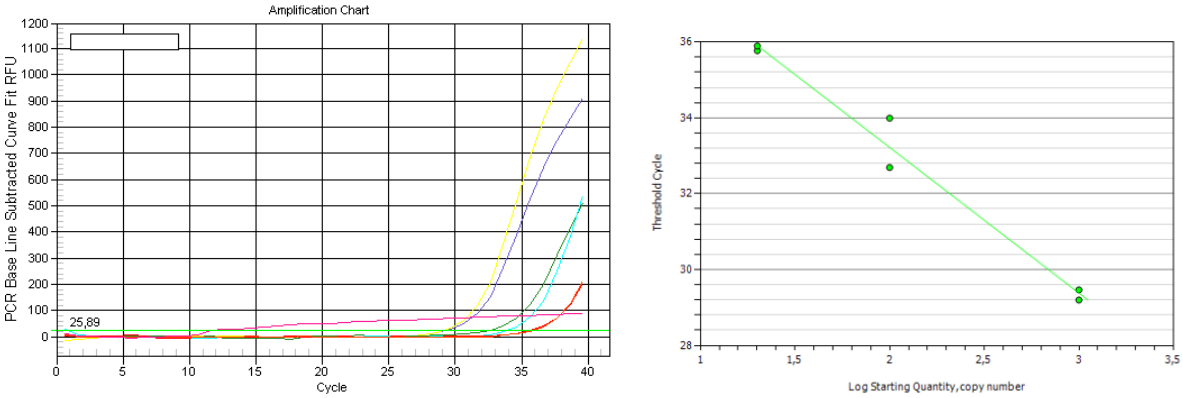

D - MBP

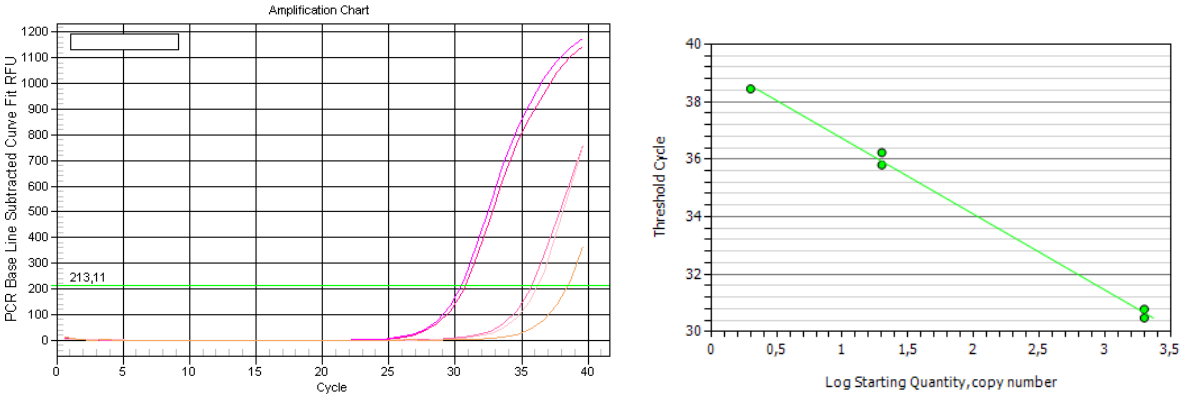

Figure 1 *Amplification curves and standard curves for HPRT, YHWAZ, TBP and MBP.*

Table 2 *PCR efficiency values.* An efficiency around 100% is the desired for appropriate primers. Besides, R^2 should be around 0,99 and the slope -3,

	Fluor	PCR Efficiency (%)	R Squared	Slope	y-Intercept
HPRT	SYBR	84,4	0,982	-3,762	41,737
YWHAZ	SYBR	100,8	0,932	-3,302	31,430
TBP	SYBR	82,2	0,979	-3,840	40,900
MBP	SYBR	109,6	0,997	-3,112	39,353

Housekeeping genes analysis

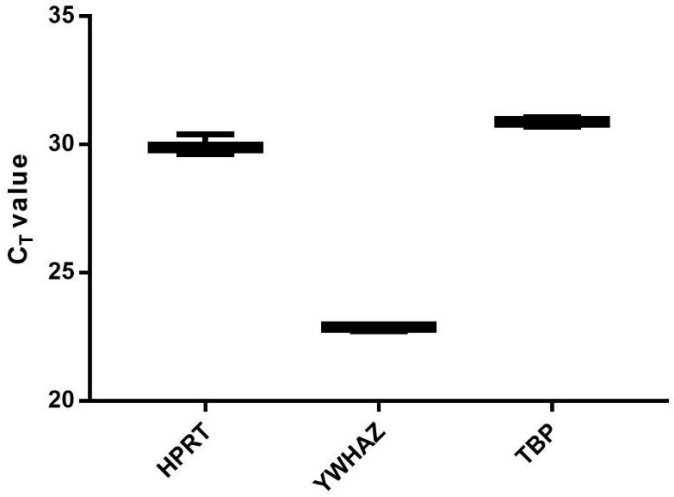

Figure 2 *C_T values for tested housekeeping genes.* YWHAZ was chosen due to the low C_T value in comparison with the other housekeeping genes. Besides, the higher values of C_T from HPRT and TBP is an indicative of low expression of the housekeeping which is not adequate.